The 7th* Chile-Cologne-Bonn-Symposium

PHYSICS AND CHEMISTRY OF STAR FORMATION

THE DYNAMICAL ISM ACROSS TIME AND SPATIAL SCALES

NEW DATE: September 26 – 30, 2022

Puerto Varas, Chile

SESSION TOPICS

Star Formation across Cosmic Time
Star Formation across Scales and Environments
The ISM and Molecular Clouds:
- feedback, quenching, triggering, turbulence
- magnetic fields, fragmentation and collapse, outflows
- abundances, chemistry and microphysical processes

Laboratory Astrophysics
Observatories and Instrumentation

SCIENTIFIC ORGANIZING COMMITTEE:

Leo Bronfman
Scott Chapman
Andrea Ferrara
Javier Goicoechea
Eva Schinnerer
Stephan Schlemmer
Gordon Stacey
Amelia Stutz
Satoko Takahashi
Ewine van Dishoeck
Ji Yang
Hans Zinnecker

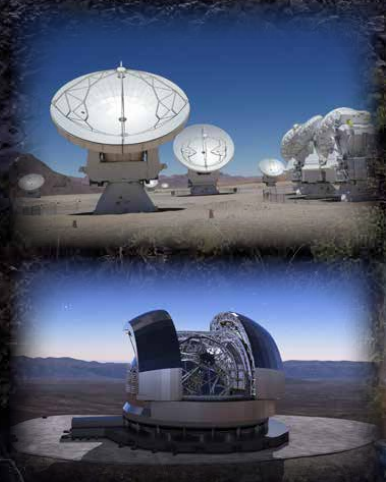

astro.uni-koeln.de/symposium-star-formation-2022

*in the series of the former Zermatt-Cologne-Bonn Symposia

LOCAL ORGANIZING COMMITTEE:

I. Breloy | R. Bustos | P. García | S. Herbst | W. Max-Moerbeck
V. Ossenkopf-Okada | D. Riquelme | R. Rodriguez | Á. Sánchez-Monge
R. Schaaf | F. Schlöder | D. Seifried | A. Stutz | J. Stutzki | S. Thorwirth

CONTACT: zermattchile2022@ph1.uni-koeln.de

The conference is managed by:
Contact: Andrea Lagarini
zermattchile2022@contactochilecom.cl

The conference is co-funded by:
CRC 956 (project ID 184018867)
Comité Mixto ESO-Chile

Abstract book

Editors: Volker Ossenkopf-Okada, Frank Schlöder, Isabelle Breloy
Release: September 26, 2022

List of sessions, talks and posters

Underlined names indicate the authors presenting at the symposium

Conference program

Monday

Start	Speaker	Title	Min.	Page
08:30	Organizers	Opening Remarks	10	
08:40	Manuel Aravena	The cosmic evolution of the molecular ISM out to the epoch of reionization	35	20
09:15	Kotaro Kohno	Unbiased surveys of dust-enshrouded galaxies using ALMA	25	21
09:40	Rodrigo Herrera-Camus	CRISTAL: a survey of gas, dust, and stars in typical, star-forming galaxies when the Universe was only $\sim$1 Gyr	20	24
10:00	Daniel Vieira	Molecular Gas Excitation of CRLE and HZ10 at z=5.7	20	27
10:20		COFFEE BREAK	30	
10:50	Matus Rybak	A new view of dusty star formation at high redshift	25	22
11:15	Kevin Harrington	A Multi-J CO and [CI] line study of single dish observations of the lensed Planck selected starbursts at cosmic noon	20	23
11:35	Edo Ibar	The molecular gas and dust content in 'typical' z$\sim$2 star-forming galaxies as revealed by ALMA	20	25
11:55	Stefanie Walch-Gassner	Stellar feedback from sub-parsec to galactic scales	35	59
12:30		LUNCH BREAK	90	
14:00	Dominik Riechers	CCAT-prime: New Science From Galaxy Evolution to Cosmic Reionization	20	26
14:20	Edith Falgarone	Chemical, radiative and statistical signatures of turbulent dissipation	25	60
14:45	Andrea Bonilla-Barroso	ONC formed via Violent Relaxation.	20	64
15:05	Sergio Molinari	Clump-to-cores fragmentation in the Galactic context: present status and preliminary indications from the ALMAGAL "statistical" survey	25	62
15:30	Emma Bordier	Can the migration scenario be at the origin of massive close binaries?	20	65
15:50	Jürgen Stutzki	Velocity-resolved [CII] Observations	20	70
16:10		COFFEE BREAK	30	
16:40	Nicola Schneider	Observational signatures of stellar feedback	25	61
17:05	Cristian Guevara	The hidden ionized carbon in M17SW	20	67
17:25	Denise Riquelme	Large Scale Mapping of the Central Molecular Zone: C+ and CO emission	20	69
17:45		Chile Folklore Show	60	
18:45		End of the Day	0	

Tuesday

Start	Speaker	Title	Min.	Page
08:30	Yasuo Fukui	High mass star formation triggered by cloud-cloud collisions	25	63
08:55	Giuliana Cosentino	Feedback from Supernova Remnants: triggering Star Formation in the ISM	20	66
09:15	Umit Kavak	Prestellar feedback in massive star-forming regions	20	68
09:35	Amelia Stutz	From collapsing clouds to protostellar clusters, the key phase of core formation and accretion	35	83
10:10	John Tobin	From protostellar to Proto-Planetary disks: Disk formation and Evolution in the Orion Molecular Cloud	25	85
10:35		COFFEE BREAK	30	
11:05	Atefeh Aghababaei	Probing accretion along filaments in creating shocks: First detection of extended SiO along filaments in the NGC6334 V	20	88
11:25	Aida Ahmadi	From core to disk fragmentation in high-mass star formation	20	89
11:45	Laura Fissel	Magnetic fields and the formation of dense gas structures in molecular clouds	25	84
12:10	Lapo Fanciullo	Studying Dust Properties, Grain Alignment And Magnetic Field Structure With Multi-Wavelength Submillimeter Polarization	20	90
12:30		LUNCH BREAK	90	
14:00	Sara Rezaei	Filament or sheet? The effects of the viewing angle on star formation	20	94
14:20	Friedrich Wyrowski	Dense clumps in the Milky Way: Physical properties and kinematics	25	87
14:45	Maria Jose Maureira	High-resolution dust mapping of Class 0 and I disks	20	91
15:05	Tom Megeath	Investigating Accretion onto Class 0 Protostars	20	92
15:25	Nadia Murillo	Formation and environment of multiple protostellar systems in Perseus	20	93
15:45		COFFEE BREAK	30	
16:15		POSTER SESSION (with coffee)	120	
18:15		End of the Day	0	

Wednesday

Start	Speaker	Title	Min.	Page
08:30	Thomas Giesen	Greetings from the Laboratory: recent developments in Laboratory Astrophysics	35	125
09:05	José Cernicharo	Broad band millimeter astronomical and laboratory observations. The case of QUIJOTE line survey of TMC-1 and the GACELA experimental setup	25	126
09:30	Octavio Roncero	Quantum calculations of formation and destruction rates of molecules for ISM models	25	127
09:55	Oskar Asvany	High-resolution spectroscopy of astrophysically relevant molecular ions	20	129
10:15	Divita Gupta	High-resolution ro-vibrational spectroscopy of cyclopropenyl cation: The ν4 C–H antisymmetric stretching band	20	130
10:35		COFFEE BREAK	30	
11:05	Thomas Henning	Laboratory Astrophysics of Cosmic Dust	25	128
11:30	Doug Johnstone	Diagnostics of stellar mass assembly uncovered via monitoring protostellar variability	25	86
11:55	Jens Kauffmann	LEGO: Observing the Milky Way to unravel Molecular Cloud Populations and Lifecycles in Galaxies	20	95
12:15		LUNCH BREAK	90	
13:45		EXCURSION	315	
19:00		CONFERENCE DINNER	300	
00:00		End of the Day	0	

Thursday

Start	Speaker	Title	Min.	Page
08:30	Johannes Staguhn	Scientific capabilities enabled by future millimeter through FIR instrumentation and observatories	35	136
09:05	John Carpenter	Current capabilities of ALMA and Roadmap to 2030	20	137
09:25	Roberto Neri	IRAM Observatories today and tomorrow	20	138
09:45	Floris van der Tak	Star and planet formation: Upcoming opportunities in the space-based infrared	20	139
10:05	Nicolas Reyes	The APEX Telescope: current status and future developments	20	143
10:25	C. Peters, G. Kausel	Introduction to the DFG and it's research funding in Chile	20	
10:45		COFFEE BREAK	30	
11:15	Gordon Stacey	CCAT-prime: status and science prospects	20	141
11:35	Urs Graf	The CCAT-prime Heterodyne Array Instrument (CHAI)	20	145
11:55	Robert Simon	The Cycling of Matter from the Interstellar Medium to Stars and back: The CCAT-prime Galactic Ecology project	20	42
12:15	Rodrigo Reeves	Chilean involvement in astronomy instrumentation projects	20	140
12:35		LUNCH BREAK	90	
14:05	Margaret Meixner	Current and Future Space/airborne Observatories for ISM studies	20	142
14:25	Hans Zinnecker	The future of FIR astronomy, after SOFIA	20	146
14:45	Alberto Bolatto	Synergies between IFU and molecular surveys	25	33
15:10	Axel Weiss	The APEX Magellanic Clouds Legacy Survey	20	43
15:30	Open discussion	FIR-perspectives after the end of SOFIA	20	
15:50		COFFEE BREAK	30	
16:20		POSTER SESSION (with coffee)	120	
18:20		DINNER BREAK	130	
20:30	Stefanie Milam	The James Webb Space Telescope: Advancing chemical and physical studies of star and planet formation	25	154
20:55	Médéric Boquien	First results of the PHANGS/JWST Treasury program on star formation in nearby galaxies	20	155
21:15	Jessica Sutter	Early Science with PHANGS-JWST: New Insights into Small Dust Grains	20	156
21:35	John Tobin	JWST/MIRI Spectroscopy and Imaging of the Class 0 protostar IRAS 15398-3359	20	157
21:55		End of the Day	0	

Friday

Start	Speaker	Title	Min.	Page
08:30	Harold Yorke	Review on: Star Formation across Different Environments	35	32
09:05	Mark Morris	Star Formation in a Strong Magnetic Environment: the Case of the Galactic Center	25	36
09:30	Aaron Bryant	Far-Infrared Imaging Spectroscopy of the Galactic Centre's Circumnuclear Disk	20	37
09:50	Cosima Eibensteiner	Comparing physical properties of two extreme dynamical environments: The centers and outskirts of nearby disk galaxies	20	38
10:10		COFFEE BREAK	30	
10:40	Sudeshna Patra	Impact of environments on star formation process: Outer versus Inner Milky Way	20	40
11:00	Simon Glover	Molecular cloud formation in metal-poor gas	25	110
11:25	Monica Rubio	Star Formation in the Magellanic Clouds	25	35
11:50	Suzanne Madden	Shine a Light: on PDRs and Molecular Clouds at Low Metallicity	20	39
12:10	Guido Garay	Massive Star Formation: from 1 pc to 100 AU scales".	25	34
12:35		LUNCH BREAK	90	
14:05	David Rebolledo	Multi-phase view of the ISM in the Carina Nebula	20	41
14:25	David Neufeld	The chemical composition of molecular clouds and what we learn from it	35	106
15:00	Maryvonne Gerin	Multi dimension analysis of molecular clouds : the example of the Orion-B clouds	25	108
15:25		COFFEE BREAK	30	
15:55	Nanase Harada	Chemistry and molecular cloud properties in nearby galaxies	25	107
16:20	Arshia Jacob	HyGAL: Characterizing the Galactic ISM with observations of hydrides and other small molecules – First Results	20	112
16:40	Wonju Kim	HyGAL, II. The absorption line survey with the IRAM 30m telescope	20	113
17:00	Manuel Merello	Hot molecular cores associated to the brightest far-infrared clumps in the Southern Milky Way	20	114
17:20	Marco Padovani	Cosmic rays: shaping dynamics and chemistry in star-forming regions	25	109
17:45	Gary Fuller	TEMPO: Tracing The Evolution of Massive Protostellar Objects: Fragmentation and Chemical Properties	20	111
18:05	Organizers	Closing Remarks	10	
18:15		End of the Day	0	

Session I: Star Formation across Cosmic Time

The cosmic evolution of the molecular ISM out to the epoch of reionization

M. ARAVENA[1]

[1] Universidad Diego Portales, manuel.aravenaa@mail.udp.cl

Remarkable progress has been made in the last few years in understanding the global properties of galaxies and how they evolve through cosmic time. A major focus has been given to studies of how the availability of molecular gas regulates the star-forming activity and galaxy growth, the eventual quenching of star formation, and how these mechanisms evolve through cosmic time. Most of these advances have been made thanks to ALMA and the upgraded capabilities of NOEMA, enabling CO line and dust continuum emission observations of thousands of galaxies and resolved interstellar medium (ISM) measurements in an increasing number of objects (in dust, CO, [CI] and [CII] line emission). In this presentation, I briefly review the latest constraints on the molecular gas content and properties based on different tracers of the molecular ISM, including recent determinations of the molecular gas fraction, gas depletion timescales, molecular gas cosmic density and resolved ISM morphologies and kinematics out to $z \sim 8$. Current studies are yielding unprecedented views of the process of galaxy assembly and feedback in the early universe.

Unbiased surveys of dust-enshrouded galaxies using ALMA

K. KOHNO[1] AND ALCS COLLABORATION

[1] Institute of Astronomy, School of Science, The University of Tokyo
kkohno@ioa.s.u-tokyo.ac.jp

The ALMA lensing cluster survey (ALCS) is an ALMA cycle-6 large program dedicated to uncovering and characterizing intrinsically faint continuum sources and line emitters with the assistance of gravitational lensing. All 33 cluster fields were selected from HST/Spitzer treasury programs including CLASH, Hubble Frontier Fields, and RELICS, which also have Herschel and Chandra coverages. Some of the ALCS fields have been observed by JWST. The total sky area surveyed reaches $\sim$134 arcmin^2 down to a depth of 0.07 mJy beam^{-1} (1σ) at 1.2 mm, yielding 141 secure continuum detections (Sun, F. et al. 2022). In this presentation, I will describe how these ALCS sources are used to examine the origin of the extragalactic infrared background light, constrain the [CII] 158 μm line luminosity function in the Epoch of Reionization, and characterize the physical properties of dust-enshrouded star-forming and active galaxies across cosmic time. We find a significant fraction of ALCS 1.2 mm continuum sources do not have any counterpart in HST/F160W band (*H*-dropout ALCS sources), and some of them are invisible even in the IRAC channel 1/2. I will also present the status of spectroscopy follow-up observations of these *H*-dropouts using ALMA.

References:

Uematsu, R., Ueda, Y., Kohno, K., et al. ApJ, submitted
Kokorev, V., Brammer, G., Fujimoto, S., et al. ApJ Suppl., submitted
Cheng, C., Yan, H., Huang, J.-S., Willmer, C. N. A., et al. ApJ, submitted
Guerrero, A., Nagar, N., et al. MNRAS, submitted
Sun, F., Egami, E., Fujimoto, S., Rawle, T., Bauer, F., Kohno, K., Smail, I., et al. 2022, ApJ, 932, 77
Fujimoto, S., Oguri, M., Brammer, G., et al. 2021, ApJ, 911, 99
Laporte, N., Zitrin, A., Ellis, R. S., et al. 2021, MNRAS, 505, 4838
Jolly, J.-B., Knudsen, K., Laporte, N., et al. 2021, A&A, 652, 128
Caputi, K. I., Caminha, G. B., Fujimoto, S., et al. 2021, ApJ, 908, 14

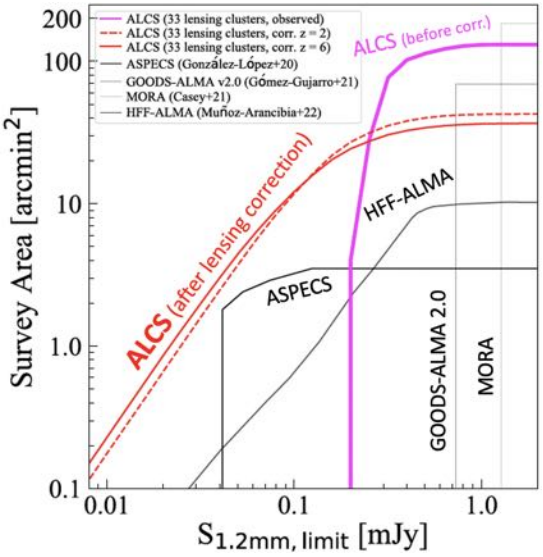

Figure 1: Comparison of deep continuum surveys using ALMA. Taken from Fujimoto et al. (in preparation)

A new view of dusty star formation at high redshift: high-resolution and high-sensitivity studies of obscured galaxies at sub-mm and radio wavelengths

M. RYBAK[1,2] AND J. A. HODGE[2]

[1] Delft University of Technology, Delft, the Netherlands, m.rybak@tudelft.nl
[2] Leiden Observatory, Leiden, the Netherlands

Beyond redshift $z \geq 1$, a significant fraction of star formation - especially in massive galaxies - is obscured by extensive dust reservoirs. Their optically thick dust screens render these galaxies largely invisible from the UV to near-IR. Instead, to identify and study these highly-obscured systems, we need to move to longer wavelengths, from mid- and far-infrared, sub-mm to the radio. Each of these provides a complementary piece of the puzzle: the mid-IR probes the older stellar populations and PAH emission; the sub-mm regime covers the dust continuum and key molecular and atomic lines; radio free-free and synchrotron emission provide independent view of star-formation and crucial information about magnetic field.

How are the immense star-formation rates of dusty galaxies triggered and maintained? What is the relationship between their molecular gas, star-formation and evolved stellar populations? What are the physical conditions of their interstellar medium? Answering these questions requires high-resolution imaging and observations of the key spectral lines such as CO and [CII], alongside the dust contunuum. The recent revolution in angular resolution and sensitivity provided by long-baseline interferometers now makes such detailed investigations possible - even deep into the Epoch of Reionization. Thanks to the exquisite resolution and sensitivity of ALMA, NOEMA, and JVLA, studies of dusty, high-redshift are now reaching the spatial scales and complexity similar to nearby galaxies and even Galactic star-forming regions.

I will showcase recent highlights from sub-mm and radio observations of high-redshift dusty galaxies:

- High-resolution ALMA imaging of dust continuum, which reveal complex morphologies indicative of dynamical interactions.
- Multi-tracer imaging of dust continuum, low-J CO, and [CII] emission, which provides the first view of gas thermodynamics on (sub-)kpc scales and evidence for extended reservoirs of cold, low-density molecular gas.
- Surveys of dense gas tracers – HCN, HCO^+, and HNC – which yield new insights on the dense-gas content of dusty galaxies and constraints on star-formation models.

A Multi-J CO and [CI] line study of single dish observations of the lensed Planck selected starbursts at cosmic noon

K.C.HARRINGTON[1], A.WEISS[2] ET AL.

[1] European Southern Observatory, Alonso de Córdova 3107, Vitacura, Santiago de Chile, Chile, kharring@eso.org

[2] Max-Planck-Institut für Radioastronomie, Auf dem Hügel 69, 53121 Bonn, Germany

The peak epoch of cosmic star formation also broadly coincides with the peak in the cosmic co-moving molecular gas mass density, at z $\sim$ 2. Only strongly lensed galaxies offer the feasibility to routinely detect multiple emission lines tracing the full CO ladder and both atomic carbon fine-structure lines for high-z galaxies. In the past few years, our team has delved into the Planck All-Sky Survey to Analyze Gravitationally-lensed Extreme Starbursts (PASSAGES) in order to conduct such systematic studies to better understand the most active star-forming galaxies in the early Universe. In this talk I will focus on the results of a state-of-the-art approach to model – simultaneously – both the detected emission lines and the dust SED. Using the largest assembly of 200 CO/[CI] lines for any uniformly selected high-z sample, we have explicitly derived the infamous alpha conversion factors without assuming any excitation corrections or typically applied values. I will discuss the implications based on such spatially unresolved measurements, including a detailed perspective on the often-used dust continuum approach to deriving the molecular gas masses. I will also briefly present our current understanding of the [CI] line excitation conditions in the context of these detailed radiative transfer models.

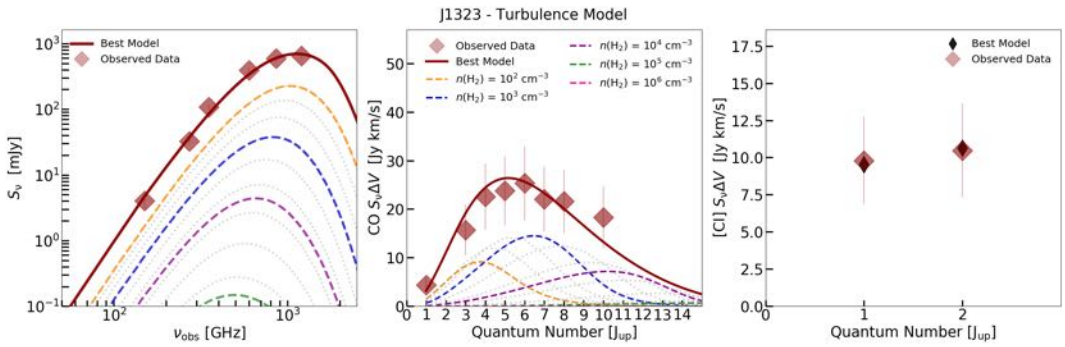

Figure 1: *Turbulence* model for the dust SED, CO and [CI] velocity-integrated line fluxes. Different dashed-colored curves denote the representative contributions to the density PDF for the molecular gas densities of log($n(\mathrm{H_2})$) = 2 (yellow), 3 (blue), 4 (purple), 5 (green) and 6 (pink) cm^{-3}. These individual density contributions have a y-axis scaled by a factor 5 for both the dust and line SED to facilitate interpretation of the dominant gas density. All observed data are shown as red diamonds. The best-fit [CI] line fluxes are plotted over the observed data. All solid red lines indicate the total best-fit, minimum-χ^2 model.

References:

Harrington, K.C. et al. 2021, ApJ, 908, 95

CRISTAL: a survey of gas, dust, and stars in typical, star-forming galaxies when the Universe was only ∼1 Gyr

R. HERRERA-CAMUS[1] ON BEHALF OF THE CRISTAL TEAM

[1] Universidad de Concepción, Chile, rhc@astro-udec.cl

The Atacama Large Millimeter/Submillimeter Array (ALMA) is revolutionizing our view of the interstellar medium (ISM) of star-forming galaxies when the Universe was only ∼1 Gyr old. In this talk I will present what we have learned from in-depth studies, focusing first on the main-sequence galaxy HZ4 at $z = 5.5$. The combination of deep ALMA and HST observations of HZ4 has revealed ISM conditions similar to those observed in local starbursts (e.g., NGC 253), a [CII] halo of neutral gas that extends beyond the star-forming disk, and the presence of a ~ 400 km s^{-1} outflow (Herrera-Camus et al. 2021). HZ4 also has a regular rotating disk already in place at $z \sim 5$, and is baryon dominated on galactic scales, with a dark-matter fraction within one effective radius of only 40% (Herrera-Camus et al. 2022). This low dark-matter fraction is only comparable to what is observed in its likely descendants: massive, star-forming galaxies at $z = 2$. The key results obtained from the ALMA observations of HZ4 has led to the ALMA Cycle 8 Large Program CRISTAL ("[CII] resolved ISM in star-forming galaxies with ALMA"; www.alma-cristal.info). CRISTAL, in combination with observations from ESO/VLT, HST, and in the very near future JWST, is producing the first systematic census on kiloparsec scales of the gas, dust, and stars in typical, star-forming galaxies between $z \approx 4 - 6$. This meeting will be a great opportunity to present the first results of our survey, and highlight its contribution to the study of the star formation activity and ISM properties of normal galaxies in the early universe.

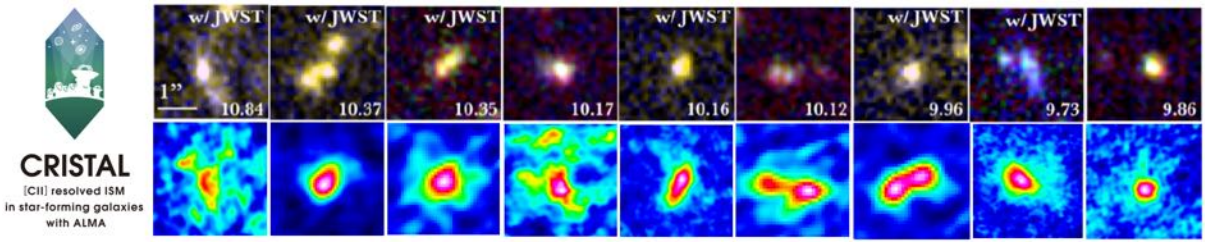

Figure 1: CRISTAL is an ALMA Cycle 8 Large Program that is observing in the [CII] 158 μm line and dust continuum 19 normal, star-forming galaxies between $z \approx 4 - 6$. The panel shows HST composites and [CII] integrated intensity maps of a subset of 10 of the 19 galaxies that are part of CRISTAL.

References:

Herrera-Camus, R., Förster Schreiber, N., Genzel, R., 2021, A&A, 649, 31
Herrera-Camus, R., Förster Schreiber, N., Price, S., 2022, arXiv:2203.00689

The molecular gas and dust content in 'typical' z$\sim$2 star-forming galaxies as revealed by ALMA

E. IBAR[1] ET AL.

[1] Instituto de Física y Astronomía. Universidad de Valparaíso eduardo.ibar@uv.cl

We show ALMA observations to 'typical' H-alpha star-forming galaxies at z=1.5-2.5 selected from the High-z Emission Line Survey (HiZELS). The galaxies have previously got AO-assisted H-alpha observations with SINFONI at $\sim$0.2" ($\sim$1kpc) resolution revealing thick rotating disks presenting massive clumps of star-formation.

Using ALMA Band-3 we observe large and massive reservoirs of cold molecular gas with masses which are usually $\sim$2-3 times larger than that seen in stars, more extended, and show smooth radial profiles without significant clumpy structures (as those seen by SINFONI). One galaxy is resolved in CO(2–1) at 0.2" resolution revealing that both phases of the ISM, ionised an molecular, have similar rotation velocity and velocity dispersion at $\sim$100km/s levels (Molina et al. 2019). We observe a flat rotation curve up to 2x its half-light radius, so assuming a thick rotating disk we can put constraints on its dynamical mass ($\sim 1.5\times10^{11}M_{\odot}$) and dark-matter fraction ($f_{\rm DM} \sim 0.6$). Even though HiZELS galaxies cover a wide parameter space in terms of gas content, their integrated properties still follow the Schmidt-Kennicutt law, similarly to 'normal' galaxies seen in the local Universe.

Using ALMA Band-7 we derive the H-alpha dust-corrected star-formation rates, finding that these 'normal' galaxies fall in the so-called 'long-lasting mode' of star-formation which could continue up to the present day at that fixed SFR (Cheng et al. 2020). Combining matched-resolution HST, ALMA, SINFONI and JVLA images (Cochrane et al. 2021), we find complex morphologies of the different phases of the ISM suggesting non-trivial global extinction corrections of these high-z galaxies.

These findings point towards the existance of large molecular gas reservoirs with complex ISM physics at high-z sustaining the peak of the cosmic star formation rate density.

References:
Molina et al. 2019, MNRAS, 487, 4856
Cheng et al. 2020, MNRAS, 499, 5241
Cochrane et al. 2021, MNRAS, 503, 2622

CCAT-prime: New Science From Galaxy Evolution to Cosmic Reionization

D.A. RIECHERS[1], ON BEHALF OF THE CCAT-PRIME COLLABORATION

[1] Universität zu Köln, riechers@ph1.uni-koeln.de

The CCAT-prime collaboration are currently constructing the Fred Young Submillimeter Telescope (FYST), a wide-field, 6-m aperture telescope to be sited at more than 5600 meters elevation on Cerro Chajnantor in northern Chile. The facility will address important astrophysical questions ranging from Big Bang cosmology through reionization and the formation of the first galaxies to star formation within our own Milky Way galaxy. This presentation will highlight how CCAT-prime will provide a tomographic view of the interstellar medium content of galaxies on megaparsec scales through cosmic history, including the star-forming galaxies driving cosmic reionization at the highest redshifts. This will be achieved through a deep line intensity mapping survey of the early universe in a suite of interstellar medium diagnostics, in particular the [CII] 158-micron cooling line from the neutral medium at $z\sim$3.5–8.0, the [OIII] 88-micron line from the ionized medium at $z>$7, and the CO rotational line ladder from the molecular medium at lower redshifts. The survey will constrain the redshift evolution of line luminosity functions of star-forming galaxies and their potential environmental dependency, the clustering of star-forming galaxies across cosmic history, and the topology of cosmic reionization by measuring the clustering of the sources of hydrogen-ionizing photons. These key constraints on cosmic evolution will critically complement in-depth studies of distant galaxies with ALMA and JWST by the mid to late 2020s, sitting at the interface to studies of the neutral intergalactic medium in the redshifted HI 21 cm line with facilities like HERA and the SKA (see CCAT-prime Collaboration 2022 for additional details).

References:

CCAT-prime Collaboration 2022, ApJS, in review (arXiv:2107.10364)

Molecular Gas Excitation of CRLE and HZ10 at z=5.7

DANIEL VIEIRA[1,2], DOMINIK A. RIECHERS[1], RICCARDO PAVESI[2], ANDREAS L. FAISST[3], EVA SCHINNERER[4], NICHOLAS Z. SCOVILLE[3], GORDON J. STACEY[2]

[1] Universität zu Köln, vieira@ph1.uni-koeln.de
[2] Cornell University
[3] California Institute of Technology
[4] Max Planck Institute for Astronomy, Heidelberg

We report some of the currently most detailed constraints on the gas excitation that sets the conditions for star formation in a galaxy protocluster environment at $z > 5$. We observe CO(5→4) and CO(6→5) lines in the dusty starbursting galaxy CRLE ($z = 5.667$) and the main-sequence (MS) galaxy HZ10 ($z = 5.654$) with the Northern Extended Millimeter Array (NOEMA). CRLE is the most luminous $z > 5$ starburst in the COSMOS field and HZ10 is the most gas-rich "normal" galaxy currently known at $z > 5$. The CO excitation of CRLE appears comparable to other $z > 5$ dusty star-forming galaxies (DSFGs). For HZ10, these line luminosity limits provide the first significant constraints of this kind for a MS galaxy at $z > 5$. We find the upper limit of $L'_{5\to4}/L'_{2\to1}$ in HZ10 could be similar to the average value for MS galaxies around $z \approx 1.5$, suggesting that MS galaxies with comparable gas excitation may already have existed one billion years after the Big Bang. For CRLE we determine the most likely values for the H_2 density, kinetic temperature and dust temperature based on excitation modeling of the CO line ladder. We also derive a total gas mass.

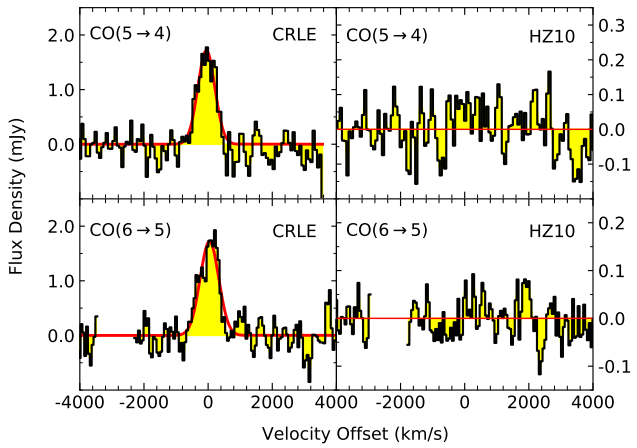

Figure 1: The CO(5→4) and CO(6→5) continuum-subtracted line spectra (histograms). Gaussian fits to the line emission are shown as red curves. Mean redshifts of $z = 5.667$ and $z = 5.654$ were adopted as the velocity reference for CRLE and HZ10, respectively. No continuum was subtracted for HZ10 since none was detected. The spectra were extracted from the peak pixel in the image cube, since the emission remains unresolved in our data.

Missing molecular gas in low-mass star-forming galaxies at cosmic noon*

M. SOLIMANO[1,3], J. GONZÁLEZ-LÓPEZ[2,1], L.F. BARRIENTOS[3] *et al.*

[1] Núcleo de Astronomía de la Facultad de Ingeniería y Ciencias, Universidad Diego Portales, Av. Ejército Libertador 441, Santiago, Chile, manuel.solimano@mail.udp.cl
[2] Las Campanas Observatory, Carnegie Institution of Washington, Casilla 601, La Serena, Chile
[3] Instituto de Astrofísica, Facultad de Física, Pontificia Universidad Católica de Chile, Av. Vicuña Mackenna 4860, 782-0436 Macul, Santiago, Chile

The molecular gas content of galaxies is deeply connected to the rates and timescales of star formation. Understanding this connection is particularly important at $z \sim 2-3$, where the cosmic star formation rate density was at its peak. However, most of what we know about molecular gas in high-z galaxies is limited to the brightest and most massive objects. In order to get a more complete picture, we have conducted a pilot survey of molecular gas in low mass ($M_{\rm stars} < 10^{10}\,{\rm M}_{\odot}$) strongly-lensed galaxies with the Atacama Compact Array. Taking advantage of the flux magnification provided by gravitational lensing, we measured (or put upper limits on) the molecular gas fraction of four "normal" star forming galaxies at $z \sim 2-3$. Using three independent tracers (CO, CI and dust continuum), we find that these galaxies seem to have 0.5-1.0 dex less gas than expected from standard scaling relations, adding evidence to a trend that was already hinted by previous studies. Our results open the possibility of a fundamentally different mode of star formation taking place in these lower mass galaxies, but also stress the need of larger samples and the reduction of systematics in tracer-to-gas mass calibrations.

* Based on work published in Solimano et al. 2021.

References:

Solimano, M., González-López, J., Barrientos, L. F, et al. 2021, A&A, 665, A42

Early Result from CRISTAL ALMA Large Program†: Connecting the interstellar and circumgalactic media of a massive merger when the universe was 1 Gyr old

M. SOLIMANO[1], J. GONZÁLEZ-LÓPEZ[2,1], M. ARAVENA[1] *et al.*

[1] Núcleo de Astronomía de la Facultad de Ingeniería y Ciencias, Universidad Diego Portales, Av. Ejército Libertador 441, Santiago, Chile, manuel.solimano@mail.udp.cl
[2] Las Campanas Observatory, Carnegie Institution of Washington, Casilla 601, La Serena, Chile

We present a study of the connection between the interstellar medium (ISM), as traced by deep, high resolution [C II] observations, and the circumgalactic medium (CGM), as indirectly traced by Lyα, in a massive merger at $z = 4.55$. This is one of the first times where we can connect the transport of gas between ISM and CGM at this redshift. The system is composed by the main sequence galaxy DC842313 (CRISTAL-1) and the extreme dusty star forming galaxy (DSFG) J1000+0234. A kinematical analysis of the [C II] data confirms previous characterization of the DSFG as a very fast rotator ($V_{\rm rot} \approx 500\,{\rm km\,s^{-1}}$), but also reveals a tentative flared disk morphology, giving a first hint of gravitational interaction. Moreover, the exquisite sensitivity of the data unveils a giant tidal tail that extends from CRISTAL-1 and intersects the DSFG in projection, making up one of the clearest views of the early stage of a merger at this redshift. However, despite the high SFR of the DSFG and the inferred gas content in the tidal tail, bright Lyα emission is preferentially seen towards CRISTAL-1. In fact, CRISTAL-1 resides in a $10^{43}\,{\rm erg\,s^{-1}}$ Lyman α blob with a very peculiar triple-peaked spectral profile, which suggests a high escape fraction according to our radiative transfer modeling. Also, we find six additional Lyα emitters (LAEs) in the MUSE FoV within $2\,000\,{\rm km\,s^{-1}}$ of the systemic redshift, confirming the presence of an overdensity. Finally we show that this system is an ideal laboratory for learning about the gas inside and around massive galaxies during their formation: Are the ISM and CGM kinematics coupled? What is the contribution of a DSFG to the properties of a Lyα blob? How is the ISM and/or CGM affected by a surrounding overdensity of LAEs?

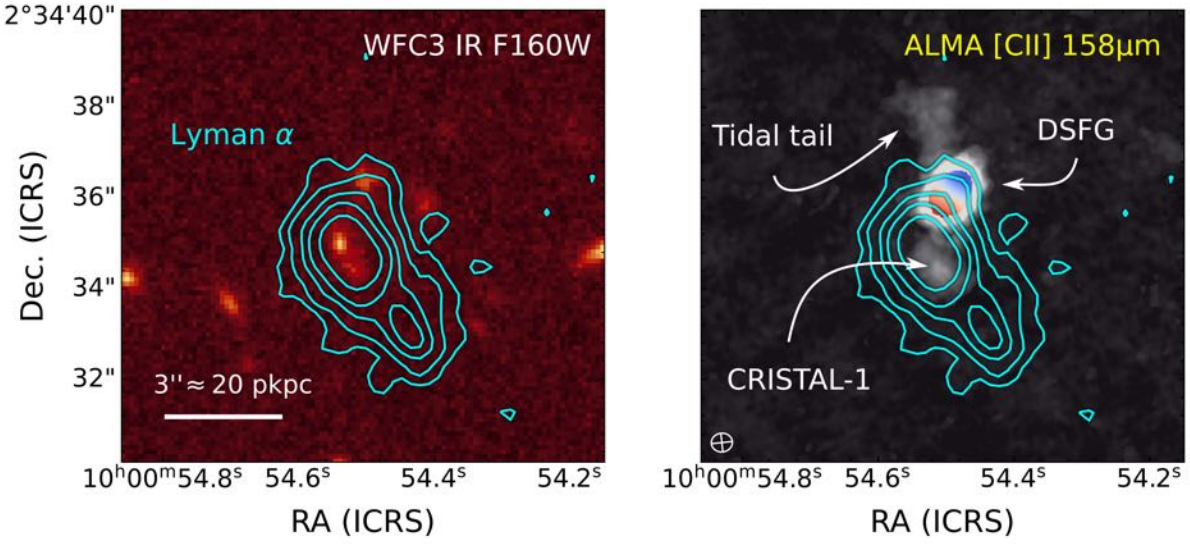

†CRISTAL is a 140h Cycle 8 program and stands for "[CII] Resolved ISM in STar-forming galaxies with ALma" (PIs: Herrera-Camus; R., Aravena M.; De Looze, I.; Förster-Schreiber, N.; González-López, J.; Spilker, J.; Tadaki, K.)

Line intensity mapping the epoch of reionization with FYST

C. KAROUMPIS[1], B. MAGNELLI[2], E.ROMANO-DÍAZ[3], M. HASLBAUER[4], AND F. BERTOLDI[5]

[1,2,3,5] Argelander Institut für Astronomie, Universität Bonn, karoumpis@astro.uni-bonn.de
[2] AIM, CEA, CNRS, Université Paris-Saclay
[4] Helmholtz-Institut für Strahlen- und Kernphysik, University of Bonn
[4] Max-Planck-Institut für Radioastronomie

We present predictions of the three-dimensional intensity power spectrum (PS) of the [CII] $158\ \mu m$ line throughout the epoch of (and post) reionization to examine the detectability of the PS in a line intensity mapping (LIM) survey with the Fred Young Submillimeter Telescope (FYST). To do so, we constructed mock [CII] tomographic scans in redshift bins at z$\approx$ 3.7, 4.3, 5.8, and 7.4 using the Illustris TNG300-1 ΛCDM simulation. Based on the PS of these tomographies, we concluded that the design of the envisioned FYST LIM survey enables a PS measurement not only in small (< 10 Mpc) shot noise-dominated scales, but also in large (> 50 Mpc) clustering-dominated scales. These measurements will make FYST the first LIM experiment that will simultaneously place constraints on (i) the relation between the star formation activity and the [CII] luminosity of galaxies and (ii) the connection between the DM halos mass and the star formation activity of the galaxies they host.

Session II: Star Formation across Scales and Environments

Star Formation across Different Environments

H. W. YORKE

hwy248@gmail.com

From some 100 million years after the Big Bang and continuing through the present, star formation has been a universal phenomenon wherever sufficient gas is present. The environments where star formation has occurred and still occurs has been extremely divergent, covering a wide range. The process of star formation itself and in particular previous star formation is a major contributor to defining the environment via feedback effects. Here, I shall discuss what defines the star forming environment and both how the environment affects star formation and how feedback effects influence the environment. Presumably I will be posing more questions than I answer.

Synergies Between IFU and Molecular Surveys

ALBERTO BOLATTO[1]

[1] University of Maryland, College Park, USA bolatto@umd.edu

The last decade has seen the maturation of optical Integral Field Units (IFUs) capable of obtaining sensitive spectroscopy over significant fields, and their use for large galaxy surveys. Some of the largest and most successful of those surveys have been ATLAS^{3D} (Capellari et al. 2011), SAMI (Croom et al. 2012), CALIFA (Sánchez et al. 2012), and MaNGA (Bundy et al. 2015). These data have help us develop a view of stellar and ionized gas kinematics, abundance and stellar population patterns, and star formation activity in galaxies. In parallel molecular gas observations permitted by sensitive interferometers such as ALMA and single dishes from Apex to the GBT are enabling an extremely complementary view of cold gas in these systems. I will review some of the recent results and emerging patterns resulting from some of these studies (EDGE-CALIFA, Bolatto et al. 2017; ALMaQUEST, Lin et al. 2019; PHANGS-MUSE, Emsellem et al. 2022), including our understanding of the relation between extinction and molecular gas, star formation activity and local galaxy parameters, and the reasons for galaxy quenching. These data are also enabling the first comparisons to large-scale ΛCDM simulations with baryons, an exciting new area of research.

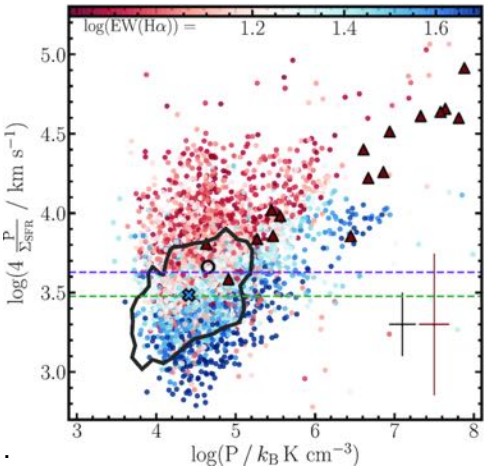

Figure 1: Momentum injection per unit mass of stars formed against interstellar medium pressure, compared with the expectations from theoretical calculations (dashed lines). Pressure is obtained from a combination of H_2 and stellar surface density. Regions with low Hα equivalent widths or extreme starbursts (triangles) are the most discrepant with the expected momentum injection by isolated supernovae. From Barrera-Ballesteros et al. (2021).

.

Figure 2: Combined CO (blue) and Hα IFU information in NGC4303 from PHANGS-MUSE (Emsellem et al. 2022).

References:

Barrera-Ballesteros 2021, MNRAS 503, 3643
Bolatto et al. 2017, ApJ 846, 159
Bundy et al. 2015, ApJ 798, 7
Capellari et al. 2011, MNRAS 413, 813
Croom et al. 2012, MNRAS 421, 872
Emsellem et al. 2022, A&A 659, 191
Lin et al. 2019, ApJ 884, L33
Sánchez et al. 2012, A&A 538, 8

Massive Star Formation: from 1 pc to 1000 AU scales

GUIDO GARAY [1]

[1] Departamento de Astronomia, Universidad de Chile, guido@das.uchile.cl

In this talk I will present the results from observations performed over the last two decades which have permitted to determine the characteristics of all the ingredients involved in the formation process of high-mass stars, from scales of parsecs to scales of 1000 AU. I start the journey presenting the characteristics of the parsec scale maternities (or massive dense cores, MDCs), then get along with the presence of filaments in MDCs, in particular their convergence giving rise to hub-filaments systems in advanced stages of evolution of MDCs. Then proceed with the characteristics of the fragmentation of MDCs in the earliest stages of evolution, leading to the formation of prestellar cores and streamers, and finally talk about the characteristics of HMYSOs and their associated components, such as disks and outflows, at the scales below 1000 AU.

Star Formation in the Magellanic Clouds

M. RUBIO[1]

[1] Departamento de Astronomía, Universidad de Chile, mrubio@das.uchile.cl

The Magellanic clouds (LMC, SMC) are the best local templates for studying the life cycle of the ISM and star formation in low metallicity environments (LMC;Z=0.5 $Z_\odot$ and SMC; Z=0.2 $Z_\odot$). Their proximity (LMC: D = 50 kpc; SMC: D = 60 kpc), provide a unique opportunity to resolve individual clouds, allowing us to conduct detailed studies of the different phases of the ISM in low-metallicity environments using various gas and dust tracers. We will present the latest results obtained at parsec resolution in the study of the physical properties of the dense and cold interstellar medium where star formation takes place, the new generation of stars and its effect of environment in these regions. These studies provide key insights into the star formation process at low metallicities, which is crucial to interpret observations of high-z galaxies.

Star Formation in the Galactic Center

MARK MORRIS[1]

[1]University of California, Los Angeles, morris@astro.ucla.edu

Copious star formation occurs in the dense Central Molecular Zone (CMZ) of our Galaxy, but at a rate that is far less than occurs in a comparable mass of gas in the Galactic disk. The combination of large turbulent velocity dispersions, a relatively strong magnetic field, and a strong tidal field all contribute to inhibiting star formation (SF) in different ways in different CMZ locations. Nonetheless, there are spectacular displays of recent and ongoing SF in the CMZ, including massive young stellar clusters, sites of abundant SF in progress, and numerous spots of protostellar or YSO activity. The discussion of SF in the Galactic center divides naturally into that taking place in the gravitational domain of the Galactic black hole (GBH, i.e., roughly within a parsec) and that taking place in the rest of the CMZ. The very strong tidal forces exerted by the GBH raise the threshold for SF considerably, and it remains debatable whether the evidence shows that SF is occurring at the present time in the central parsec, but the presence of the young nuclear cluster shows that a dramatic SF event occurred 4 or 5 million years ago, probably accompanied by a major episode of accretion onto the GBH. The implications of that event will be discussed. In the CMZ, the presence of giant molecular clouds that are almost entirely devoid of SF indicates that SF requires a trigger that is not present everywhere. The dominant provocation of SF is likely to be cloud compression, either by large-scale shocks or by orbital motion of clouds into a region of enhanced tidal compression and/or enhanced external pressure. The recent hypotheses for where SF takes place in the CMZ will be discussed. They are constrained by the recent orbital determinations of the massive Arches and Quintuplet clusters.

Far-Infrared Imaging Spectroscopy of the Galactic Centre's Circumnuclear Disk

A. BRYANT[1], A. KRABBE[2], C. ISERLOHE[2] AND C.FISCHER[2]

[1] Deutsches SOFIA Institut, Universität Stuttgart, Germany, bryant@irs.uni-stuttgart.de
[2] Deutsches SOFIA Institut, Universität Stuttgart, Germany

The inner few 100 pc of the Milky Way's Galactic Centre serve as a rich laboratory for the study of star formation in extreme environments, and provide the unique opportunity to observe the workings of a galactic nucleus – complete with central supermassive black hole – at high resolution. Among the most pressing questions is how a population of young, massive stars could have formed in the inhospitable surroundings of Sgr A*. Finding a solution to this "paradox of youth" demands a characterisation of the key star formation ingredient, dense molecular gas. The closest molecular reservoir is the Circumnuclear Disk (CND), which appears as a clumpy ring surrounding the star cluster with an inner radius of 1.5 pc. The structure features a number of filaments and streamers, and the physical states of the various ISM phases remain inconclusively characterised. We used the Far Infrared Field-Imaging Line Spectrometer (FIFI-LS) on board the Stratospheric Observatory for Infrared Astronomy (SOFIA) to obtain spatially resolved maps of far-infrared emission lines of the region with an angular resolution approximately 4 times higher than previous published data. Together, these lines span a range of tracers of the atomic, molecular and ionised gas phases, and are used as diagnostics of the physical state of the CND. Armed with this information, we can make inferences on the role of the CND in the formation of a central star cluster.

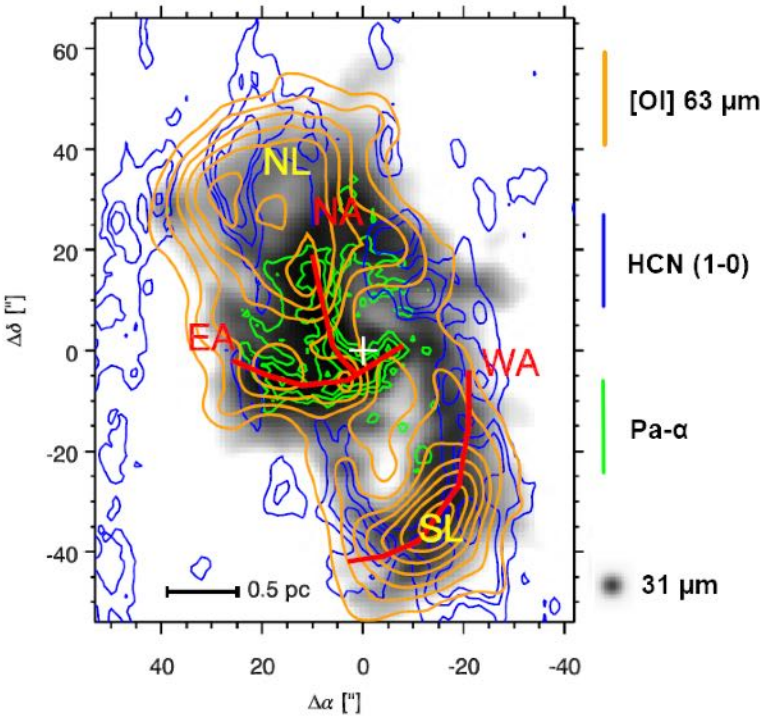

Figure 1: The Circumnuclear Disk and Mini-Spiral as seen in multiple tracers, including FIFI-LS spectral data. From Iserlohe et al. 2019.

References:

Bryant, A., Krabbe, A. 2021, New Astronomy Reviews, vol. 93
Iserlohe, C., Bryant, A., Krabbe, A., et al. 2019, ApJ, 885, 169

Comparing physical properties of two extreme dynamical environments: The centers and outskirts of nearby disk galaxies

C. EIBENSTEINER[1], F. BIGIEL[1], A. BARNES[1],
AND THE PHANGS COLLABORATION

[1] Argelander Institut für Astronomie, Universität Bonn, Auf dem Hügel 71, 53121, Bonn, Germany
eibensteiner@astro.uni-bonn.de

The centers of galaxies are extreme environments, characterized by strong tidal forces, rapid rotational timescales, high gas density and star formation rates. On the other hand, outskirts of spiral galaxies are low in gas densities and star formation rates. The key link connecting these two environments in disk galaxies is dynamics: driving mass flows from the outermost regions, filling their centers with fresh star-forming material.

In my talk, I will present both of these extreme environments. Firstly, I present high resolution 2-4″ (∼75-150 pc) and high sensitivity observations at 2 and 3 mm covering the central 50″ (∼1.9 kpc) of the nearby, gas-rich, very actively star-forming double-barred spiral galaxy NGC 6946 obtained with the IRAM Plateau de Bure Interferometer (Eibensteiner et al. 2022). In this work we studied dynamical features of the inner, small-scale bar of NGC 6946 and its effects on the emission of molecular lines. Together with ancillary data (from 8 additional galaxy centers), we investigate weather the ratio of HCN/HNC is kinetic temperature sensitive and whether the HCN/HCO+ ratio can reflect AGN activity. This first survey paper highlights the diagnostic potential of covering the full 2 and 3 mm bands while pushing to molecular cloud scales in extragalactic environments.
In the second part of my talk, I will present a 10 pointing mosaic VLA observation of neutral atomic hydrogen (HI) towards M83 (Eibensteiner et al. 2022, to be submitted). We analyze the kinematics of the super-extended HI disk (5 times the optical radius) in terms of non-circular motions and line widths. We further investigate outer disk mass flow rates and their role in fueling M83's center with fresh gas.
I will finish the talk by connecting these two environments (centers and outskirts) by presenting work in progress on MeerKat HI observations towards three nearby spiral galaxies together with PHANGS-ALMA CO observations of their centers.

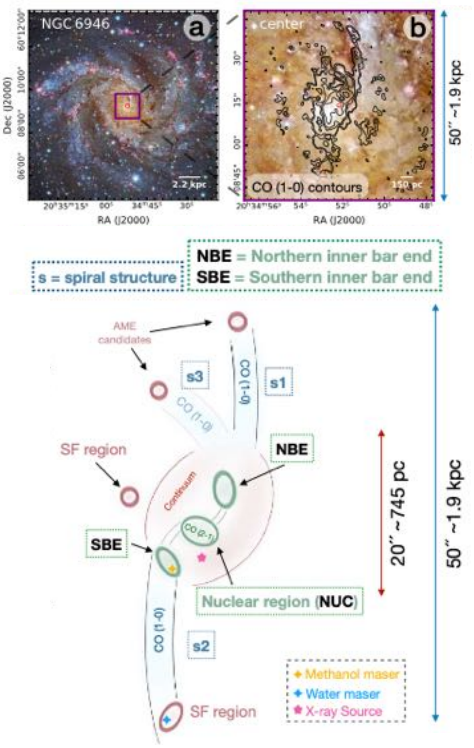

Figure 1: The center of NGC 6946. The sketch shows one of NGC6946's dynamical features: the small scale inner bar (green colors).

References:
Eibensteiner, C., et al. 2022, A&A, Volume 659, id.A173, 37 pp.

Shine a Light: on PDRs and Molecular Clouds at Low Metallicity

SUZANNE C. MADDEN[1] AND THE LMC$^+$ CONSORTIUM

[1] CEA/DSM/IRFU/Departement d'Astrophysique, AIM, CEA, Saclay suzanne.madden@cea.fr

The fundamental processes of star formation in galaxies involve the intricate interplay between the fuelling of star formation via molecular gas and the feedback from recently formed massive stars. This process, by which galaxies evolve, is closely connected to the global and intrinsic ISM properties, such as the structure, density, pressure, metallicity, thermal balance, etc. The necessary fuel to feed star formation is considered to be molecular with CO as our convenient proxy to assess the total molecular gas and thus a calibrator of star formation activity in the local universe as well as at high redshifts. Our unresolved studies of local universe, low metallicity dwarf galaxies, show that the meagre quantity of molecular gas deduced via CO, confronted with the high efficiency with which these galaxies are forming stars, is enigmatic, leaving the conversion of observed CO to total H_2 in low-metallicity galaxies a veritable challenge to ascertain. This complicates our understanding and simulations of molecular clouds to star formation in metal-poor, early-universe galaxies for which our local low-metallicity galaxies may be references. On the other hand, our modelling of unresolved dwarf galaxies demonstrates that the *relatively bright far-infrared [CII] line can be used to quantify the total H_2 reservoir.*

To better understand the effects of local conditions on the H^+-H^0-H_2 and the C^+-C^0-CO transitions in molecular clouds, we have zoomed into our nearest low metallicity galaxy, the Large Magellanic Cloud (LMC), with a SOFIA Legacy Program (LMC$^+$), targeting the southern molecular ridge, with the largest spectral map obtained by SOFIA (45′ x 20′; 660pc x 300 pc) at 2.5pc resolution. This study exploits new observations of [CII]158μm and [OIII]88μm along with a new ALMA CO map covering the same region. The observations will be be confronted with photodissociation region and photoionisation modelling to quantify the fractions of CO-dark gas reservoir compared to the CO-bright gas and the local intrinsic conditions which control these fractions. The LMC$^+$ map shows that the [CII] emission peaks toward the massive star forming regions (N158 N159 N160), while clearly extended throughout the mapped region, in contrast to the CO, most often found in clumps, some of which do not coincide with [CII]. Preliminary analyses show variations of [CII]/CO over several orders of magnitude in just this region. The FIR luminosity, varying over 2 orders of magnitude in this area, is extended, resembling the distribution [CII] more than the CO. The [CII]/FIR varies over a much narrower range than the [CII]/CO: from $\sim$1% at low values of FIR, decreasing to $\sim$ 0.05% at high FIR luminosities. Some questions this project plans to address are: how do the properties and structure of ISM phases vary from the proximity of star- forming sites to the extended, more diffuse, lower visual extinction (Av) phases? What local conditions favor CO-dark vs.CO-bright molecular gas?

These data bring the first extensive study of the heating and cooling variations in low-metallicity star forming and quiescent regions at 2.5 pc scales and by extension will potentially bring new insight on the physical conditions of PDRs/molecular clouds and star formation in early-universe galaxies, where [CII]158μm and [OIII]μm are now observed.

Impact of environments on star formation process: Outer versus Inner Milky Way

SUDESHNA PATRA[1], NEAL EVANS[2], JESSY JOSE[1], KEE-TAE KIM[3], MARK HEYER[4], JENS KAUFFMANN[5], MANASH R. SAMAL[6], SWAGAT DAS[1]

[1] Indian Institute of Science Education and Research (IISER) Tirupati,
inspire.sudeshna@gmail.com
[2] Department of Astronomy The University of Texas at Austin, [3]Korea Astronomy and Space Science Institute, [4]Department of Astronomy University of Massachusetts Amherst, [5]Haystack Observatory MIT, [6]Astronomy & Astrophysics Division, Physical Research Laboratory

Star forming environments within Milky Way change with increasing galactrocentric distance and the role of environments (especially, metallicity) on star formation processes is one of the fundamental differences. The physical and chemical conditions in outer Milky Way are different from those in the inner Galaxy and Solar neighbourhood. The metallicity, gas surface density, and interstellar radiation field are lower in the outer part.

Pioneering studies by Gao & Solomon (2004a,b) showed strong correlation between dense gas tracers and star formation. In order to get the actual mass of dense gas contributing to star formation we need molecular tracers like HCN, $\mathrm{HCO^+}$ which are more sensitive to the volume density.

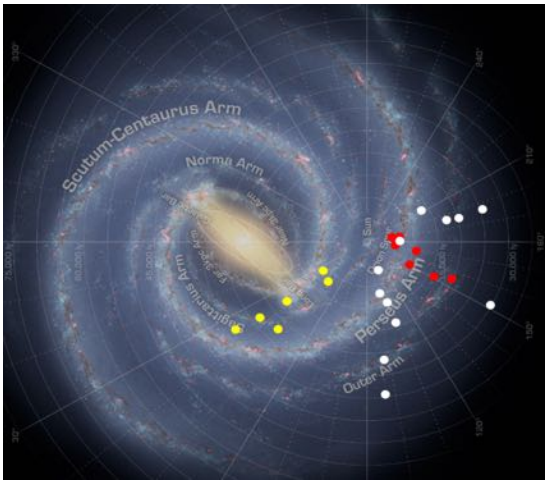

Figure 1: Spatial distribution of 19 outer Milky Way star-forming regions (indicated by red and white points) and 6 inner Galaxy targets (indicated by yellow points) with respect to Sun and Galactic center explored in this study.

We have selected 19 star-forming regions in the outer Milky Way ($\mathrm{R_G} > 9.5$ kpc) to explore the two fundamental questions : **(i) How dense gas tracers depends on environments, especially metallicity ? (ii) Role of metallicity and Galactocentric distance on star formation processes, such as star formation rate (SFR), instantaneous star formation efficiency (SFE) and Initial mass function (IMF).**

These star forming regions are observed using HCN, $\mathrm{HCO^+}$ using 14-m telescope from Taeduk Radio Astronomy Observatory, KASI and complemented with UKIDSS (JHK) data. With this systematic and uniformly sensitive millimeter and IR data sets, we compare the star formation process of the outer Galaxy regions with that of inner Galaxy regions studied by Evans et al. 2020.

References:

Gao, Y., & Solomon, P. M. 2004a, ApJ, 606, 271
Gao, Y., & Solomon, P. M. 2004b, ApJS, 152, 63
Evans, Neal J., I., Kim, K.-T., Wu, J., et al. 2020, ApJ, 894, 103
Patra, S., Evans, Neal J., Kim, K.-T., et al., AJ (under review)

Multi-phase view of the ISM in the Carina Nebula

DAVID REBOLLEDO[1,2], ANNE GREEN[3], MICHAEL BURTON[4], GUIDO GARAY[5]

[1] Joint ALMA Observatory, david.rebolledo@alma.cl, [2] National Radio Astronomy Observatory, [3] University of Sydney, [4] Armagh Observatory, [5] Universidad de Chile

The Carina Nebula Complex is a spectacular star-forming region located at a distance of 2.3 kpc, which is close enough to observe a wide range of size scales in detail. With more than 65 O-stars and more than 900 young stellar objects identified it is also the nearest analogue of more extreme star forming regions, such as 30 Doradus. In this talk I will present the results of a major effort to study the relationship between the different gas phases in the Carina region from 100 pc to 0.01 pc using the Australia Telescope Compact Array, the Mopra telescope and ALMA. At large scales, CO image combined with far-infrared data from Herschel revealed the overall molecular mass and its distribution across the CNC (Rebolledo et al. 2016). An extremely detailed map of the HI 21-cm line across the whole nebula revealed a complex filamentary structure in the atomic gas, which allowed the identification of regions where phase transition between atomic and molecular gas is happening (Rebolledo et al. 2017). Most recently, we have released a 1-3 GHz radio continuum image across the whole Caria region, revealing a complete and espectacular view of the ionized gas in the region (Rebolledo et al. 2021). At small scales, ALMA high spatial resolution observations of molecular line tracers (Figure 1) and dust showed that the level of stellar feedback effectively influences the fragmentation process in clumps, and provides further evidence for a higher level of turbulence in the material with a higher level of massive stellar feedback (Rebolledo et al. 2020).

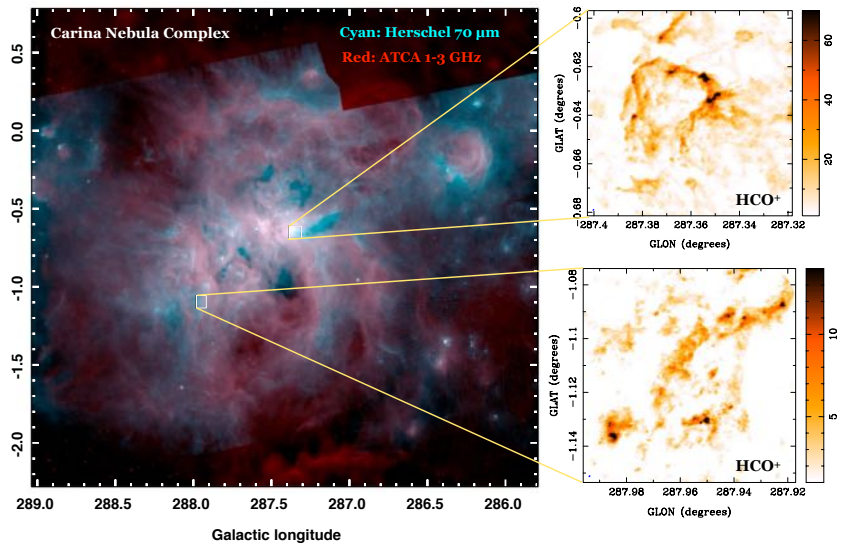

Figure 1: **Left:** Color composite image of the CNC. Cyan shows the Herschel 70 μm, red color shows the ATCA 1-3 GHz continuum map released by Rebolledo et al. (2021). **Right:** Integrated intensity map of the HCO^+ in both regions with different physical properties observed with ALMA (Rebolledo et al. 2020). The maps are in units of K km s^{-1}.

References:

Rebolledo, D., Burton, M. J., Green, A., et al., 2016, MRAS, 446, 2406
Rebolledo, D., Green, A., Burton, M. J., et al., 2017, MRAS, 472, 1685
Rebolledo, D., Guzmán, A. E., Contreras, Y., 2020, et al., ApJ, 891, 113
Rebolledo, D., Green, A., Burton, M. J., et al., 2021, et al., ApJ, 909, 93

The Cycling of Matter from the Interstellar Medium to Stars and back: The CCAT-prime Galactic Ecology project

R. SIMON[1], F. BIGIEL[2], U. U. GRAF[1], Y. OKADA[1], V. OSSENKOPF-OKADA[1], M. RÖLLIG[1], N. SCHNEIDER[1], J. STUTZKI[1], & THE CCAT-PRIME COLLABORATION[3]

[1] I. Physikalisches Institut, Universität zu Köln, simonr@ph1.uni-koeln.de
[2] Argelander-Institut für Astronomie, Universität Bonn
[3] CCAT observatory Inc.

The Fred Young Submillimeter Telescope (FYST) at the CCAT-prime observatory is a novel 6 m aperture telescope enabling highly sensitive wide field observations at submillimeter wavelengths to address science topics ranging from the formation of stars and the evolution of the interstellar medium (ISM) in the Milky Way and nearby galaxies to galaxies in the early universe and cosmology. It will be deployed near the summit of Cerro Chajnantor at 5600 m altitude in the Atacama desert and become operational in early 2024.

This talk will focus on presenting the CCAT-prime Galactic Ecology project (GEco), which is one of the key science projects of the observatory designed to improve our understanding of the matter cycle in the interstellar medium of galaxies from the assembly of clouds to the formation of filaments and cores within them and eventually stars, which in turn provide stellar feedback. The GEco project employs high spectral resolution observations with the CCAT-prime Heterodyne Array Instrument (CHAI), a dual frequency array receiver built at the Universität zu Köln, which will allow for unprecedented large scale surveys of atomic and molecular clouds in the Milky Way (including the Galactic Center), the Magellanic clouds, and other nearby galaxies in key diagnostic spectral lines. CHAI will initially target the CO 4-3 and [CI] 1-0 lines. The second, higher frequency, channel will become available later and cover the CO 7-6 and [CI] 2-1 lines which can be observed in parallel.

Our surveys will yield new insights into the processes of feeding the Milky Way clouds through CO-dark gas, dissipation of turbulence traced in low-velocity shocks, dynamics and feedback in massive star forming regions in the Milky Way and nearby galaxies, and their dependence on environmental conditions including metallicity.

Our observations are not only the much needed complement to existing and ongoing large scale surveys in the FIR (Herschel, SOFIA; continuum, [CII] and [OI] fine structure lines), (sub)mm lines and continuum, and longer wavelength spectral lines of, e.g., the CO molecule, but also invaluable for the interpretation of observations in terms of the underlying physics and microphysics involving modelling. They will thus constitute a data set of high legacy value.

The APEX Magellanic Clouds Legacy Survey

A. WEISS[1], K. GRISHUNIN[1], M. CHEVANCE[2], K. HARRINGTON[3], ET AL.

[1] MPIfR, Bonn, Germany, aweiss@mpifr-bonn.mpg.de
[2] Universität Heidelberg, Germany, [3]ESO Chile

In the local universe, star formation (SF) is exclusively associated with molecular clouds. Understanding the efficiency of this process, the environmental conditions under which SF occurs and the impact of feedback from newly formed massive stars on this process is one of prime goals of current astronomical research. Observations resolving the molecular gas distribution in different environments in nearby galaxies typically reach ∼50-100 pc even with ALMA (e.g. the PHANGS survey, Sun et al. 2020). Star forming filaments and clumps identified in MW surveys as the nursery for SF happens at much smaller scales (e.g. Lada 1987, Padoan et al. 2020). The proximity of LMC and SMC offers the unique opportunity to bridge nearby galaxy and MW studies, by allowing to observe the molecular gas distribution and kinematics at an, for extra-galactic studies, unprecedented spatial resolution of 5 pc even with APEX.

In this talk we will present the first results from our ongoing APEX Large Program to image both Magellanic Clouds in the CO(3–2) emission line using the LASMA 7 pixel array receiver. Our project is designed such that it will improve over the currently best available CO survey in the LMC by a factor of 8 in sensitivity (5σ cloud mass limit ≈300M$_\odot$), 6 in terms of spatial resolution and a factor of 4 in areal coverage. Observations started in 2019 and the survey is half completed by now (see Fig. 1). Together with an general overview on the survey, we will present an analysis of the cloud properties and their relation to SF. We will also discuss how feedback from the R136 cluster affects the molecular cloud properties in the vicinity of the Tarantula Nebula.

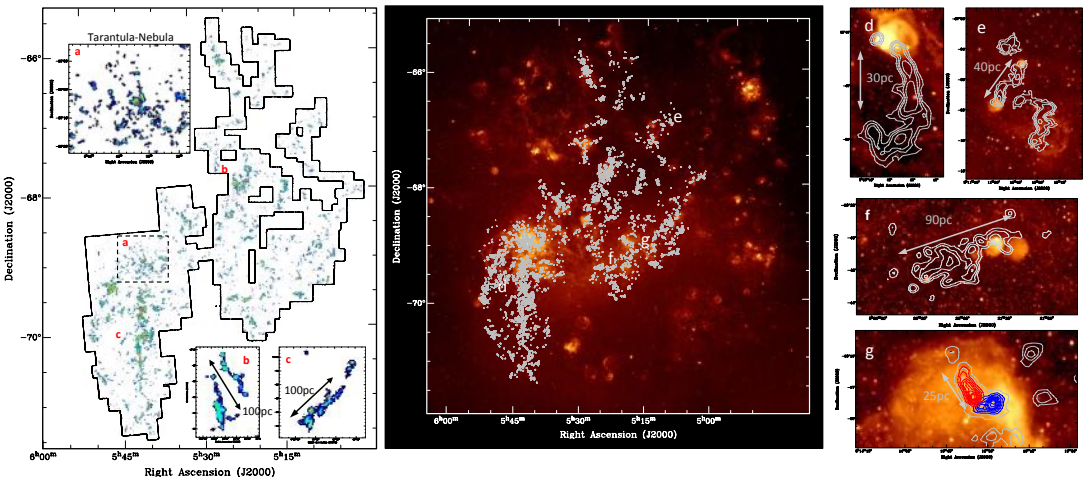

Figure 1: Left: Moment zero map of the CO(3-2) emission in the LMC observed so far with zooms on the 30Dor region and selected filaments. Center: contours of the CO moment zero maps overlayed on H$_\alpha$. Right: Zooms on SF filaments (H$_\alpha$, CO contours). The bottom panel shows an example of an outflow or colliding flows detected in CO on H$_\alpha$.

References:

Lada 1987, IAUS, 115, 1; Padoan et al. 2020, ApJ 900, 82; Sun et al. 2020, ApJ 901, 8

Milky Way Clouds as Templates for Clouds in External Galaxies

A. BEMIS, A. R.[1], B. WILSON, C. D.[2]

[1] Leiden Observatory, Niels Bohrweg 2, 2333 CA Leiden, The Netherlands
bemis@strw.leidenuniv.nl
[2] McMaster University, 1280 Main Street West, Hamilton, Ontario, Canada

Relative to nearby galaxies, Milky Way clouds provide our highest-resolution view of molecular cloud structure, and this structure holds important information on the physics of the interstellar medium (ISM). Recent results of the Herschel Gould Belt Survey (HGBS) and Herschel imaging survey of OB Young Stellar objects (HOBYS) provide H2 column density maps of a sample of Milky Way clouds that can be decomposed and analyzed to compare with current models of ISM physics. In nearby galaxies, we must employ more complex methods to derive information on the underlying structure of clouds, which involves studying molecular transitions with sensitivities to various gas densities. This project synthesizes the results of HGBS and HOBYS with molecular line observations to derive the emissivity of these transitions in individual clouds/clumps. We model the emissivity of these transitions using decomposed column density maps and RADEX to test the applicability of this method to nearby galaxies. This project makes use of data of multiple-J transitions of CO, HCN, and HCO+ from the JCMT and Nobeyama 45m telescopes. We plan to extend this to archival ALMA data that contain continuum observations of dust and molecular line emission.

Classification of ionized nebulae in the PHANGS-MUSE sample: a Bayesian approach

E. CONGIU[1], G. BLANC[1,2], AND THE PHANGS TEAM

[1] Departamento de Astronomía, Universidad de Chile, Santiago, Chile, econgiu@das.uchile.cl
[2] Observatories of the Carnegie Institution for Science, Pasadena, CA 911P1, USA

The PHANGS-MUSE survey offers us an unprecedented view of the ionized interstellar medium of nearby star-forming galaxies (Emsellem et al. 2022). The high spatial resolution ($\sim$50 pc) allows us to identify and isolate single emitting clouds, while the broad spectral range offered by MUSE@VLT gives us the opportunity to study their properties in detail. However, to study nebulae and their role in galaxy evolution, their correct classification (e.g., in HII regions, planetary nebulae, supernova remnants/shock ionized regions) is critical. To solve this problem, many classification schemes have been developed in the literature in the last few decades (e.g., Ciardullo et al. 2002, Blair et al. 1997). Several problems still exist: 1) most of them focus on a single class of nebulae, 2) there is significant overlap between some of them, so they do not provide unique classifications, and 3) they typically have been developed using only limited amounts of physical information. In this talk, I will present the results of a new algorithm I developed that aims to reliably and objectively classify nebulae taking advantage of the wealth of information provided by the PHANGS-MUSE data. It exploits the Bayesian odds ratio principle to return a classification based on the comparison between the regions' properties and models representing the different classes of nebulae. This algorithm is applied to the $\sim$40000 nebulae identified across the 19 PHANGS-MUSE galaxies, the most extensive catalog of classified ionized nebulae in nearby galaxies compiled so far.

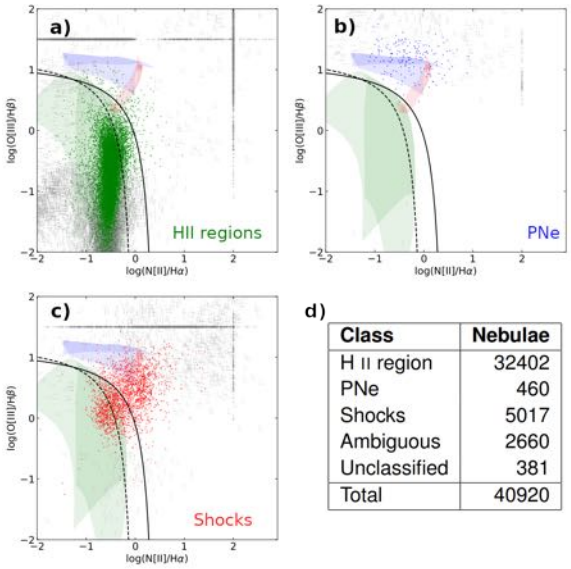

d)

Class	Nebulae
H II region	32402
PNe	460
Shocks	5017
Ambiguous	2660
Unclassified	381
Total	40920

Figure 1: *Panel a), b) and c):* Plots showing how the different classified nebulae are positioned in the diagnostic diagrams from Baldwin et al. 1981. Shaded areas represent the models used for the classification. Solid black lines are the relation from Kewley et al. 2001 while the dashed black lines are from Kauffmann et al. 2003. Colored regions have well measured lines, while grey points have at least one line flux which is an upper limit. *Panel d)* Table showing how the nebulae in our catalog are distributed across the different classes. For *unclassified* nebulae the classification algorithm did not converge, while for *ambiguous* nebulae no model has a probability larger than the threshold used for the classification.

References:

Emsellem, E., Schinnerer, E., Santoro, F. et al. 2022, A&A, 659, 191
Ciardullo, R., Feldmeier, J. J., Jacoby, G. H. et al. 2002, ApJ, 577, 31
Blair, W. P., Long, K. S. 1997, ApJS, 108, 261
Baldwin, J. A., Phillips, M. M., Terlevich, R. 1981, PASP, 93, 5

The bulk molecular medium across local galaxies
New insights from comprehensive multi-CO line mapping campaigns

JAKOB DEN BROK[1]

[1] AIfA, Universität Bonn, Auf dem Hügel 71, 53121 Bonn, Germany, jdenbrok@uni-bonn.des

A robust knowledge of the distribution, amount, and physical/chemical state of the cold molecular (H_2) gas is key to understanding galaxy evolution. With the help of multi-CO line observations, it is possible to study the molecular gas distribution and disentangle numerous physical and chemical processes that shape and govern the molecular ISM. In my talk, I will present the key findings from two recent papers (den Brok et al. 2021, 2022) focusing on the IRAM 30-m large program CLAWS as well as additional large program (EMPIRE) and ALMA data. My presentation will include a discourse on:

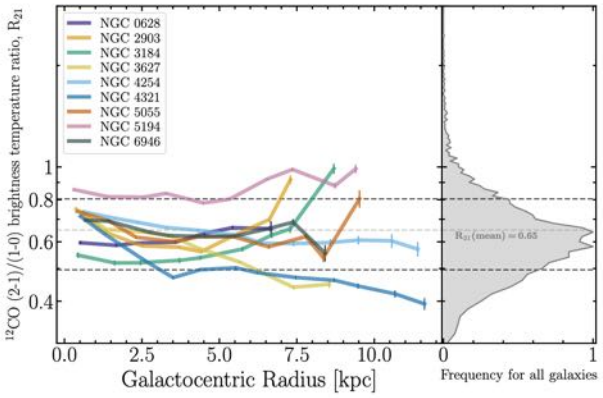

Figure 1: Lines show the radial R_{21} trend of individual galaxies. Histogram shows the sample-wide R_{21} distribution. Figure from den Brok et al., (2021).

(i) Benchmarking the CO(2-1)/(1-0) (R_{21}) line ratio across nearby galaxies: We provide a comprehensive and systematic characterization of the global R_{21} value in nearby spiral galaxies and investigate the drivers of variations with other galactic properties. We find significant galaxy-to-galaxy offsets (see Fig. 1), which to some extent can be explained due to systematic uncertainties of the telescope itself (e.g., flux calibration). I will motivate that care needs to be taken regarding observational uncertainties when carrying out such an analysis. After accounting for these uncertainties, we find substantial variation within the individual galaxies, including differences inside and outside of the galactic centers and between the arm and interarm regions. We trace these changes back to the impact of physical drivers (e.g., diffuse gas fraction or increase of turbulence). In particular, we find that the star formation rate density seems to be well correlated with changes in the R_{21} value, and hence can potentially be used as a proxy when estimating variation in the line ratio.

(ii) Exploring CO isotopologue line ratio trends across M51 from our IRAM 30m large program CLAWS: For the first time, we obtain resolved mapping data of faint CO isotopologues (^{13}CO, C^{18}O, C^{17}O) at 1mm and 3mm wavelengths across the disk of M51. With the help of such CO isotopologues, it is possible to better constrain the physical and chemical conditions of the bulk molecular gas. I will present results from my first paper on this survey, where we study potential explanations for changes in CO isotopologue emission such as indications for CO abundance variations due to selective nucleosynthesis and changes in the optical depth. Based on our analysis, we conclude that variation in opacity is the dominant driver for the observed CO line ratio trends on large (kpc) scales, while CO abundance variations seem to only play a minor role. I will conclude with an outlook on additional ongoing work with these surveys and show some of my work in progress.

References:

den Brok, J. S., Chatzigiannakis, D., Bigiel, F., et al. 2021, MNRAS, 504, 3221
den Brok, J. S., Bigiel, F., Sliwa, K., et al. 2022, arXiv e-prints, arXiv:2201.05165

Revealing the cold ISM properties at 150pc in a strongly lensed UV-bright star-forming galaxy at Cosmic Noon

J. González-López[1,2], M. Solimano[2], and M. Aravena[2]

[1] Las Campanas Observatory, Carnegie Institution of Washington, Casilla 601, La Serena, Chile, jgonzalez@carnegiescience.edu

[2] Núcleo de Astronomía de la Facultad de Ingeniería y Ciencias, Universidad Diego Portales, Av. Ejército Libertador 441, Santiago, Chile

Strong gravitational lensing has become a prime tool for resolving the star-forming interstellar medium of high redshift galaxies down to sub-kpc scales. While the first ALMA studies focused on intrinsically luminous lensed targets, recent work has pioneered the study of star formation and molecular gas in fainter, lower mass and lower metallicity galaxies, which are more representative of the global population at z∼2.

Here we present the findings of high resolution imaging of CO emission observations of SGASJ0033, a UV-bright strongly lensed, but otherwise typical, main sequence galaxy at z=2.4. The magnification corrected properties of SGASJ0033 make it more representative of the general SFG population at $z \approx 2$ than the massive and/or starbursty systems targeted in previous work.

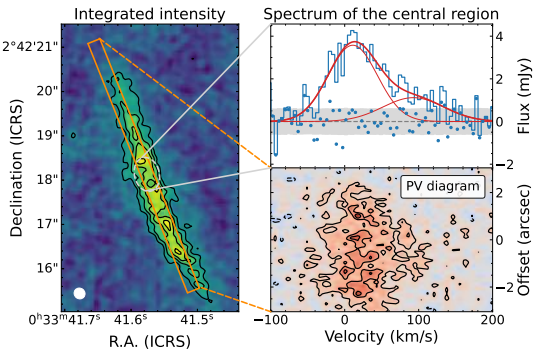

Figure 1: *Left:* Velocity-integrated intensity map of the CO(4-3) line. *Top right:* CO(4-3) spectrum extracted from the central region of the arc, the line profile exhibits a broad high-velocity component. *Bottom right:* Position-velocity diagram extracted from the orange pseudo-slit in the left panel. The presence of various local peaks suggests a clumpy ISM.

Our 0.2" beam CO map reveals a well resolved and extended molecular gas component with clear indications of being clumpy both spatially and kinematically (Fig. 1). When compared to PSF-match restframe UV continuum and Hα, from HST and SINFONI respectively, we find that the CO emission is more compact in the center than the SFR tracers, indicating a radial change in star-formation efficiency. In fact, our resolved SFR surface density and molecular gas surface density put the resolved regions of SGASJ0033 closer to the locus of starbursts galaxies, with depletion times ranging between 20-100 Myr. Without gas replenishment, the galaxy will cease forming stars just because of the extreme current rates. Additionally, HST and SINFONI observations also reveal ionized gas outflows arising from an active nucleus. The CO spectrum from the same region shows a higher velocity component consistent with a molecular gas outflow.

Our multi-phase gas observations show that the star-formation activity in a normal main-sequence galaxy can be very extreme when looked at sub-kpc scales. In this case, both star-formation activity and AGN feedback will regulate SFR at different spatial scales and all this information is lost in low spatial resolution observations. SGASJ0033 serves as a example of how "normal" can have a different meaning when galaxies are studied in detail and how gravitational lensing is key in revealing the processes of galaxies.

GMC Analyses on FIRE-2 Mergers

HAO HE[1], CHRISTINE WILSON[1], CONNOR BOTTRELL[2] AND JORGE MORENO[3].

[1] McMaster University, heh15@mcmaster.ca
[2] University of Tokyo
[3] Pomona College

In this talk, I will present new results using FIRE-2 simulations to study giant molecular cloud (GMC) properties in galaxy mergers. Due to the rarity of mergers in the local universe, we do not have large samples of mergers that are close enough to study individual GMC properties. The FIRE-2 merger simulations provide us with a new window to study how GMCs evolve during a merging event. In this study, we conduct a pixel-by-pixel analysis on the molecular gas properties in both undisturbed control galaxies and mergers in the simulation. In the velocity dispersion σ_v versus gas surface density $\Sigma_{\rm mol}$ diagram, the data points from FIRE-2 galaxies follow a similar trend as that seen in observations of PHANGS normal spiral galaxies. However, the GMCs of FIRE-2 galaxies sits at the lower surface density/velocity dispersion end compared to PHANGS galaxies, with a maximum $\Sigma_{\rm mol}$ barely reaching 100 $M_\odot$ pc^{-2}. Instead, the data points from the simulated galaxies lie closer to the green-valley galaxies, such as M31. We suspect the low $\Sigma_{\rm mol}$ might be caused by the low gas mass fraction due to the choice of simulation initial conditions. For the simulated mergers, we find $\Sigma_{\rm mol}$ is still low compared to several observed mergers. On the other hand, the gas in simulated mergers has high σ_v that is comparable to the observed mergers. We calculate the virial parameters $\alpha_{\rm vir}$ of GMCs in the simulated mergers and the $\alpha_{\rm vir}$ in simulation are much higher than that of normal spiral galaxies both in observations and simulations. This is consistent with our expectation that feedback from starburst activities will disperse the surrounding GMCs and make clouds less bound.

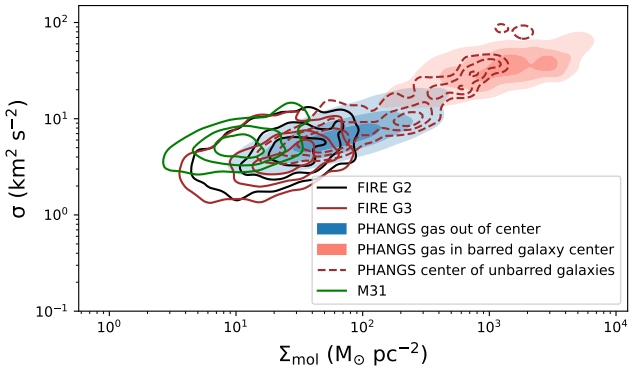

Figure 1: *σ_v vs $\Sigma_{\rm mol}$ for isolated G2 (black solid line) and G3 (brown solid line) galaxies compared to PHANGS galaxy sample (Sun et al. 2020) and M 31 (Sun et al. 2018).*

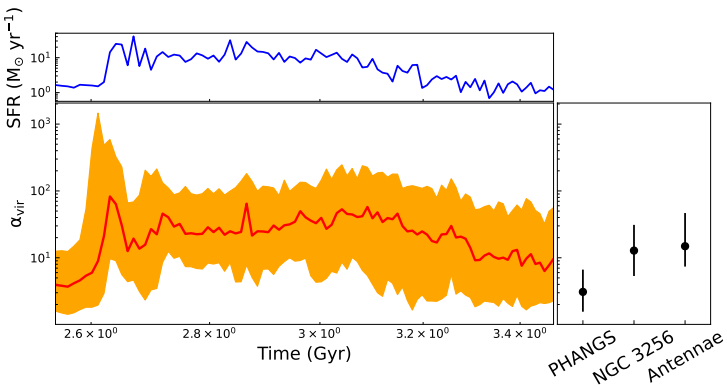

Figure 2: *The variation of viral parameter $\alpha_{\rm vir}$ during the final coalesce for G2&G3 mergers with e2 orbit. The red line is the mass weighted median for the $\alpha_{\rm vir}$ in simulation. The orange shaded region includes data within 16th and 84th quantile of $\alpha_{\rm vir}$ values. The right box show the observed $\alpha_{\rm vir}$ range for PHANGS, NGC 3256 and Antennae galaxies.*

Sun, J., Leroy, A. K., Schruba, A. 2018, AJ, 860, 172
Sun, J., Leroy, A. K., B., Schinnerer, E., et al. 2020, ApJL, 901, L8

Star formation in the Magellanic Clouds: Across metallicities and environments

VENU M. KALARI[1]

[1] Gemini Observatory/NSF's NOIRLab, Casilla 603, La Serena, Chile venu.kalari@noirlab.edu

Star formation processes vary by metallicity– quantifying these effects may significantly impact our current view of star formation and galaxy evolution in the early Universe. However, it has been challenging to observationally quantify any differences between star formation properties as a function of metallicity. In this talk, I present a combination of radio (ALMA/APEX), adaptive-optic and speckle infrared, and optical ground-based imaging and spectroscopy of star forming regions in the Magellanic Clouds, ranging from metallicities of 1/2-1/10 solar. From such multi-wavelength observations pushing observational frontiers in a diverse range of environments, one can being building a picture of how star formation properties vary across a variety of scales.

References:

Kalari V. M. et al. 2022, *Sharpest optical imaging of the R136 star cluster*, ApJ subm.
Kalari V. M. et al. 2020, *Resolved star formation in the metal-poor star-forming region Magellanic Bridge C*, MNRAS, 499, 2534
Kalari V. M. et al. 2018, *Pillars of Creation among Destruction: Star Formation in Molecular Clouds near R136 in 30 Doradus*, ApJ, 857, 132
Kalari V. M. et al. 2018, *The Magellanic Bridge Cluster NGC 796: Deep Optical AO Imaging Reveals the Stellar Content and Initial Mass Function of a Massive Open Cluster*, ApJ, 852, 71

The GMC-scale distributions of the molecular gas density and kinetic temperature in the central region of the AGN-starburst hybrid galaxy NGC 613

H. KANEKO[1,2], T. TOSAKI[1], K. TANAKA[3] AND Y. MIYAMOTO[4]

[1] Joetsu University of Education, hkaneko@juen.ac.jp
[2] National Astronomical Observatory of Japan
[3] Keio University
[4] Fukui University of Technology

We present position-position-velocity cubes of the physical and chemical properties of the molecular medium in the central region of the active galaxy NGC 613 at a resolution of 0.″8 ($\sim$ 68 pc) and a velocity resolution of 10 km s^{-1}. In constructing cubes of the gas kinetic temperature, molecular hydrogen volume density, and fractional abundances of four molecules (C^{18}O, HCN, HCO^{+}, and CS), eight molecular lines and a method based on hierarchical Bayesian (HB) inference were used. The derived mean volume densities $n_{\rm H_2}$, kinetic temperatures $T_{\rm kin}$, and gas surface densities $\Sigma_{\rm H_2}$ (converted from the column densities) ranged $10^{3.21-3.85}$ cm^{-3} and $10^{2.34-2.64}$ K, and $10^{1.01-2.28}$ $M_\odot$ pc^{-2}, respectively.

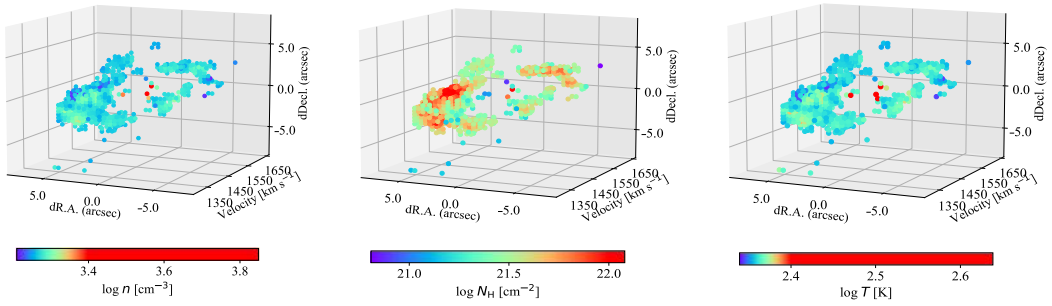

Figure 1: Position-position-velocity views of the volume density, number density, and gas kinematic temperature of the central region of NGC 613.

The correlation between $\Sigma_{\rm H_2}$ and the star formation rate (SFR) $\Sigma_{\rm SFR}$ shows two distinct sequences. The molecular clouds in the southwest region of the star-forming ring exhibited a $\sim$ 0.5 dex higher $\Sigma_{\rm SFR}$ than those of the eastern region, which follow the Kennicutt–Schmidt law. We examined the origin of the higher SFR and the star formation efficiencies (SFE: $\Sigma_{\rm SFR}/\Sigma_{\rm H_2}$) in the southwestern clouds. The clouds in the southwestern and other regions exhibited no systematic difference in the mean volume densities, which are often invoked as drivers of SFE variation. We suggest that the availability (or deficiency) of molecular gas in the southwestern region, where no significant gas supply is evident along the offset ridges in the bar, is responsible for the higher SFE.

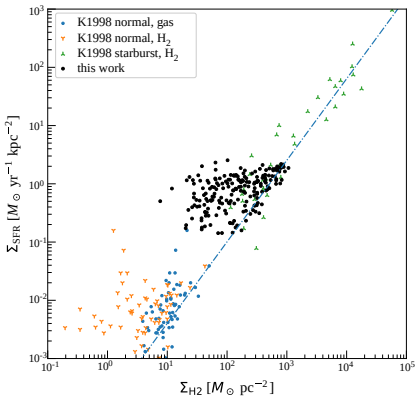

Figure 2: The correlation between $\Sigma_{\rm H_2}$ and $\Sigma_{\rm SFR}$ in comparison with the galactic-scale correlation shown in Kennicutt (1998).

Observations of the Magellanic Corona and the LMC's Feedback Driven Wind

D. KRISHNARAO[1,2,†]

[1] Colorado College, [2] Johns Hopkins University, [†] NSF Astronomy & Astrophysics Postdoctoral Fellow, dkrishnarao@coloradocollege.edu

Recent measurements of a relatively high mass for the LMC imply the LMC should host a massive Magellanic Corona, a collisionally ionized, warm-hot gaseous halo at the virial temperature ($\sim\ 10^{5.4}K$) initially extending out to the virial radius (100 - 130 kpc). Such a Magellanic Corona would have shaped and fed the formation of the Magellanic Stream (e.g. Lucchini et al. 2020). Here we show direct observational evidence for this Magellanic Corona via highly ionized oxygen (O VI), and indirect detections via C IV and Si IV, seen in UV absorption toward background quasars using data from *HST* and *FUSE* (Krishnarao et al. 2022; in review) We find that the Magellanic Corona is part of a pervasive multiphase Magellanic CGM seen in many ionization states with a declining projected radial profile out to at least 35 kpc from the LMC and a total ionized CGM mass of $\log(M/M_{\odot})\ 9.1 \pm 0.2$. The evidence for the Magellanic Corona is a crucial step forward in characterizing the Magellanic Group and its nested evolution with the Local Group and helps diagnose the impact of galactic scale winds emerging from star formation feedback in the LMC. In our upcoming work from an accepted HST Legacy Archival Program (PI: Kat Barger), we will directly measure and map this galactic scale outflow and the Magellanic Corona using hundreds of sightlines towards stars in the LMC from the ULYSSES program (Roman-Duval et al. 2020). We will conduct the highest resolution survey of any galactic wind to date, allowing us to measure star formation feedback effects on the CGM, (e.g. 30 Doradus starburst region), which will provide insight as to how stellar feedback affects galaxies when it cannot be resolved.

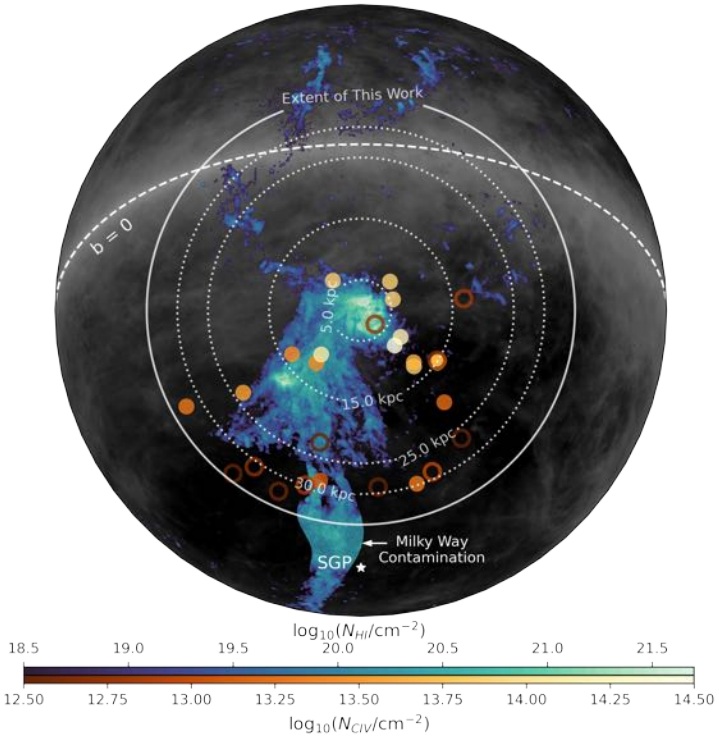

Figure 1: Map centered on the LMC showing Magellanic 21-cm H I emission in blue-scale and circles showing C IV column densities measured with *HST*. open circles show upper limits and dotted circles mark LMC impact parameter.

References:

Lucchini, S., D'Onghia, E., Fox, A. J., et al. 2020. Nature, 585, 203–206
Krishnarao, D., Fox, A. J., D'Onghia, E., et al. 2022, Nature, in review post referee
Barger, K., ... Krishnarao, d., et al. 2021, HST Proposal. Cycle 29, ID. 16602
Roman-Duval, J., et al. 2020, RNAAS, 4, 11

Star formation in galactic bar environments – a poorly understood process

J. NEUMANN[1], D. A. GADOTTI[2], A. FRASER-MCKELVIE[3], CARS AND MANGA TEAM

[1] Institute of Cosmology and Gravitation, U. of Portsmouth, justus.neumann@port.ac.uk
[2] Durham University
[3] ICRAR, The University of Western Australia

About half of all nearby barred galaxies show signatures of ongoing star formation along the bar, while the other half presents itself with a curious absence of star formation. Despite the presence of cold molecular gas observed as radial flows along the edge of the bar towards the galaxy centre, the local environment seems to be able to suppress star formation. Simulations indicate that a combination of shear and turbulence within the fast-flowing gas might be responsible. However, it is not clear how star-forming bars fit into this picture and how the dynamical state of the bar is related to other properties of the host galaxy.

In this talk I present some results from our works using integral-field spectroscopic data from MUSE and from the MaNGA survey to investigate the distribution of star formation in barred galaxies and how it relates to properties of the host. In addition, I will review some recent efforts to characterise the star formation efficiency in bars highlighting the power of combined molecular-IFU surveys that will eventually help us to determine the main mechanism that regulates star formation in bar environments.

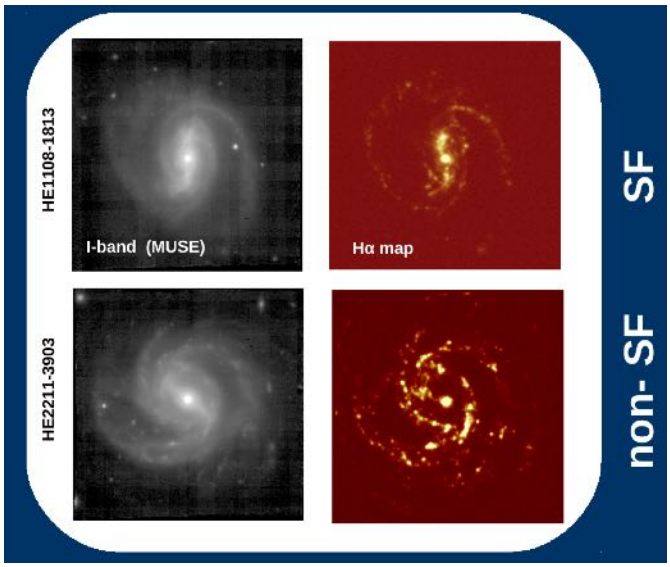

Figure 1: Example of a star-forming (SF) and a non-star-forming (non-SF) bar from Neumann et al. (2019). The left column shows collapsed i-band images from MUSE observations, while Hα maps are presented in the right column. Both galaxies actively form stars along the spiral arms and in the centre, but only HE 1108-1813 also forms stars along the bar.

References:
Neumann, J., Gadotti, D. A., Wisotzki, L., et al. 2019, A&A, 627, A26

Spatially resolved star formation rates of 10,010 galaxies from stellar population analysis

J. NEUMANN[1], D. THOMAS[1], C. MARASTON[1] AND MANGA TEAM

[1] Institute of Cosmology and Gravitation, U. of Portsmouth, justus.neumann@port.ac.uk

Star formation activity is one of the main characteristics to trace galaxy evolution on large scales and to learn about the physical processes of star formation on small scales. A big pool of diagnostic methods across the electromagnetic spectrum from ultraviolet to far-infrared to trace recent star formation has been established over the years (e.g. Kennicutt 1998; Kennicutt & Evans 2012). A complete stellar population analysis through full spectral fitting with model spectra offers probably the most direct probe of recent star formation by delivering a full decomposition of stellar ages. In this approach, star formation rates (SFRs) are obtained by integrating the masses of young stellar populations within a given age interval, depending on the adopted definition of *current* star formation.

In this talk, I will present spatially resolved SFRs of 10,010 galaxies from our recently published MaNGA FIREFLY Value-Added-Catalogue (VAC) of stellar populations in the MaNGA survey using integral-field spectroscopic data. Using the SFRs from the VAC allows us to self-consistently compare them to other local properties such as stellar surface mass density, metallicity of the youngest stars or dust attenuation. In addition, by inspecting the full star formation history, we are also able to explore how star formation varies across a wide range of spatial and temporal scales.

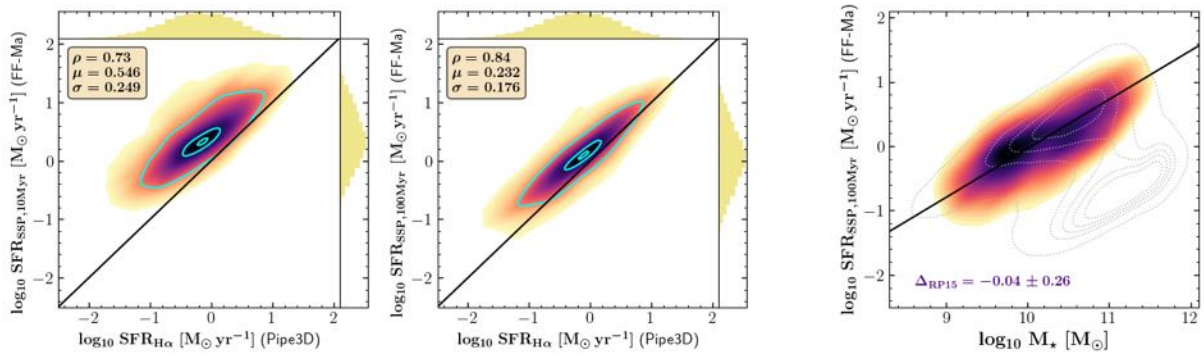

Figure 1: Left and middle panel: Comparison between SFRs obtained by integrating the star formation history over the last 10 and 100 Myr, respectively, with SFRs from Hα measurements. Right panel: SFR-M$\star$ relation for star-forming galaxies in our sample overplotted with grey contours indicating the distribution of SDSS galaxies. The black solid line marks the star formation main sequence as determined in Renzini & Peng (2015). Figure adopted from Neumann et al. (2022).

References:

Kennicutt, Jr., R. C. 1998, ARA&A, 36, 189
Kennicutt, R. C., & Evans, N. J. 2012, ARA&A, 50, 531
Neumann, J., Thomas, D., Maraston, C., et al. 2022, MNRAS, in press, arXiv:2202.04082
Renzini A., Peng Y.-j., 2015, ApJ, 801, L29

Self-contained modeling of CO isotopologues in M51 – an application of the Dense Gas Toolbox to CLAWS

J. PUSCHNIG[1], J. DEN BROK[1], F. BIGIEL[1] & THE CLAWS TEAM

[1] Argelander-Institute for Astronomy, University of Bonn, Germany
johannes.puschnig@uni-bonn.de

Gas density is a key parameter regulating the collapse of molecular clouds (Jeans 1902, McKee & Ostriker 2007). Thus it plays an important role in theories of star formation and is closely connected to galaxy evolution. However, from an observational point of view, gas density is not directly accessible, but must be constrained from e.g. multi-transition observations of rotational lines, taking advantage of the fact that each transitions traces only a certain range of conditions (temperature, density). The caveat is that most molecular lines that are easily accessible in extragalactic observations (e.g. ^{12}CO) are optically thick and the optical depth is typically unknown. This introduces large uncertainties in the derivation of the density from multi-line spectroscopy.

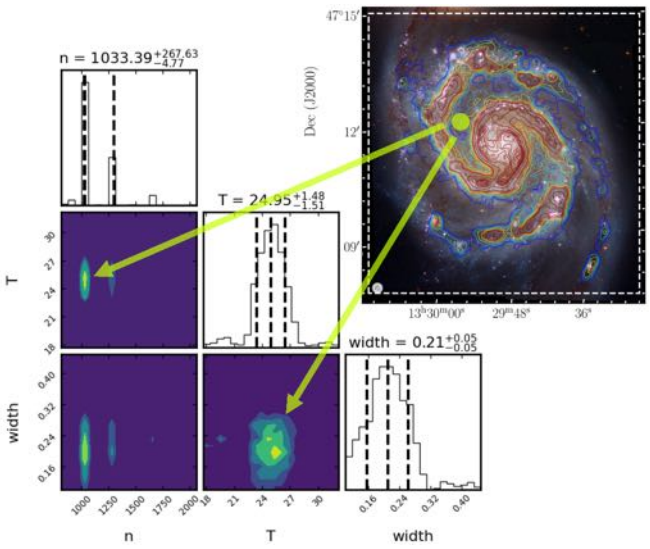

Figure 1: Breaking the n-T degeneracy via application of the `Dense Gas Toolbox` (Puschnig et al. in prep) on CO multi-line spectroscopy of the CLAWS survey (den Brok et al. 2022).

To overcome this issue, we take advantage of the *CO isotopologue Line Atlas within the Whirpool galaxy Survey* (CLAWS; den Brok et al. 2022), a deep survey in M51 (Whirlpool galaxy) targeting ^{12}CO up to the J=3–2 transition as well as the faint and optically thin isotopologues ^{13}CO, C^{18}O and C^{17}O up to the J=2–1 level. That way, the derivation of density and temperature through radiative transfer models now becomes more robust and reliable, as the models can be applied to a self-contained system of CO molecules.

In order to solve the problem, we apply a novel radiative transfer code – `The Dense Gas Toolbox` (DGT; Puschnig et al. in prep; Leroy et al. 2017). The models assume that the molecular emission lines emerge from a log-normal density distribution rather than from a single density. Using Bayesian statistics, i.e. Markov chain Monte Carlo (MCMC), the mass-weighted mean density, as well as temperature and width of the distribution could be inferred.

We will present the most reliable constraints on density variations across the M51 galaxy disk to date. A preliminary result for a single region in the galaxy is presented in the figure above. The data and model successfully break the degeneracy between density and temperature.

References:

Jeans, J. H., 1902, Phil. Trans. of the Royal Society of London, Series A, 199, 1
McKee, C. F. & Ostriker, E. C., 2007, ARA&A, 45, 565
den Brok, J. S. & Bigiel, F. & Sliwa, K. et al. 2022, arXiv e-prints, arXiv:2201.05165
Leroy, A. K. & Usero, A. & Schruba, A. et al. 2017, ApJ, 835, 217L

Optical emission-line diagnostics of the simulated interstellar medium in different environments

T.-E. RATHJEN[1], S. WALCH[1], T. NAAB[2] AND SILCC PROJECT[3] ET AL.

[1] I. Physikalisches Institut, Universität zu Köln, Zülpicher Str. 77, 50937 Köln, Germany, rathjen@ph1.uni-koeln.de
[2] Max Planck Institute for Astrophysics, Karl-Schwarzschild-Str. 1, 85748 Garching, Germany
[3] https://hera.ph1.uni-koeln.de/~silcc/

We present the first results from applying optical emission-line diagnostics via post-processing to high-resolution MHD simulations of the multi-phase ISM with a range of initial gas surface densities, Σ, from 10 to 100 $M_\odot$ pc^{-2}.
Our simulations are part of the SILCC simulation framework and incorporate all major thermal and non-thermal stellar feedback mechanisms necessary to model a self-consistent ISM. We follow the evolution of massive stars with a sub-grid sink particle approach and account for stellar winds, ionising UV radiation via radiative transfer, radiation pressure on dust with FUV heating in thermal equilibrium, Type II supernovae and cosmic ray acceleration.

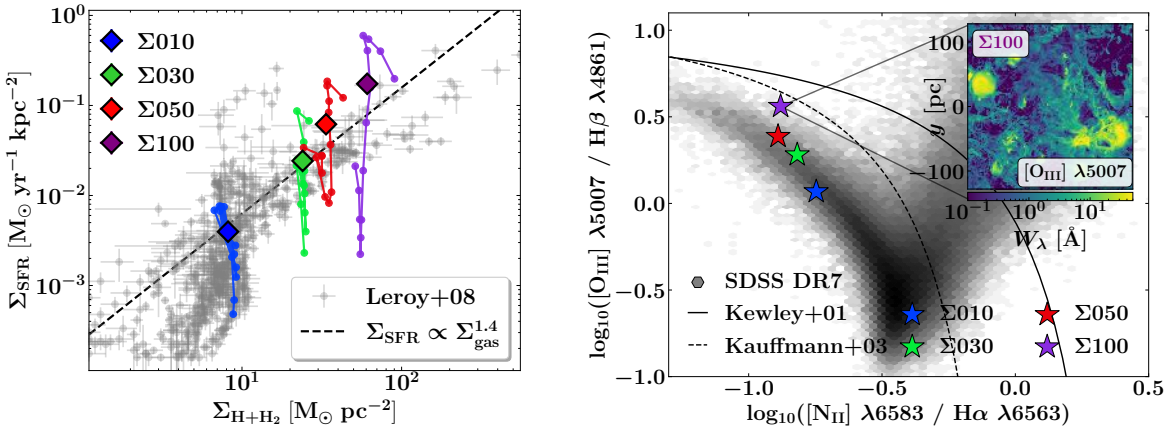

Figure 1: **Left:** Kennicutt-Schmidt relation for ISM simulations with increasing initial gas surface densities. The data points are averaged over 10 Myr bins. Solid diamonds indicate global averages. **Right:** BPT diagram of ISM simulations in different environments. The inset shows the [O$_{III}$] emission map for the model with the highest gas surface density $\Sigma 100$. Galaxy observations are shown in grey.

We couple the simulations to the photo-ionisation code CLOUDY and predict the optical line emission originating from each simulation cell based on its gas temperature, gas density, radiation energy density and spectral shape of the ionising source. Afterwards, we integrate the emission along the line of sight while accounting for attenuation by dust. We can predict the impact of observables like metallicity, temperature and ionisation parameters on emission line scaling relations. We analyse the emission sources and find that in high surface density environments up to 30% of the total emission originates from shock excited and diffuse ionised gas instead of HII regions, leading to a shift in the BPT diagram away from the star-forming sequence.

Probing the ionized gas in the core and outburst of the nearby starburst galaxy M82 with FIFI-LS/SOFIA

C. FISCHER[1], W. VACCA[2], C. ISERLOHE[1], S. LATZKO[1] AND A. KRABBE[1]

[1] Deutsches SOFIA Institut, University of Stuttgart, fischer@dsi.uni-stuttgart.de
[2] USRA - SOFIA

Over the last couple of years the core and outflows of the nearby starburst Galaxy M82 has been mapped in [OIII] 52μm with FIFI-LS on SOFIA. We re-reduced the data with newly available water vapor values for telluric correction and used dynamic properties from the high S/N PACS [OIII] data to optimize the line fitting of the FIFI-LS data. We combine the data with [OIII] 88μm from PACS/Herschel to derive the electron density and investigate the structure of the ionized gas in the core and the outflow. We can then compare this to the structure of e.g. the atomic gas from literature and see if and how it supports the cloudlet model for the outflows.

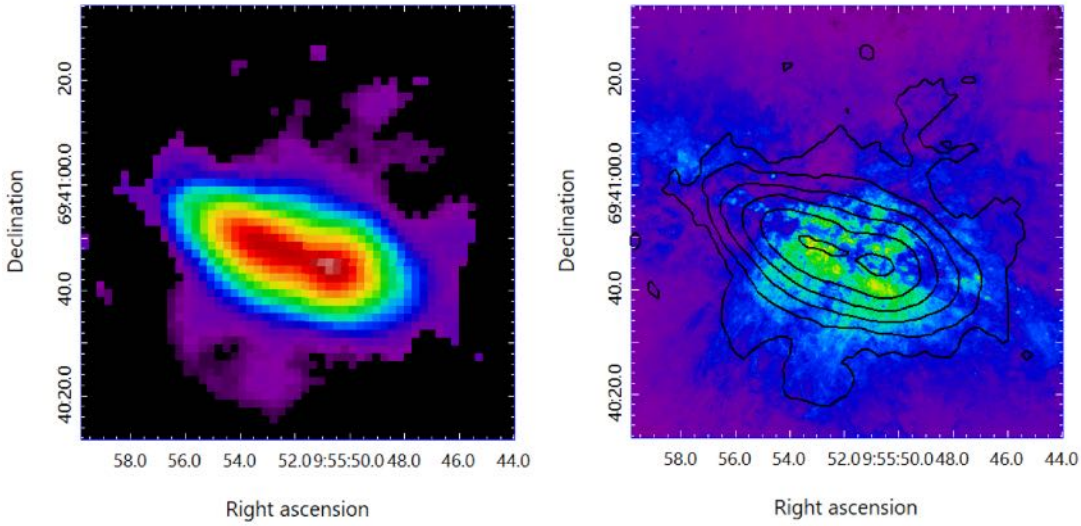

Figure 1: left: the integrated line flux for the [OIII] 52μm line from the FIFI-LS measurements; right: contours from the [OIII] 52μm line flux over a Hubble Halpha image

Infrared view of the multiphase ISM in NGC 253

A. BECK[1], C. FISCHER[1], C. ISERLOHE[1], M. KAŹMIERCZAK-BARTHEL[1], A. KRABBE[1], S. T. LATZKO[1], V. LEBOUTEILLER[2], S. C. MADDEN[2], J. P. PÉREZ-BEAUPUITS[3,4], AND L. RAMAMBASON[2]

[1] Deutsches SOFIA Institut, University of Stuttgart, abeck@dsi.uni-stuttgart.de
[2] Laboratoire AIM, CEA/Service d'Astrophysique
[3] Max-Planck-Institut für Radioastronomie
[4] Centro de Astro-Ingeniería, Pontificia Universidad Católica de Chile

NGC 253 is the closest ($3.5\,\mathrm{Mpc}$) starburst galaxy and thus an ideal laboratory to study the various mechanisms of heating and cooling of the interstellar medium (ISM). The impacts of an active galactic nucleus (AGN) or a nuclear starburst on the surrounding environment in general, but also in NGC 253 in particular are not completely understood. Fine-structure lines in the mid-infrared and far-infrared spectral range, which are often only mildly affected by extinction and self-absorption, are perfect to study the ISM in very dusty sources such as starburst-galaxies.
In this study we present a combined data set from SOFIA (Fig. 1), *Spitzer*, and *Herschel* observations of the nuclear region in NGC 253. We use the line flux ratios [OIII]$52/88\,\mu$m, [NII]$122/205\,\mu$m, and [SIII]$19/33\,\mu$m to determine the local electron density. The line ratios are insenstive to the temperature, but depend strongly on the electron density. Further, we use ([NeII]$13\,\mu\mathrm{m}$ + [NeIII]$16\,\mu$m) / Hu α line flux ratio to calculate the Ne/H abundance ratio (Fig. 2), which serves as a measure for the metallicity in the nuclear region of NGC 253 (Beck et al. 2022). We also will show preliminary results from our ongoing, more sophisticated modelling approach with `MULTIGRIS` (Lebouteiller & Ramambason 2022, Ramambason et al. 2022).

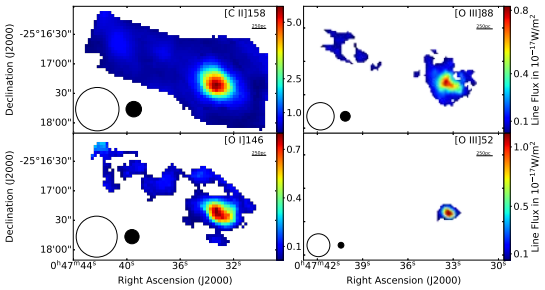

Figure 1: Line flux maps for the four different emission lines observed with SOFIA/FIFI-LS. Bottom left of each plot shows the extraction aperture used to extract the line flux from the nucleus. Filled circle show the PSF size at the observed wavelength.

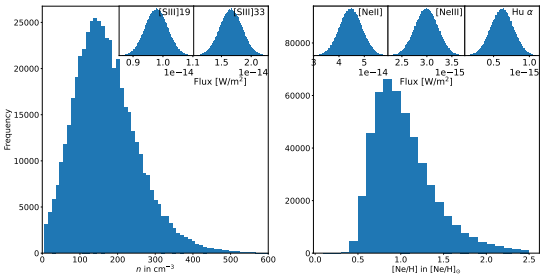

Figure 2: Results from the Monte-Carlo simulation to determine the density (from the [SIII]$19/33\,\mu$m line flux ratio) and subsequent the metallicity (using the ([NeII]$13\,\mu\mathrm{m}$ + [NeIII]$16\,\mu$m) / Hu α ratio).

References:
Beck, A., Lebouteiller, V., Madden, S. C., et al. 2022, A&A, accepted
Lebouteiller, V. & Ramambason, L. 2022, A&A, accepted
Ramambason, L., Lebouteiller, V., Bik, A., et al. 2022, A&A, accepted

Session IIIa: The ISM and Molecular Clouds: feedback, quenching, triggering, turbulence

Stellar feedback from sub-parsec to galactic scales

S. WALCH[1]

[1] I. Physics Institute, University of Cologne, Germany, walch@ph1.uni-koeln.de

Throughout their life, stars are sources of radiation, momentum and kinetic energy. The so-called stellar feedback includes not only radiation and radiation pressure, but also stellar jets, outflows, winds, and supernovae, where the latter two processes are only relevant for massive stars ($M_\star > 8\ \mathrm{M}_\odot$). The mass, energy and momentum delivered to the surrounding interstellar medium (ISM) via stellar feedback is believed to strongly influence the evolution of star-forming molecular clouds, locally quenching star formation as the cold and dense molecular gas is heated and dispersed. I will review our current understanding on the relative impact of these different feedback processes on the dynamics and multi-phase structure of the interstellar medium in star-forming galaxies.

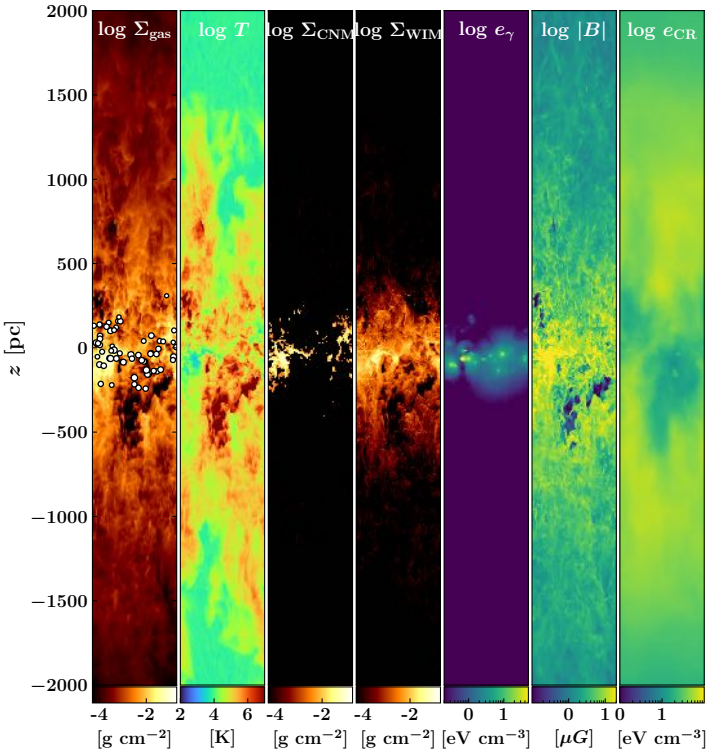

Figure 1: Overview of a stratified disk ISM simulation with initial gas surface density of 100 $\mathrm{M}_\odot\,\mathrm{pc}^{-2}$. The simulation includes all major thermal- and non-thermal stellar feedback processes, i.e. early feedback in the form of HII regions created by ionising radiation as well as stellar winds, core-collapse supernovae (SN) explosions at the end of the lifetime of each massive star and the acceleration of cosmic rays in SN remnants. We show the simulation viewed edge-on, at 50 Myr after the onset of star formation. The columns are (from left to right): the total gas column density, $\Sigma_{\rm gas}$, mass-weighted temperature projection, T, the column densities of the cold neutral medium (CNM) and the warm ionised medium (WIM), the energy density of the ionising radiation, e_γ, the mass-weighted magnetic field, $|B|$, and the energy density of cosmic rays, $e_{\rm cr}$. White circles in the first column depict stellar clusters (realised with a sub-grid sink particle approach). From the intricate and highly non-linear combination of stellar feedback channels a multi-phase ISM emerges. A mass-loaded galactic wind is launched by the interplay of a volume-filling hot gas created from overlapping SN remnants and an additional long-lived cosmic ray pressure gradient.

References:

Rathjen, T., Naab, T., Girichidis, P., Walch, S., et al. 2021, MNRAS, 504, 10
Walch, S., Girichidis, P., Naab, T., et al. 2015, MNRAS, 454, 23

Intermittency of turbulent dissipation: chemical, radiative and statistical signatures

E. FALGARONE[1], P. LESAFFRE[1], T. RICHARD[1], P. HILY-BLANT[2], B. GODARD[3,1], A. LEHMANN[1], A. VIDAL-GARCIA[1] AND G. PINEAU DES FORÊTS[3,4]

[1] Ecole Normale Supérieure, edith.falgarone@ens.fr,
[2] Université Grenoble Alpes, [3] Observatoire de Paris, [4] Université Paris-Saclay

Turbulent dissipation is a central issue in the star and galaxy formation process. Its fundamental property of space-time intermittency, well characterised in incompressible laboratory experiments, remains elusive for cosmic turbulence which is multi-phase, compressible, magnetised, and coupled to gravity. Progress in our understanding of cosmic turbulence intermittency requires the combination of state-of-art observations, modelling and numerical simulations.
Magneto-hydrodynamical (MHD) simulations dedicated to turbulent dissipation in a non-ideal fluid showed that dissipation is concentrated in fractal structures of intense velocity shear, current and ion-neutral drift [1]. Similar structures are now found in simulations of compressible magnetised turbulence. Most (but not all) can be classified as shocks, current sheets or rotational discontinuities [2]. The observable chemical signatures of shocks are computed self-consistently [3] but a direct comparison with observations is still in its infancy.

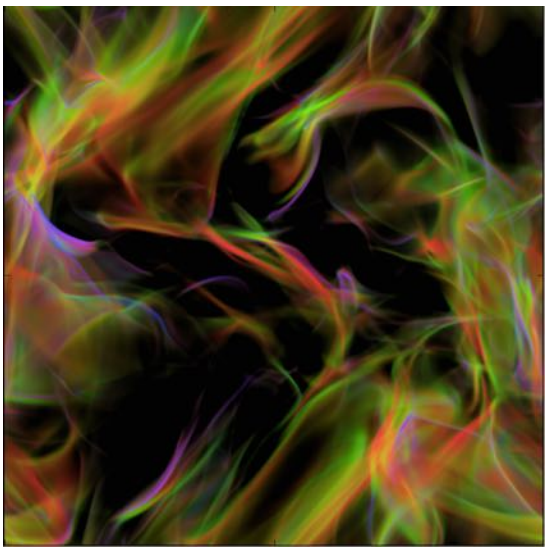

Figure 1: *Extrema of dissipation in numerical simulations of MHD turbulence [1] due to compressible viscosity (blue), solenoidal viscosity (green) and ohmic resistivity (red).*

In a highly turbulent diffuse molecular cloud, a statistical analysis of the spatial velocity increments of the CO(2-1) line, singled out the positions of extreme velocity shears. They outline a parsec-scale elongated structure [4], bright in CO line emission, but almost undetected in the dust continuum. High-angular resolution observations unveil similarly elongated structures embedded within the parsec-scale large velocity shear. Not only the orientation of these structures is preserved over three-orders of magnitude in scales, but also the magnitude of the velocity differences, providing quantitative constraints to numerical simulations.
Finally, the highly concentrated heating associated to intermittent turbulence dissipation opens chemical routes at the origin of specific molecular tracers accessible to observations in the local and high-redshift universe [6,7,8,9]. The route is far from being paved but these recent results unveil a possible role of intermittent turbulent dissipation in seeding the growth of molecular cloud structures.

References:
1 Momferratos, G. et al. 2014 MNRAS 443, 86, **2** Richard T. et al. 2022 A&A in press, **3** Lesaffre P. et al. 2020 MNRAS 495, 816, **4** Hily-Blant P. et al. 2008 A&A 481, 367, **5** Hily-Blant P. et al. 2022 A&A in prep., **6** Godard B. et al. 2019 A&A 622, 100, **7** Lehmann A. et al. 2022 A&A 658, 165, **8** Falgarone et al. 2017 Nature 548, 430, **9** Vidal-Garcia A. et al. MNRAS 2021 506, 255

Observational signatures of stellar feedback

N. SCHNEIDER[1], S. KABANOVIC[1] AND THE FEEDBACK CONSORTIUM[2]

[1] I. Physik. Institut, University of Cologne, kabanovic@ph1.uni-koeln.de

Massive stars play a key role in the evolution of the interstellar medium (ISM) in galaxies because they impact the ISM through ionization, stellar winds, and supernova explosions. This stellar feedback regulates the physical conditions of the ISM, sets its emission characteristics, and ultimately governs the star formation activity.
The gas is heated by UV radiation and cools via far-infrared cooling lines, in particular the [CII] 158 μm line and the [OI] 63 μm line. Spectrally resolved observations of these lines are extremely valuable not only to characterize the gas density and temperature of the photodissociation region, but also for tracing the dynamics of the gas.
The SOFIA legacy project FEEDBACK (Schneider et al. 2020) performed extended maps in these lines in 11 Galactic massive star-forming regions. I will present on behalf of the FEEDBACK consortium the first results of this program: we discovered in all FEEDBACK sources expanding bubbles seen in the [CII] line (Lusisi et al. 2021, Tiwari et al. 2021, Beuther et al. 2022), driven by stellar winds, that trigger further star formation; we detected large amounts of cold [CII] that is associated with atomic hydrogen (Kabanovic et al. 2022), and we observed dynamic signatures of molecular cloud assembly (Schneider et al. 2022).
I will also give an outlook how we will quantify the relationship between star formation activity and energy injection and the negative and positive feedback processes involved, and how to link that to other measures of activity on scales of individual massive stars, of small stellar groups, and of star clusters.

References:
Beuther, H., et al., 2022, A&A, 659, 77
Kabanovic S., et al., 2022, A&A, 659, 36
Luisi M., et al., 2021, Science Advances, 9 Apr 2021, Vol. 7
Schneider, N., et al., 2020, PASP, PASP, 132, 104301
Tiwari, M., et al., 2021, ApJ, 914, 117

Clump-to-cores fragmentation in the Galactic context: present status and preliminary indications from the ALMAGAL "statistical" survey.

S. MOLINARI[1], P. SCHILKE[2], C. BATTERSBY[3], P.T.P. HO[4], A. SANCHEZ-MONGE[2], M.T. BELTRAN[5], H. BEUTHER[6], G. FULLER[7], R. KLESSEN[8], Y.-W TANG[4], S. WALCH[2], Q. ZHANG[9] AND THE ALMAGAL TEAM

[1] Istituto Nazionale di Astrofisica-IAPS Rome (I)sergio.molinari@inaf.it
[2] Universtität zu Köln (D)
[3] University of Connecticut (USA)
[4] Academia Sinica (TW)
[5] Istituto Nazionale di Astrofisica-OAA Arcetri (I)
[6] MPIA Heidelberg (D)
[7] University of Manchester (UK)
[8] ITA-ZAH Universität Heidelberg (D)
[9] Harvard-CfA (USA)

A large fraction of stars form in clusters containing high-mass stars, which affect the local and galaxy-wide environment. Yet fundamental questions about the physics responsible for fragmenting molecular Clumps into Cores are still open. What are the physical processes governing the fragmentation of cluster forming clumps, and how do they evolve with time? How do high-mass cluster-forming cores gain mass? How is this influenced by internal feedback from cores into clump gas?
After reviewing from an evolutionary and Galactic context viewpoint the present status from the ALMA data published so far, we will present the first indications emerging from the ALMAGAL "statistical" survey of more than 1000 dense ($S \geq 0.1$ g cm^{-2}) and massive (M$\geq$500 M$_{\odot}$) parsec-scale clumps resolved at a minimum linear scale of 1000AU, sampling the full evolutionary path from IRDCs to UCHII regions from the tip of the Galactic Bar to the Solar circle and beyond.

Star formation triggered by cloud-cloud collisions

YASUO FUKUI[1]

[1] Univ Nagoya, fukui@a.phys.nagoya-u.ac.jp

Formation of high mass stars and massive clusters has been an issue of keen interest. Recent observations and theoretical studies provided growing evidence for collisions between clouds as a key mechanism to trigger the formation of massive objects at various scales ranging from a single O star to massive clusters having $10^6\,\mathrm{M_O}$. In this talk I will summarize these works on the Galaxy, the Magellanic system, and the Antennae galaxies, and will discuss the future prospects of the relevant research.

ONC formed via Violent Relaxation.

ANDREA BONILLA-BARROSO[1], JAVIER BALLESTEROS-PAREDES[1]

[1]Instituto de Radioastronomía y Astrofísica, UNAM, campus Morelia. PO Box 3-72. 58090. Morelia, Michoacán, México, a.bonilla@irya.unam.mx

There are currently two models for the formation and evolution of molecular clouds: the gravo-turbulent and global, hierarchical and chaotic collapse model. In order to discern between these scenarios we analyzed the velocity dispersion of stars in simulations of stellar clusters formed in molecular clouds undergoing a global collapse and stellar clusters inside molecular clouds dominated by turbulence.
We found that if the cloud is collapsing then its stars exhibit a constant velocity dispersion as a function of mass, as predicted by Lynden-Bell. Instead in the turbulent scenario, massive stars exhibit a larger velocity dispersion than low-mass stars.
We also used data from Gaia EDR3 to analyze the stars in the Orion Nebula Cluster and show that the stars in the ONC have a constant velocity dispersion. This suggests that the cloud that gave origin to the ONC should have been in global, hierarchical and chaotic collapse rather than being supported by turbulence against collapse over many high-density free-fall times.

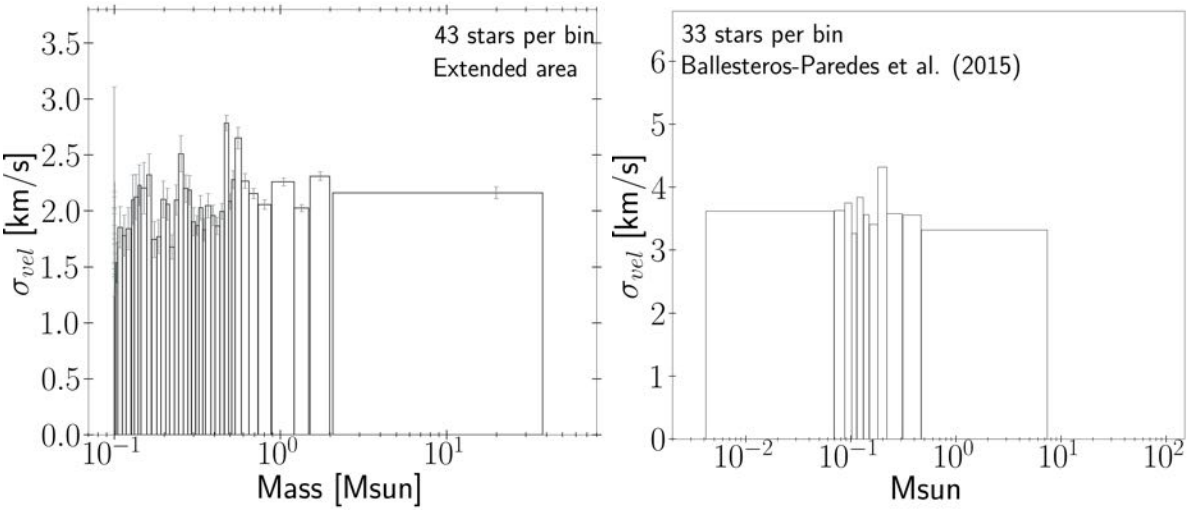

Figure 1: Left panel: Velocity dispersion per mass bin for sinks in runs of global hierarchical and chaotic collapse. Stars show a fairly flat velocity dispersion as a function of the mass. Right panel: Velocity dispersion per mass bin for stars of the ONC. It can be seen that the velocity dispersion per mass bin remains nearly constant suggesting that the ONC has been suffering global collapse.

References:

Lynden-Bell D., 1967, MNRAS , 136, 101
Bonilla-Barroso, A., Ballesteros-Paredes, J., Hernández, J., et al. 2022, MNRAS, 511, 4801

Can the migration scenario be at the origin of massive close binaries?

E. BORDIER[1,2], A. FROST[2], H. SANA[2], W.-J. DE WIT[1]

[1] European Southern Observatory (ESO), Alonso de Cordova 3107, Vitacura, Santiago, Chile, emma.bordier@eso.org
[2] Institute of Astronomy, KU Leuven, Celestijnenlaan 200D, B-3001 Leuven, Belgium

The formation of high-mass stars has seen some significant progress over the past years. Still, being deeply embedded in their natal envelope, a definitive observational sequence for their formation is lacking, unlike their low-mass counterparts. Most main sequence (MS) massive stars (70%) belong to short-period binaries, a fact that does not reflect the binary parameters measured among populations of newly born massive stars.

To bridge the gap between these two regimes, we need to obtain strong constraints on the origin of the pairing mechanism and the orbital properties at birth. Migration has been proposed as a formation scenario in which massive binaries formed at large separations would harden on a time-scale of 2 Myr.

Being one of the youngest clusters in our Galaxy, M17 is an unprecedented laboratory where pre-main sequence binaries can be caught. In my talk, I will describe how optical interferometry (e.g. GRAVITY) is the best opportunity to characterise massive stellar systems just after they have reached the MS and probe the starting point of massive stellar evolution. From the interferometric model fitting of visibility amplitudes and closure phases, I will present statistics on young high-mass multiplicity tracing 1-100mas in M17, including multiplicity and companion fraction (MF and CF). These results will be compared to other studies involving different stellar populations and covering different mass regimes. Finally, I will discuss the connection with the current star formation theories and relate with the migration scenario.

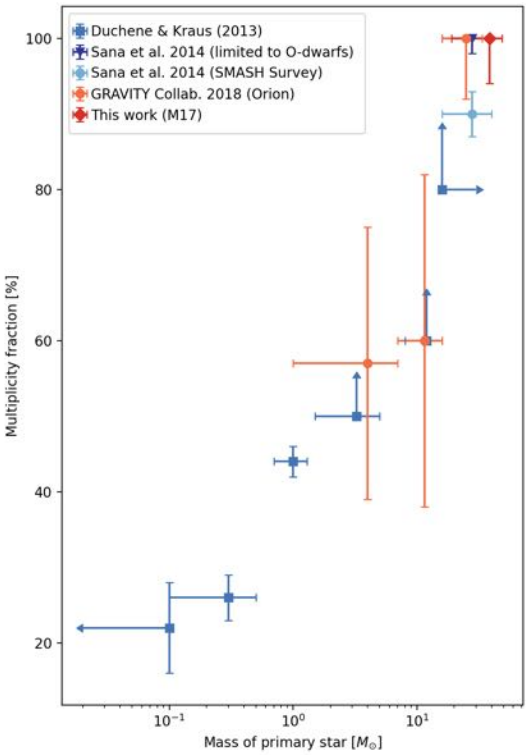

Figure 1: MF of stars in various systems as a function of the primary mass. (*Source: Bordier+2022*)

References:

Bordier, E., Frost, A. J., et al. (2022) arXiv, arXiv:2203.05036 - 2022arXiv220305036B
Ramírez-Tannus, M. C., Backs, F., et al. (2021) A&A, 645, L10 - 2021A&A...645L..10R
Oliva, G. A., & Kuiper, R. (2020) A&A, 644, A41 - 2020A&A...644A..41O
Ramírez-Tannus, M. C., Kaper, L., et al. (2017) A&A, 604, A78 - 2017A&A...604A..78R
Sana, H., Ramírez-Tannus, M. C., et al. (2017) A&A, 599, L9 - 2017A&A...599L...9S

Feedback from Supernova Remnants: triggering Star Formation in the ISM

G. COSENTINO[1] AND THE SHREC COLLABORATION.

[1] Department of Earth, Space and Environment, Chalmers University of Technology,
giuliana.cosentino@chalmers.se

Supernova remnants (SNRs) drive large-scale shocks that locally enhance the density of the surrounding material but also inject vast amounts of energy and momentum that largely perturb and disperse the Interstellar Medium (ISM). The interplay between these two effects is considered paramount in regulating the star fromation efficiency in galxies. However, how SNRs affect the conditions of density and temperature of the ISM is not well constrained from an observational point of view. In this talk, I will present our work aimed to address this question. I will show our study of the large scale shock triggered by the SNR W44 on the molecular cloud G034 (Figure 1). I will show how the shock, probed by Silicon Monoxide (SiO) and observed with ALMA, enhances the density of the processed gas to values compatible with those required for massive star formation and has helped to shape the cloud. I will also present our exploratory large single-dish observing program SHREC, aimed to observe the molecular shock tracer SiO(2-1) toward a sample of $\sim$30 SNRs known to be interacting with molecular clouds. I will introduce the aim and technical aspects of SHREC and present the first results obtained toward the SNRs IC443. IC443 is a well known SNR, expanding into and interacting with a nearby toroidal molecular cloud. Toward the major site of interaction, known as clump G, we estimate the mass of the shocked gas to be 100 Msun. The shock driven by IC443 into this material enhances its density by a factor >10, to value consistent with those required to ignite star formation. Finally, we estimate that between 35-50% of the momentum injected by IC443 is transferred to the nearby molecular material. Our work therefore indicates that the molecular ISM is an important carrier of the SNR momentum and that the SNR-molecular cloud interaction play a crucial role in the regulating star formation in galaxies.

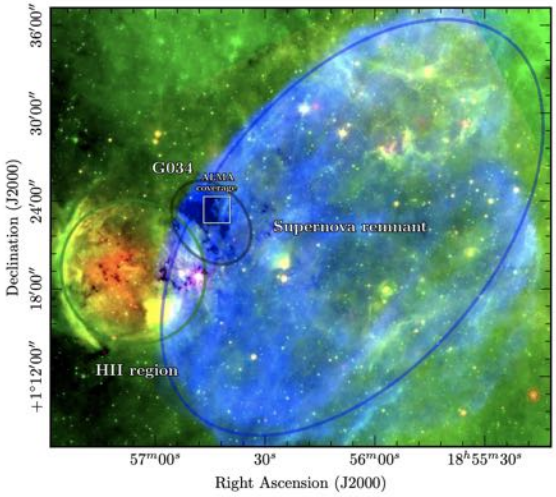

Figure 1: Three-colour image of G034 showing its position (black circle) between W44 (blue circle) and the HII region G034.758−00.681 (green circle). Red is 24 μm emission (MIPSGAL; Carey et al. 2009), green is 8 μm emission (GLIMPSE; Churchwell et al. 2009), and blue shows a combined JVLA+GBT 21cm continuum map (THOR; Beuther et al. 2016). The white square indicates the ALMA mosaic area and the grey shadow corresponds to Av$\geq$20 mag.

References:

Beuther, H., Bihr, S. et al. 2016, A&A, 595, 21
Carey, S.-J., Noriega-Crespo, A., et al., 2009, PASP, 121, 76
Churchwell, E., Babler, B. L., PASP, 121, 213

The hidden ionized carbon in M17SW

C. GUEVARA[1], J. STUTZKI[1], AND V. OSSENKOPF-OKADA[1]

[1] 1st Physics Institute, University of Cologne guevara@ph1.uni-koeln.de

Our simultaneous observations of [^{12}CII] and its isotope [^{13}CII] towards M17SW and other Galactic star-forming regions (Guevara et al. 2020) have shown that C^+ is optically thick, and even under self-absorption effects that mimic velocity components. Through a simple radiative transfer model composed of two layers, one background layer in emission and one foreground layer in absorption, we fit the [^{12}CII] and [^{13}CII] line emission simultaneously through multiple Gaussian components and to recover the "hidden" [^{12}CII] emission at both layers in selected individual positions (Fig. 1). We found that the velocity profile is much simpler than expected, with column densities up to 10^{19} cm^{-2}. The nature of the foreground layer is still under investigation.

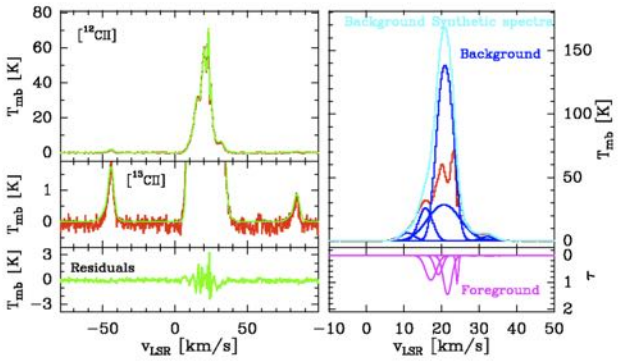

Figure 1: M17SW multicomponent analysis toward one of the positions (Guevara et al. 2020).

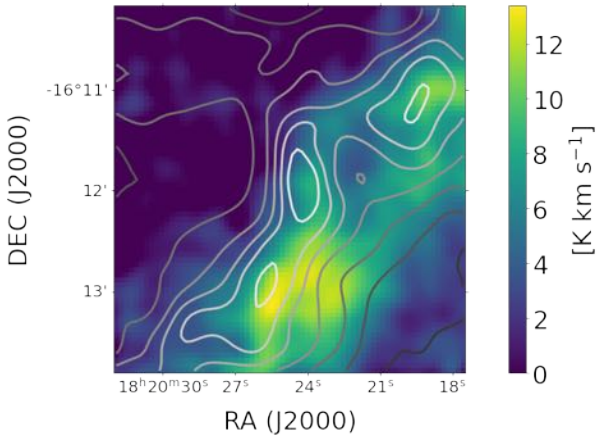

Figure 2: M17SW integrated intensity map of $[^{13}CII]_{F=1-0}$ in colors and $[^{12}CII]$ in contours (levels at 88, 176, 264, 352, 440, 528, 616, 704, 792 and 880 K km s^{-1})).

M17 is one of the brightest and most massive star-formingregions in the Galaxy located at a distance of 1.9 kpcs (Wu et al. 2019). M17SW is where the HII region is localized, and it is associated with a giant molecular cloud and PDR interface. M17SW is considered as a prototype of an edge-on PDR. The HII region is ionized by a highly obscured ($A_V > 10$ mag) cluster of many (>100) OB stars (Hoffmeister et al. 2008). Recent observations at high spectral resolution and signal-to-noise (S/N) towards M17SW grant us to not only detect $[^{13}CII]$ but also spatially map it in small contained regions (Fig. 2). From the map, we can see how its distribution is completely different, spatially and in intensity. The maps allow us to repeat the same multi-component analysis mentioned above and derive the full C^+ spatial structure hidden by the self-absorption effects and uncover its true distribution.

References:

Guevara, C., Stutzki, J., Ossenkopf-Okada, V., et al. 2020, A&A, 636, A16
Hoffmeister, V. H., Chini, R., Scheyda, C. M., et al. 2008, ApJ, 686, 310
Wu, Y. W., Reid, M. J., Sakai, N., et al. 2019, ApJ, 874, 94

Prestellar feedback in massive star-forming regions

Ü. KAVAK[1] AND C+ SQUAD TEAM

[1] SOFIA Science Center, USRA, NASA Ames Research Center, M.S. N232-12, Moffett Field, CA 94035, USA, ukavak@sofia.usra.edu

The role of feedback in the self-regulation of star formation is a major problem in astrophysics. Stellar feedback is the sum of all the processes by which massive stars inject energy, momentum, and mass into the interstellar medium (ISM). This feedback is thought to be responsible for regulating the rate of star formation, turbulence on various scales, and the evolution of galaxies. From an observational point of view, it has been difficult to determine the relative importance of prestellar and main sequence feedback mechanisms. We examine stellar feedback mechanisms during the protostellar phase through jets and outflows and during the main sequence phase feedback via stellar winds. To solve this issue, we make use of the velocity-resolved [C II] observations at 158 μm provided by Stratospheric Observatory for Infrared Astronomy (SOFIA) observatory. Recent [C II] 158 μm observations of Orion Nebula from SOFIA C+ SQUAD Large Program (led by A. G. G. M. Tielens) revealed an expanding bubble, the Veil shell, being powered by stellar winds of θ^1 Ori C, the most luminous star in Orion (20,000 $M_\odot$ km s^{-1}, Pabst et al. 2019). By examining channel maps and position-velocity (PV) diagrams spanning the entire Veil shell from this program, we identify [C II] emitting cavities at different velocities ranging from 1-2 km s^{-1} to 15 km s^{-1} relative to the Veil shell ($v_{\rm LSR}$ = 13 km s^{-1}). To understand the origin of these cavities, we estimate their energetics with SOFIA observations and morphology utilizing Spitzer 8 micron, IRAM 30m CO observations, Herschel PACS and SPIRE, and ESO Hα observations of the Orion Nebula. The momentum and dynamical timescales of these cavities imply that the cavities in Orion are formed by outflows from massive stars with luminosities ranging from 10^3 to 10^5 $L_\odot$, which correspond to B and O type stars. Specifically, we find that these cavities were created together by the fossil protostellar outflow of θ^1 Ori C (Kavak et al., 2022a) and by active outflow from less-massive stars, especially B-type stars (Kavak et al., 2022b). The momentum deposited during prestellar feedback is $\sim$10% of the momentum that Veil shell has, deposited through stellar winds from θ^1 Ori C (Pabst et al., (2019), Kavak et al., 2022(a,b)). Moreover, by creating cavities, these fossil shells may already have broken the Veil shell, and outflows from less massive stars may have made the Veil shell porous. These studies show that prestellar feedback from massive stars plays an important role in determining the future morphology of HII regions.

For the first time, the velocity-resolved SOFIA [C II] line observations enable us to quantify the relative importance of pre-stellar and main sequence stellar feedback. The SOFIA Feedback Legacy Program, which surveys a sample of massive star-forming regions spanning a range of stellar and environmental properties, will provide invaluable input for simulations of the Galaxy evolution (Schneider et al., 2020).

References:

Pabst, C., Higgins, R., et al., 2019, Nature, Volume 565, p.618-621
Schneider, N., Simon, R., et al., 2020, PASA, Volume 132, 19 pp.
Kavak, U., Goicoechea, J. R., et al. 2022a, A&A, Volume 660, A109
Kavak, U., Bally, J., Goicoechea, J. R., et al. 2022b, A&A, Accepted

Large scale mapping of the Central Molecular Zone: C^+ and CO emission

D. RIQUELME[1], R. GÜSTEN[1], A. HARRIS[2], M. A. REQUENA-TORRES[2], ET AL.

[1] Max-Planck Institute for Radioastromy, riquelme@mpifr-bonn.mpg.de
[2] Maryland University

We map several molecular lines in the complete Central Molecular Zone (CMZ) of the Galactic Center (GC) at the APEX telescope, and the [CII] emission using the upGREAT receiver onboard SOFIA. These observations reveal gas flows at large scales (important for the fueling and star formation history of the GC) and between clouds, physical and chemical properties, the fraction of "CO-dark" gas, and address the known (current) lack of star formation in the GC. We aim to establish the GC as a template for the interpretation of observations of the central regions of external galaxies. In this talk we will report the large scale imaging from the SOFIA and APEX surveys and we will present detailed studies towards Sgr B and Sgr C regions mainly focusing on the detailed imaging of the 158 μm [CII] spectral line, and 63 μm [OI] spectra from a sample of bright regions.

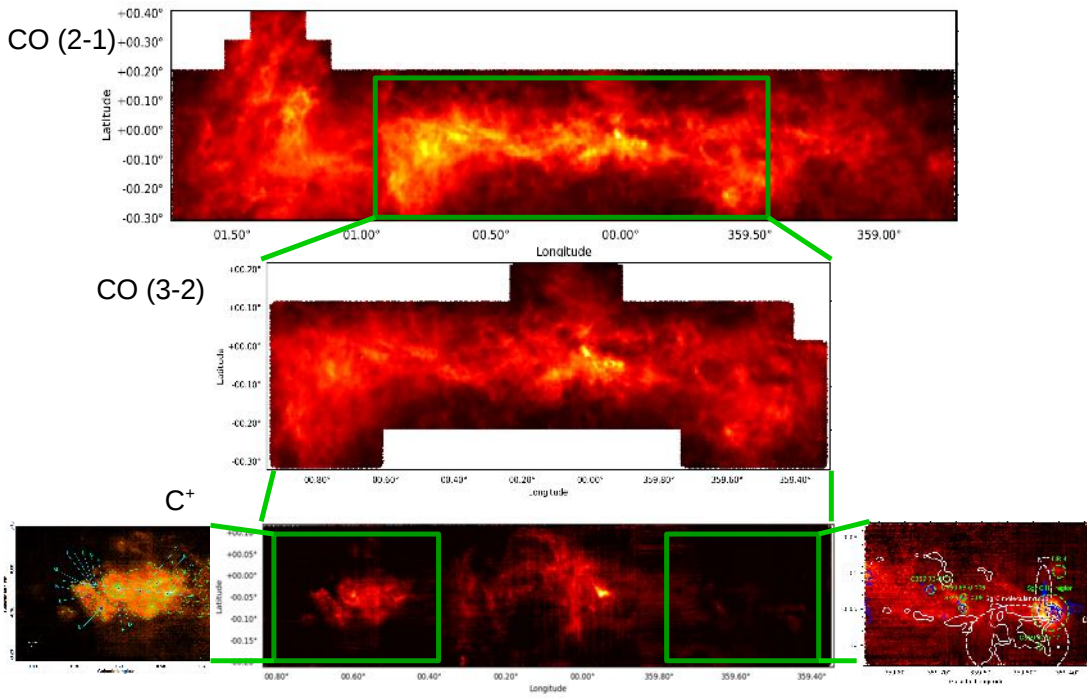

Figure 1: Top: CO (2-1) image of the CMZ observed with the PI230 receiver at the APEX telescope. Middle: CO (3-2) image of part of the CMZ observed with the LAsMA receiver at the APEX telescope. Bottom: [CII] image of part of the CMZ observed with the upGREAT receiver at SOFIA telescope (center). Left image shows a zoom in the Sgr B region (Harris et al, 2021) and right image shows a zoom towards Sgr C region (Riquelme et al., in prep).

References:

Harris, A., Güsten, R. et al, 2021, ApJ, 921, 33

Velocity-resolved [CII] Observations

J. STUTZKI[1]

[1] I. Physikalisches Institut, Universität zu Köln; stutzki@ph1.uni-koeln.de

Due to the ramp-down of SOFIA, the unique opportunity of high-resolution spectroscopic astronomical observations in the Far-Infrared spectral regime is gone. I will review the importance of velocity-resolved spectroscopy versus line-integrated observations for the important FIR-cooling lines of [CII] 158 μm (and [OI] 63 and 145 μm) with GREAT over the last decade.
Velocity resolved spectroscopy allows to address several topical areas: The fractal structure of the ISM implies that high spectral resolution observations help to avoid line-of-sight confusion in identifying small-scale spatial structure and hence clumpiness of the interstellar medium. High S/N line profile with high spectral resolution unambiguously identify weak additional velocity components in the line profiles, that are otherwise missed observationally. Absorption spectroscopy against bright Galactic background sources allows to identify and disentangle the multitude of line-of-sight components through the Milky Way. Self-absorption by cool foreground layers, showing up as narrow dips in the spectral line profiles, identify otherwise overlooked components of the ISM. Both topics can only be addressed at high spectral resolution. The identification of the isotopic line of [^{13}CII] and high S/N measurements of its line profile allow to derive firm numbers on the source intrinsic column density, unaffected by self-absorption.
I will exemplarily review the results that GREAT/SOFIA has provided over the last decade in these areas. The detailed insight into the complex structure of the ISM thus possible for the Milky Way and local galaxies raises the question to what extent it influences the interpretation of integrated line intensities of far-out galaxies, where these details cannot be observed.

California Molecular Cloud: gas kinematics of a rotating “sleeping giant”

R. ÁLVAREZ-GUTIÉRREZ[1], A. STUTZ[1], ET AL.

[1] Universidad de Concepción, Chile, rodralvarezz@gmail.com

Here I discuss the mass distribution and kinematic analysis done on the L1482 filament, located in the California Molecular Cloud (CMC), presented in Álvarez-Gutiérrez et al. (2021). The CMC has comparable gas mass to Orion ($\sim$1e5 $M_\odot$), and is at the $\sim$median mass of Milky Way clouds. Meanwhile, the CMC has only $\sim$177 YSOs (and 1 B-star), so has been dubbed a "sleeping giant". We focus on the L1482 filament, one of the most dense in the CMC, which contains $\sim$50% of the YSOs in the cloud. Using Gaia data we measure a distance of 511 pc. Then we measure the line mass (M/L) profile of L1482. The M/L profile lies below the ones of structures located in Orion, which are more active in terms of star formation, such as the ONC, Orion ISF, or L1641. We interpret the increase of the M/L profiles as a progression towards star formation. Next we analyze the gas radial velocities using IRAM 30m data. The velocity centroid of $C^{18}O$ (and other tracers) shows a velocity gradient perpendicular to the long axis of the filament. This gradient is linear and anti-symmetric about the center of the filament and presents an inner and outer component (Fig. 1). We interpret this velocity gradient as filament rotation. Using a simple solid-body rotation toy model, we show that the centripetal force, compared to gravity, increases toward a break at ~ 0.25 pc from the center of the filament (see figure below); when the ratio of forces approaches unity, the profile turns over. This analysis implies outside-in evolution on timescales of a few times 6 Myr. This filament has practically no star formation, a perpendicular Planck plane-of-the-sky (POS) magnetic field morphology, and POS “zigzag” morphology, which together with the rotation profile lead to the suggestion that the 3D shape is a corkscrew filament with a helical magnetic field. These results suggest evolution toward higher densities as magnetized rotating filaments shed angular momentum. With our recently obtained IRAM 30m data, we will continue our analysis of new gas radial velocity maps that extend the observations to the entirety L1482, covering different physical conditions in the gas (varying M/L, SFRs, and feedback conditions) and how they correlate with the dense gas velocities.

References:
Álvarez-Gutiérrez R. H., Stutz A. M., Law C. Y., et al., 2021, ApJ, 908, 86

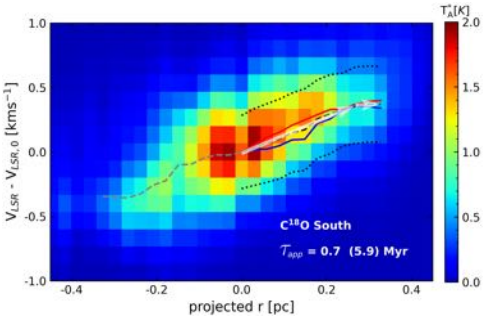

Figure 1: Velocity vs. projected radius r map for $C^{18}O$ L1482-South. The blue and red curves represent the velocity gradient for r ≤ 0 pc and r ≥ 0 pc.

Diffusion-advection effects in photon-dissociation regions

B. ALEENA[1], V. OSSENKOPF-OKADA[1], AND M. RÖLLIG[1]

[1] Institute of Physics I, University of Cologne, Germany, baby@ph1.uni-koeln.de

Molecular clouds are not static but species are transported through them by random motions. Quantifying this transport is essential for understanding the underlying physical conditions in a molecular cloud. We investigated the diffusion-advection effects in the multi-fluid gas of photon-dissociation regions (PDRs). A turbulent mixing-length theory along with molecular and thermal diffusion is included in the KOSMA-τ PDR model. The KOSMA-τ PDR model solves the chemistry, level populations, and energy balance simultaneously in a spherical geometry.

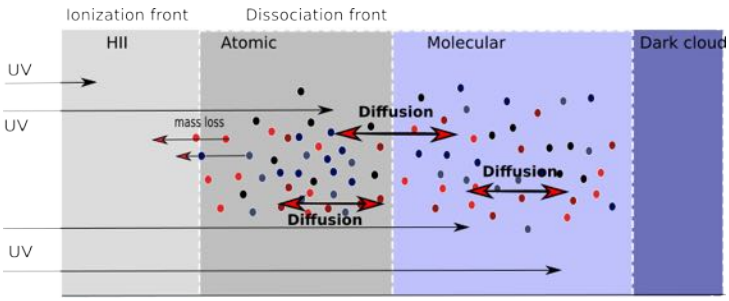

Figure 1: A simplified PDR model that shows mass loss from the surface of the PDR to the nearby regions and diffusion of species within the PDR. Diffusion mixes species within the PDR.

We demonstrate how diffusion flows influence the chemistry of the PDRs. We were able to derive the limits of the total diffusion coefficient and coherence length of turbulent flows as a function of the radius of the cloud. Diffusion increases the surface temperature and results in different chemical pathways compared to the non-diffusive case. It increases the abundance of H^+, He^+, OH^+, CH^+, and decreases that of He, CH, CO in the warm gas at intermediate optical depths. The density profiles of C, C^+, HCO, and HCO^+ are shifted towards the cloud center. The H/H_2 ratio is changing as a function of the diffusion velocity, with knock-on effects for the whole PDR chemistry. The line intensities from C, C^+, $C^{18}O$, CH^+, CO, and HCO^+ show significant differences for different diffusion-advection scenarios. Hence, C, CO, and other organic molecules can be used as a probe to understand non-stationary chemistry effects measuring changes in the PDR stratification from the diffusion and advection of gas.

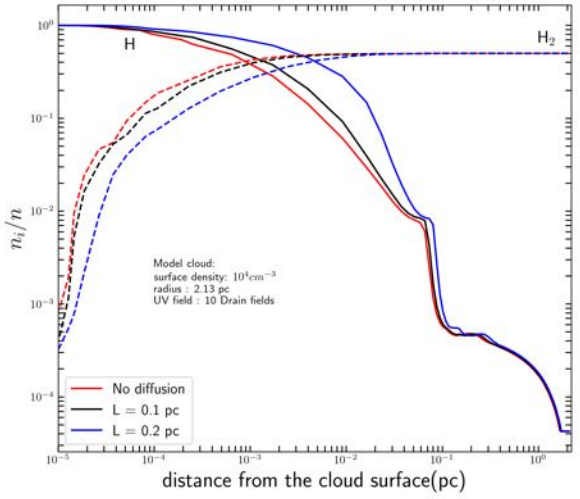

Figure 2: The fractional abundance of H and H_2 with and without diffusion. Two different turbulence coherence lengths were tested.

Shock compression and self-gravity: two ways to form filaments?

S. GANGULY[1], S. WALCH[1], D. SEIFRIED[1] AND S. D. CLARKE[2]

[1] I Physikalisches Institut, Universität zu Köln ganguly@ph1.uni-koeln.de
[2] Academia Sinica, Institute of Astronomy and Astrophysics

Molecular clouds are threaded with filamentary sub-structures. How exactly the different filaments form, however, remains an open question. We investigate the dynamics of forming structures by evaluating the contribution of different energy terms (kinetic, thermal, magnetic and gravitational) in young molecular clouds. For this purpose, we use the SILCC-Zoom and SILCC deep-zoom simulations, which follow the self consistent formation of molecular clouds from 100 parsec scales down to a maximum resolution of around 0.008 pc (1600 AU). The simulations include a galactic potential, self-gravity, magnetic fields, supernova driven turbulence, as well as a non equilibrium chemical network. We identify structures (sheets, filaments, and cores) inside selected regions using a dendrogram algorithm, and follow the dynamical behaviour of the hierarchically forming structures. We find that, of our two prominent larger filamentary structures, one is more quiescent and close to self gravitating, while the other is shock compressed and leads to smaller scale gravitationally bound regions. By studying the morphology of the forming structures, we further observe that in both cases, core-like structures appear at around 0.1 pc, and are embedded inside filaments.

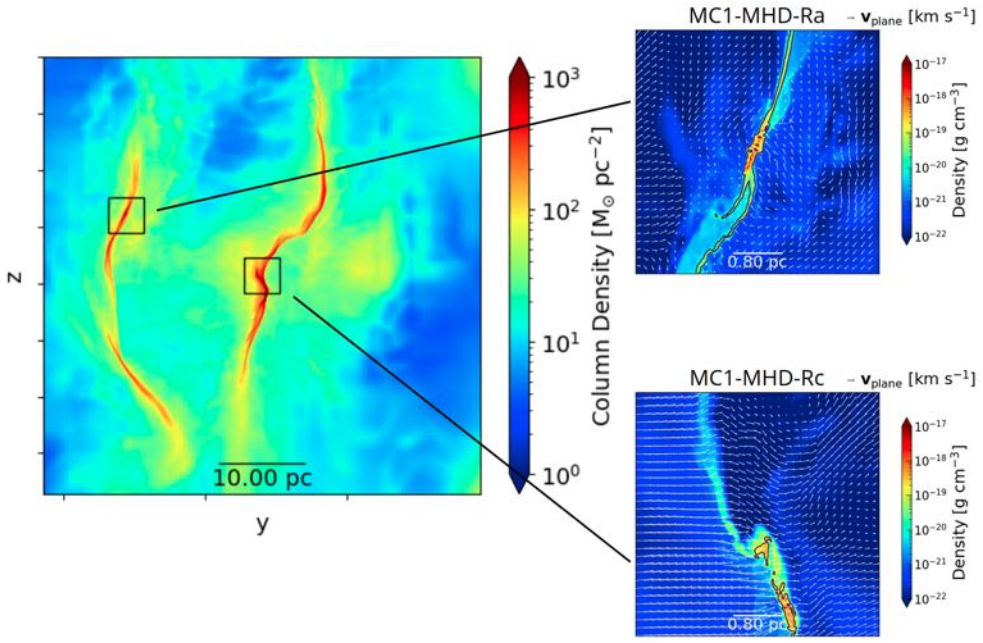

Figure 1: Column density map of a 50 parsec region in the SILCC-Zoom cloud MC1-MHD. The two highlighted boxes show density slices from two analyzed regions of size 4 parsec, with the planar velocity field shown using arrows. The contours represent a prominent dendrogram structure inside the analyzed region in each case. Of the two regions, MC1-MHD-Ra is relatively quiescent and self-gravity dominated, while MC1-MHD-Rc represents a shock layer.

Understanding Feedback Processes in the RCW36 Massive Star Forming Region.

P. García[1,2], L. Bonne[3], N. Schneider[4] and the FEEDBACK Consortium

[1] Chinese Academy of Sciences South America Center for Astronomy, National Astronomical Observatories, CAS, Beijing 100101, China, pablo.garcia@cas.nao.cn. [2] Instituto de Astronomía, Universidad Católica del Norte, Chile. [3]SOFIA Science Center, NASA Ames Research Center, USA. [4]I. Physik. Institut, University of Cologne, Germany.

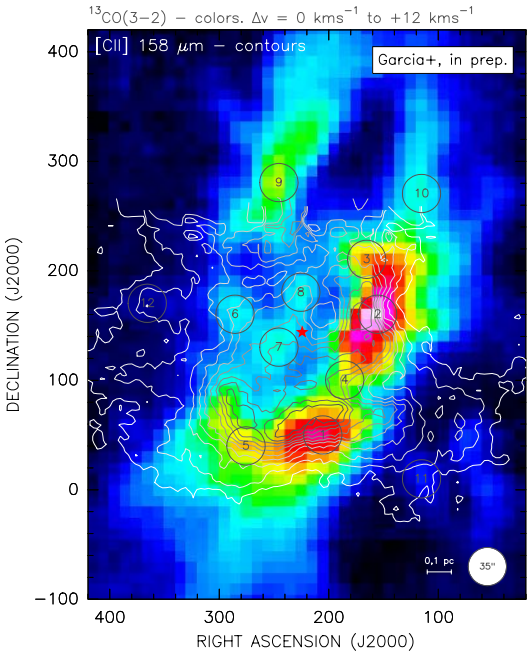

Figure 1: *RCW36 outlined in ^{13}CO(3-2) (colors) and [CII] (contours) integrated intensity emission [2]. The location of the massive star candidates in the region are shown by the ★ symbol [1]. Black open circles (∼ 35"), labeled 1 to 12, show the targeted positions for our XDR/PDR analysis, including ongoing HCO$^+$(2-1,3-2,4-3), H^{13}CO$^+$(2-1), ^{13}CO(2-1,6-5), CO(2-1,4-3,6-5), [CI](1-0) observations with the APEX Telescope and our available [CII], [OI], CO(3-2), and ^{13}CO(3-2) data sets.*

The mechanical (stellar winds and supernovae explosions), radiative (X-ray, UV, and Far-UV radiation fields), and cosmic-rays feedback of massive stars on their environment regulates the physical conditions in the interstellar medium (ISM). The simple geometry of the bipolar RCW36 H II region in the Vela C molecular cloud, composed of a central cavity with a stellar cluster [1], surrounded by a dense molecular ring, makes it an ideal testbed to study the relative importance of the radiative feedback processes at play. Unique [CII] 158 μm and [OI] 63 μm observations obtained as part of the SOFIA upGREAT C$^+$ Legacy Project FEEDBACK [4], in combination with recently obtained $^{12/13}$CO(3-2) (APEX) observations (see Fig. 1), and X-ray and dust continuum ancillary data, all together, have revealed a complex picture of the region: the presence of an expanding (v_{exp} ∼ 1.0 – 1.9 km s^{-1}) central molecular ring; blue-shifted expanding shells (v_{exp} ∼ 5.2 km s^{-1}) in the bipolar cavities possibly due to the hot plasma created by stellar winds; and leakage of the warm gas and the hot plasma from the H II region; among others [2]. Overall, the observed multistage expansion morphology and emission leakage in the region point to a scenario where stellar feedback evolves in a structure of filaments, sheets, and lower-density ambient gas, determined by the density structure that make up the Vela C molecular cloud. In order to assess the spatial influence of stellar feedback processes on the gas physical conditions in the region, further analysis will explore the radial influence of XDRs, PDRs, and CRs (constrained via PDR modeling) at targeted positions (see Fig. 1) in the main gas structures of RCW36, located close and far (from 0.1 pc to 1.0 pc in projection) from the central cluster [3]. For this purpose, a multi-species multi-wavelength observing campaign is ongoing to measure the HCO$^+$(2-1,3-2,4-3), H^{13}CO$^+$(2-1), ^{13}CO(2-1,6-5), CO(2-1,4-3,6-5), and [CI](1-0) transitions with the APEX Telescope. **REFERENCES: [1]** Baba, D., Nagata, T., Nagayama, T., et al. 2004, ApJ, 614, 818; **[2]** Bonne, L., Schneider, N., García, P., et al. 2021, submitted to ApJ. **[3]** García, P., Bonne, L., Schneider, N., et al. 2022+, in prep. **[4]** Schneider, N., Simon, R., Guevara, C., et al. 2020, PASP, 132, 104301.

Self-absorption in [CII], ^{12}CO, and HI in RCW 120. Building up a geometrical and physical model of the region

S. KABANOVIC [1], N. SCHNEIDER[1], V. OSSENKOPF-OKADA[1] AND FEEDBACK CONSORTIUM

[1] I. Physikalisches Institut, Universität zu Köln, Zülpicher Str. 77, 50937 Köln, Germany,
kabanovic@ph1.uni-koeln.de

It is a long-lasting question to which extent expanding HII regions, that appear circular in IR images, are indeed 3D bubbles. We investigated the 3D structure of the archetypical HII region RCW 120, using [CII] $158\,\mu\mathrm{m}$ observations from the SOFIA FEEDBACK legacy project, ^{12}CO and ^{13}CO (3$\rightarrow$2) lines from APEX, and HI and continuum data from the CGPS.

Two radiative transfer model were used on the set of observed lines. A line profile analysis with the 1D non-LTE radiative transfer code SimLine proves that the CO emission cannot stem from a spherically symmetric molecular cloud configuration. With the multicomponent two-layer model we quantified the amount of material located in the warm emitting background layer and the cold absorbing foreground. Hereby we obtained that a substantial amount of the C^+ column is hidden in a cold absorbing foreground layer. From HI self-absorption studies (HISA), we find that this surrounding layer is atomic with $T \sim 30\,\mathrm{K}$, has a low density $\sim 500\,cm^{-3}$ and an extend of about $\sim 5\,\mathrm{pc}$.

To determine the spatial distribution of the warm emitting and cold absorbing layer we apply a Gaussian mixture model to cluster the data cube by spectra with similar spectral shapes. This allows us to initialize the two-layer model for an entire spectral cube with a few initial parameters.

The model results suggest that RCW 120 developed out of a flat molecular cloud, enveloped by HI, and most of the CO is located inside the torus compressed by the stellar wind from the central star. The sudden morphological change in the cold foreground layer towards red-shifted velocities might indicate that the torus is still in formation and accreting mass.

A multi-wavelength study of the W33 Main ultracompact HII region

SARWAR KHAN[1], JAGADHEEP D. PANDIAN[2], MICHAEL R. RUGEL[1], KARL M. MENTEN[1], ANDREAS BRUNTHALER[1], F. WYROWSKI[1], AND DHARAM V. LAL[3]

[1] Max-Planck-Institut für Radioastronomie, Auf dem Hügel 69, 53121 Bonn, Germany, skhan@mpifr-bonn.mpg.de
[2] Indian Institute of Space Science and Technology (IIST), Trivandrum 695 547, India
[3] National Centre for Radio Astrophysics - Tata Institute of Fundamental Research, Post Box 3, Ganeshkhind P.O., Pune 411007, India

W33 is a star forming complex of the Milky Way with giant molecular clouds at different evolutionary stages. This complex chemical environment is influenced by a multitude of factors such as its density, turbulence, local radiation fields and the location of other stars. Here we study the dynamics of ionized gas around the W33 Main which hosts the brightest radio source in the region. We used the Giant Meterwave Radio Telescope (GMRT) to observe the H167α radio recombination line (RRL) at 1.4 GHz, and RRL data acquired in the GLOSTAR survey. The Global-View on Star formation in the Milky Way (GLOSTAR) is an unbiased survey of the Galactic Plane from 4−8 GHz covering 145 square degrees from 358° $\leq \ell \leq$ 60°, | b | $\leq$ 1°, and the Cygnus X region. The survey was carried out using the *Karl. G. Jansky* Very Large Array (VLA) in the compact D-configuration and the more extended B-configuration and the 100m Effelsberg radio telescope. In addition, archival data from submillimeter to near-infrared wavelengths were used to study the dust emission and identify young stellar objects.

The radio continuum data from GMRT and GLOSTAR show the presence of two sources, one associated with W33 Main and another arc-like region of diffuse emission, G12.81-0.22. The GLOSTAR RRL data reveal a velocity gradient across W33 Main and G12.81−0.22 at a higher resolution. The velocity gradient does not appear to be homogeneous but has a complicated velocity structure (Fig. 1). We determined the electron temperature to be 6300 K and 4800 K in W33 Main and G12.81−0.22 respectively. We derived the physical properties of the W33 Main molecular clump by modelling the dust emission using data from the ATLASGAL and HiGAL surveys. Our results are consistent with the region being a relatively evolved site of massive star formation. We conclude that the gas dynamics and physical properties of G12.81−0.22 are consistent with the HII region being in an evolved phase with a slowing expansion due to the pressure difference.

To expand the work on W33 Main, we are creating an unbiased catalogue of Galactic HII regions using the RRLs observed in the GLOSTAR survey. Also, we are using the GLOSTAR and ATLASGAL surveys to do a comprehensive study of the molecular environments these HII regions originate from.

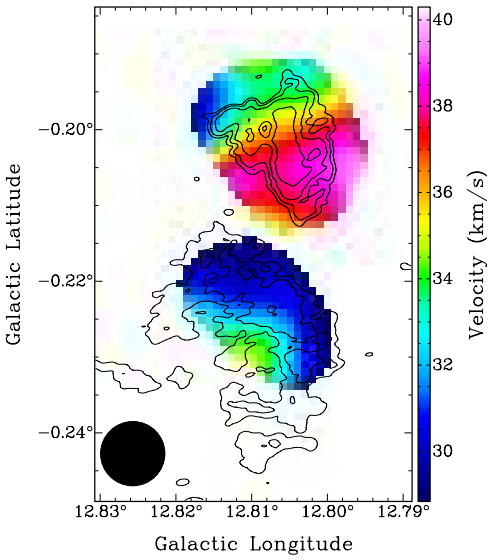

Figure 1: Velocity field map of W33 Main and G12.81−0.20 obtained from the Gaussian fitting of GLOSTAR stacked recombination lines. The maps are overlaid with contours of the radio emission at 1400 MHz. The black filled circle represents the GLOSTAR beam size (25″).

Radiative Feedback: Multi-line Study of the Photo-dissociation Regions in M17-SW and M42

R. KLEIN[1], A. REEDY[2], S. COLDITZ[3], D. FADDA[1], CH. FISCHER[3], A. KRABBE[3], L. LOONEY[4], W. VACCA[1], AND THE FIFI-LS TEAM

[1] USRA/SOFIA, NASA Ames, CA, USA, rklein@sofia.usra.edu
[2] Caltech, Pasadena, CA, USA
[3] Deutsches SOFIA Institut, Stuttgart, Germany
[4] Department of Astronomy, University of Illinois, Urbana, IL, USA

Photo-dissociation regions (PDRs) are the places where the radiative feedback by massive stars on molecular clouds happens. The molecular gas is photo-dissociated and then ionized by UV radiation. The UV radiation below 13.6 eV heats the gas via the photo-electric effect on dust grains. Cooling happens through the dust continuum and a handful of far infrared (FIR) fine-structure lines. FIFI-LS, the FIR spectrometer onboard the US-German airborne observatory, SOFIA, can map these main cooling processes efficiently.

We observed the well-studied PDRs, M17-SW and M42, with high spatial resolution in all major FIR cooling lines of the ionized and neutral medium. By comparing the observed line intensities to model predictions, we mapped the physical conditions of the ionized and neutral layer of the PDR. The [OIII] line ratio readily provides the electron density maps in the ionized layer just above the PDR. The analysis of the [OI], [CII], CO and continuum emission with the PDR Toolbox allowed us to map the gas density and UV radiation field strength over the region. We also estimate the optical depth effects to the [OIII]63μm line and the contribution of the PDR to the ubiquitous [CII] emission for each map position. While the applied model is comparatively simple, a consistent picture of the spatial variation of the physical parameters over the mapped region could be derived. Based on these findings the processes and energetics in the PDR can be studied further possibly by applying more detailed models together with more data from other wavelengths.

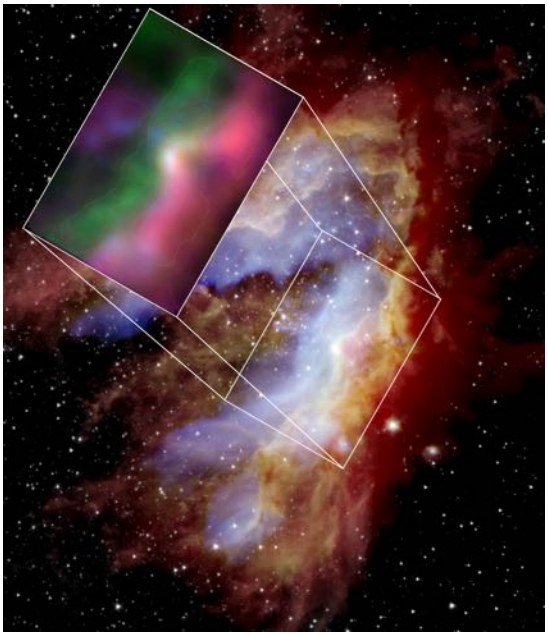

Figure 1: M17-SW Overview: Background - M17 (3.6μm - white, 20μm - blue, 37μm - green, 70μm - red; Lim et al. 2020); the box shows the approximate location of the FIFI-LS maps. The inset shows the PDR layers traced by [OI]63μm (green), [OI]146μm (yellow), and [CII]158μm (magenta)

References:

Lim, W., De Buizer, J. M., & Radomski, J. T. 2020, ApJ, 888, 98

Dense gas kinematics in a high-mass star-forming region: New ALMA-IMF Large Program observations of N2H+(1-0) in the G351.77 protocluster

N. SANDOVAL-GARRIDO[1], A. STUTZ[1], R. ALVAREZ-GUTIERREZ[1], S. REYES-REYES[1] AND J. SALINAS[1]

[1] Universidad de Concepción, Concepción, Chile nsandovalgarrido@gmail.com

The principal physical characteristics of protoclusters like G351.77 are that they are (a) gas dominated by mass, and (b) massive compared to individual and even 1000's of stars that form within. Despite their importance as the main sites of massive star and star cluster formation, their formation mechanisms are still under debate. Within the theoretical ideas proposed to explain protocluster properties, including their gas kinematics, are gravitational collapse, turbulence, magnetic instabilities, and cloud collisions, amongst others. Thanks to ALMA-IMF Large Program, where 15 massive protoclusters were observed in different bands, spectral lines, and continuum images (Ginsburg et al. 2021; Motte et al. 2021), we got access to the massive filamentary protocluster G351.77. This project is focused on the kinematic study of the dense gas in G351.77 using 3 mm data of the N_2H^+ (1-0) line. The G351.77 protocluster is located at a distance of $\sim$ 2 kpc from the Sun. Thanks to ALMA, we accessed to N_2H^+ line emission of the dense gas down to $\sim$ 2000 AU resolution, which allows us to resolve down to the scales of individual cores – the sites of individual star formation. I combined the 12M array, ACA, and Total Power data for imaging of the N_2H^+ spectral cube. The moment 0 maps a clear filamentary structure of dense gas in the protocluster that follows the direction of the maternal filament (not covered by these data). The moment 1, or mean velocity, calculated over the isolated component (Stutz et al., in prep) exhibits two key features: 1) a large scale gradient $\sim$ perpedicular to the maternal filament, and 2) cores located in $\sim$ all measures velocity components (no preference for components, so all are "fertile"), see Figure 1. In the next steps, I am developing Nestfit 2-component (in velocity) fits to the full hyperfine line complex to obtain more detailed results on both small and large scales.

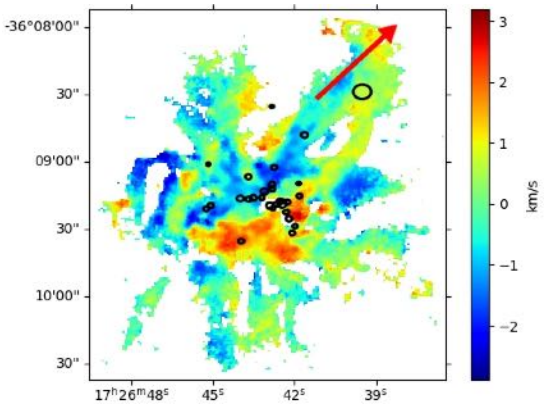

Figure 1: ALMA-IMF G351.77 N_2H^+ Moment 1 map derived from the combination of 12M array, ACA and TotalPower data, using only the isolated hyperfine component. The black ellipses show the cores derived from the continuum image of N_2H^+ and the red arrow shows the direction of the main filament. The axis "x" and "y" show the ICRS coordinates, Right Ascension and Declination respectively.

References:

Ginsburg, A. et al. 2021, arXiv, arXiv:2112.08183
Motte, F. et al. 2021, arXiv, arXiv:2112.08182

Cold Atomic filaments in the Galactic plane as traced by HI self-absorption

J. SYED[1], H. BEUTHER[1], AND J.D. SOLER[1]

[1] Max-Planck-Institut für Astronomie, syed@mpia.de

Stars form in the dense interiors of molecular clouds. The dynamics and physical properties of the atomic interstellar medium (ISM) set the conditions under which molecular clouds and eventually stars will form. It is therefore critical to investigate the relationship between the atomic and molecular gas phase of the ISM to understand the global star formation process. Using the high angular resolution data from The HI/OH/Recombination line survey of the Milky Way (THOR), we aim at constraining the kinematic and physical properties of the atomic hydrogen gas toward the inner Galactic plane.

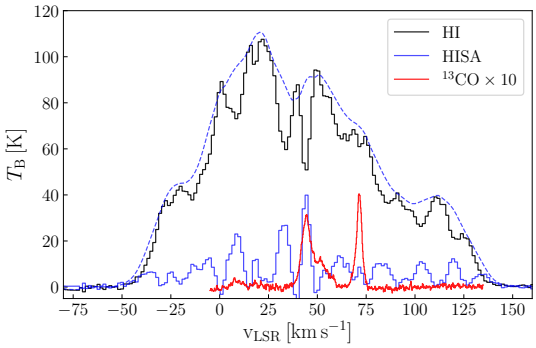

Figure 1: HI, HISA, and ^{13}CO spectrum (Syed et al. in prep.). The black curve shows an example spectrum of HI emission. The dashed blue curve shows an obtained self-absorption baseline. The blue curve represents the final extracted HISA spectrum. The GRS ^{13}CO spectrum is shown in red and has been multiplied by a factor of ten for better visibility.

HI self-absorption (HISA) has proven to be a viable method to detect cold atomic hydrogen clouds in the Galactic plane. With the help of a newly developed self-absorption fitting routine, we have extended upon previous case studies to identify HI self-absorption toward a sample of Giant Molecular Filaments (GMFs). We find the cold atomic gas to be spatially correlated with the molecular gas in some regions within these filaments. In other regions, however, the molecular gas appears to be decoupled from the cold atomic clouds as no significant spatial correlation is evident. The column densities of the cold atomic gas traced by HISA are usually on the order of $\sim 10^{20}$ cm^{-2} while those of molecular hydrogen traced by ^{13}CO are an order of magnitude higher. The HISA column densities are attributed to the cold gas that accounts for a fraction of the total atomic gas budget within the clouds. With this ongoing work, we will present possible explanations on the different findings as the physical properties that are traced by HISA are likely to vary with environment.

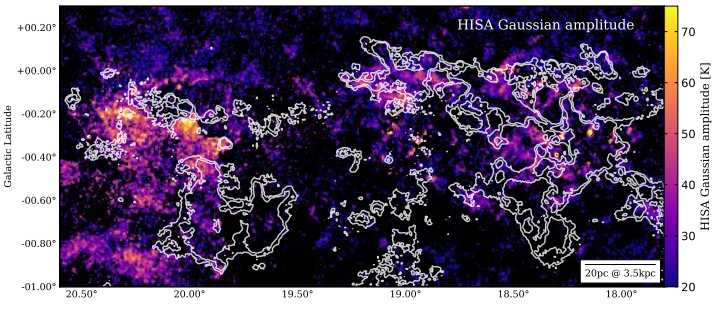

Figure 2: Fit HISA amplitude (Syed et al. in prep.). This map presents the fit peak intensity of the extracted HISA spectra toward GMF20.0-17.9. The white contours show the integrated ^{13}CO emission.

References:

Syed, J., Wang, Y., Beuther, H., et al. 2020, A&A, 642, A68
Wang, Y., Bihr, S., Beuther, H., et al. 2020, A&A, 634, A139

Turbulence Amplification During Gravitational Collapse

R. GUERRERO-GAMBOA[1], AND E. VÁZQUEZ-SEMADENI[1].

[1] Instituto de Radioastronomía y Astrofísica, UNAM, campus Morelia. 58090. Morelia, Michoacán, México, r.guerrero@irya.unam.mx

The turbulent (K) and gravitational (W) energies within molecular clouds (MCs) and their substructures are close to equipartition ($K \sim |W|$) or virialization ($2K \sim |W|$). This suggests that the turbulent motions may be driven by gravity. To investigate the amplification of turbulence during the gravitational contraction of a prestellar turbulent core, we perform analytical estimates and numerical simulations considering spherical coordinates and define the ratio g of the one-dimensional turbulent velocity dispersion, $\sigma_{1\mathrm{D}}$, to the gravitational velocity v_{g}. Under the assumptions of equipartition and virialization between the turbulent and the gravitational energies, we analytically find $g_{\mathrm{eq}} = \sqrt{1/3} \approx 0.58$ and $g_{\mathrm{vir}} = \sqrt{1/6} \approx 0.41$, respectively. Then, we run a set of AMR numerical simulations of purely hydrodynamic (HD) and magnetohydrodynamic (MHD) prestellar turbulent cores, and a non-turbulent control one. We find that the HD turbulent simulations collapse essentially at the same rate as the non-turbulent case. The ratio measured in the simulations approaches a virial-like value $g_{\mathrm{sim}} \approx 0.39$, even though the system is out of equilibrium, suggesting the necessity of considering more terms in the virial theorem, such as the time derivative of the moment of inertia and the energy loss by dissipation. Also, the MHD simulations were performed using different values for the initial strength of the magnetic field resulting in a non-monotonic behavior of the energy transfer as the field strength is increased (Fig. 1).

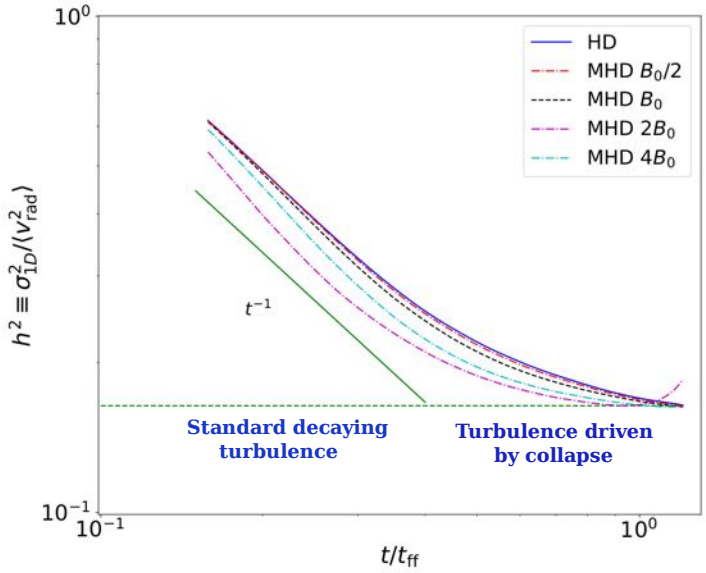

Figure 1: Evolution of the ratio between the one-dimensional to the radial velocity dispersion for HD and MHD simulations, and a non-monotonic behavior with the magnetic field strength.

References:

Guerrero-Gamboa, R. & Vázquez-Semadeni, E. 2020, ApJ, 903, 136

Extended [CII] and CO 3-2 mapping of the M17 nebula

PARIT MEHTA[1], JÜRGEN STUTZKI[1], ROLF GÜSTEN[2], NICOLA SCHNEIDER [1], CRISTIAN GUEVARA [1]

[1] Institute for Astrophysics, University of Cologne, 50937 Cologne, Germany
[2] Max-Planck-Institut für Radioastronomie, 53121 Bonn, Germany

We present high-resolution, large-scale maps of ionized, neutral and molecular gas in the M17, one of the brightest and most massive star forming regions in the galaxy. For the first time, M17 has been mapped in the [CII] ionized carbon fine-structure line at 158 μm and OI line at 63 μm as part of FEEDBACK, a SOFIA legacy program studying the interaction of massive stars with their environments. We here present first results of the [CII] map covering an area of $\sim$24x24 sq. arcminutes around the star forming region. The new spectroscopically resolved [CII] data is complemented by new ^{12}CO and ^{13}CO (J=3-2) maps from APEX, atomic [CI] emission maps obtained formerly at NANTEN2 and upcoming observations of ^{12}CO, ^{13}CO and C^{18}O (J=2-1), which will enable a comprehensive analysis of the excitation conditions and chemical structure of the extended region.

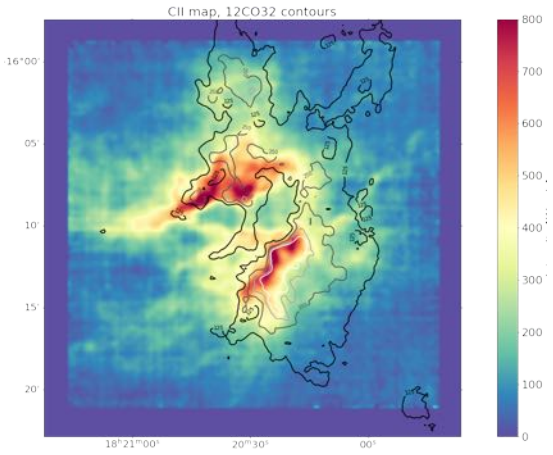

Figure 1: [CII] emission in M17 from the FEEDBACK survey using upGREAT onboard SOFIA, with contours of ^{12}CO (J=3-2) emission derived using data from APEX. The contours are on a grey scale at 25% (black), 50%, 75% and 90% (white) of the peak emission. The color bar at the right represents integrated intensities in K km/s.

The [CII] emission in M17N has the peak intensities around 800 K km/s. But the intensity of ^{12}CO (J=3-2) is much weaker, in stark contrast to the south. This is also true for HI and UV-flux intensities. The ^{12}CO emission appears to be clumpier in M17N as compared to M17SW. The dominant ^{12}CO velocity component at $\sim$20 km/s has a line integrated intensity of $\sim$400 K km/s as compared to the maximum intensity of $\sim$745 K km/s in the southern PDR.The main emission line is centered at 20 km/s, and T_{mb} peaks at $\sim$80 K. The ^{12}CO emission has a fairly complex velocity structure extending across $\sim$50 km/s at the baseline. Most of the warmest gas at T_{mb} $\sim$80 K is along the ionization front of M17N and $\sim 7'$ north of it.

The emission regions of [CI], [CII] and CO in M17 SW have been previously shown to be spatially extended and to coincide. [CII] has been detected at particularly high extinctions where UV photons are not expected to ionize carbon, suggesting clumpiness in the medium. It is also expected to spot outflows of molecular and ionized gas in the extended M17 region, whose energy output is dominated by O and B stars and consequential star formation due to stellar feedback processes. Our analyses may also have implications for galaxy-scale winds, by affecting the chemical evolution of galaxies and mass-metallicity relation through outflows.

Session IIIb: The ISM and Molecular Clouds: magnetic fields, fragmentation and collapse, outflows

Protoclusters: the key phase of core formation and accretion

A. STUTZ[1] & THE ALMA-IMF TEAM

[1] Departamento de Astronomía, Universidad de Concepción,Casilla 160-C, Concepción, Chile

Protoclusters are gas-dominated systems where star clusters are born. Studying massive protoclusters is an absolute requirement for investigating the origin of the IMF and the emergence of star clusters in the typical, yet extreme environments where massive stars are born. Accessing individual star formation cites within these protoclusters, the "cores", is also a key requirement for testing hypotheses that aim to explain the origin of stellar masses. And this requires both the frequency grasp and resolution capabilities of ALMA.

In this framework, the ALMA large Program ALMA-IMF observed 15 massive (2.5–33$\times10^3$ $M_\odot$) nearby (2–5.5 kpc) protoclusters selected to span a range in evolutionary stages. ALMA-IMF data were observed at 1.3 mm and 3 mm, capturing a wealth of spectral lines and importantly the continuum emission at approximately homogenous sensitivity reaching point-like cores down to $\sim$ 0.2 $M_\odot$(1.3 mm) and $\sim$ 0.6 $M_\odot$(3 mm). We emphasize that the ALMA-IMF data are also observed at matched spatial resolution down to $\sim$2 kAU, making inter-comparisons across different regions down to our resolution limit robust. In this talk I will address the ALMA-IMF sample, the evolutionary classification, initial results on core mass functions, examples of chemical diversity, and the dense gas kinematics in the hearts of the 15 protoclusters (e.g. see Motte et al., 2022, and Fig. 1).

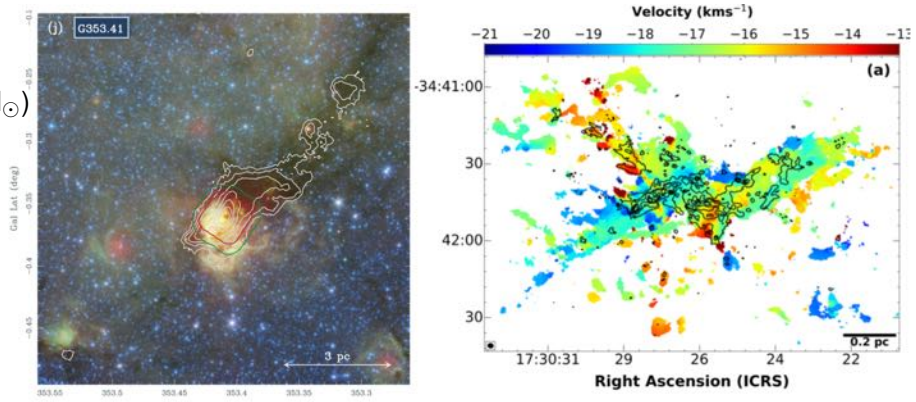

Figure 1: Figures from Motte et al. (2022). G353.41 as example target of the ALMA-IMF Large Program. *Left:* ATLASGAL 870 μm emission contours overlaid on the Spitzer 3-color image (red:green:blue $\rightarrow$ 24:8:3.6 μm). The green (red) contour indicates the ALMA 12 m array mosaic coverage at 3 mm (1.3 mm). *Right:* G353 ALMA-IMF moment 1 (mean velocity) map of N_2H^+ (1-0) isolated hyperfine satellite line. Contours indicate 1.3 mm continuum emission. Cores are almost all located inside the back contours. A network of filaments interacting in the center of the protocluster are visible. See Motte et al. (2022) for more details.

References:

Motte, F., et al., 2022, A&A, 622, A8

Magnetic fields and the formation of dense gas structures in molecular clouds

L. M. FISSEL[1]

[1] Queen's University, laura.fissel@queensu.ca

Star formation is known to be an extremely inefficient process, due to regulation from a combination of turbulent gas motions, feedback from young stars, and magnetic fields. In recent years large area dust polarization maps covering entire molecular clouds from *Planck*, and BLASTPol (Figure 1), and detailed maps of individual filaments with HAWC+ and JCMT/POL2, have allowed us to investigate the role of magnetic fields in star formation over a wide range of scales and density regimes.

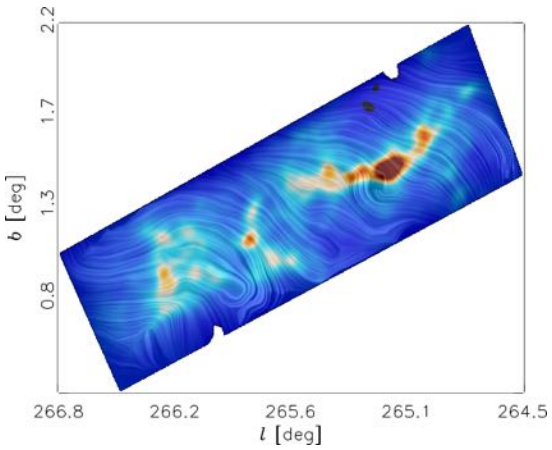

Figure 1: Inferred magnetic field map of the Vela C molecular cloud made from 500 μm BLASTPol Polarization data.

In this talk I will discuss what we have learned about magnetic fields in molecular clouds, and the role they play in the formation of the dense filaments and clumps that are the preferred locations of star formation. I will focus on two methods: analyzing the probability distribution functions of polarization maps, and examining the changing alignment of the magnetic field with molecular gas in different density regimes (Figure 2). By statistically comparing polarization maps with simulations of magnetized star formation, we find our observations best match simulations with dynamically important magnetic fields on large (> 1 pc) scales. Magnetic fields therefore appear to play an important role in the formation of both low- and high-density molecular gas sub-structures within star-forming regions, and possibly set where gravitationally unstable gas most efficiently forms.

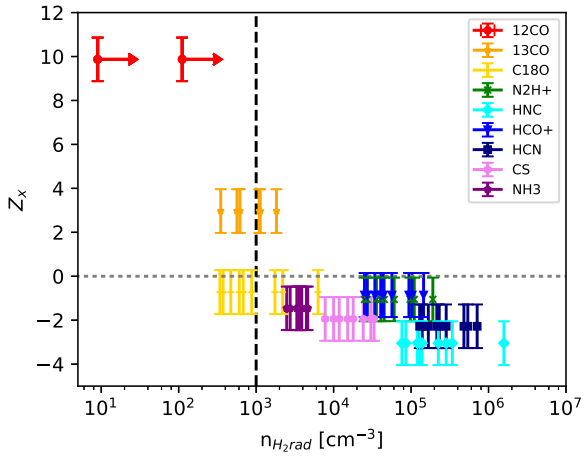

Figure 2: Relative alignment of the BLASTPol inferred magnetic field and structures in different MOPRA molecular line maps versus their characteristic density for different values of excitation temperature and integrated line intensity (Fissel et al. 2019). The average relative alignment is quantified by the projected Rayleigh statistic $Z_{\rm x}$: $Z_{\rm x} > 0$ indicates parallel alignment, $Z_{\rm x} < 0$ indicates perpendicular alignment.

References:

Fissel, L., et al., 2016, ApJ, 824, 134
Fissel, L., et al., 2019, ApJ, 878, 110

From protostellar to Proto-Planetary disks: Disk formation and Evolution in the Orion Molecular Cloud

A. John J. Tobin[1] and B. Patrick D. Sheehan[2]

[1] National Radio Astronomy Observatory, jtobin@nrao.edu
[2] Northwestern University

We have conducted a survey of 328 protostars in the Orion star forming regions at 40 AU (0.1") resolution using ALMA (0.87 mm). This large sample constitutes the majority of the protostars in Orion. We will show the results from a statistical characterization of the size, masses, and physical density structure of disks throughout the protostellar phase. Protostellar disks are significantly more massive than proto-planetary disks around more evolved young stars. The median dust mass of the Orion protostellar disks is 17.5 $M_\oplus$, inferred from observations of dust continuum. There is a systematic decrease in disk masses from Class 0 to Flat Spectrum, but there is substantial scatter in the observed masses for each class. The median protostellar disk masses are at least 4 times larger than the proto-planetary disks around pre-main sequence stars. Thus, there is substantially larger reservoir of gas and dust available for planet formation in the protostellar phases and the protostellar disks may better represent the initial conditions for planet formation. We will also present current evidence of substructure in protostellar disks which may be a sign of ongoing planet formation.

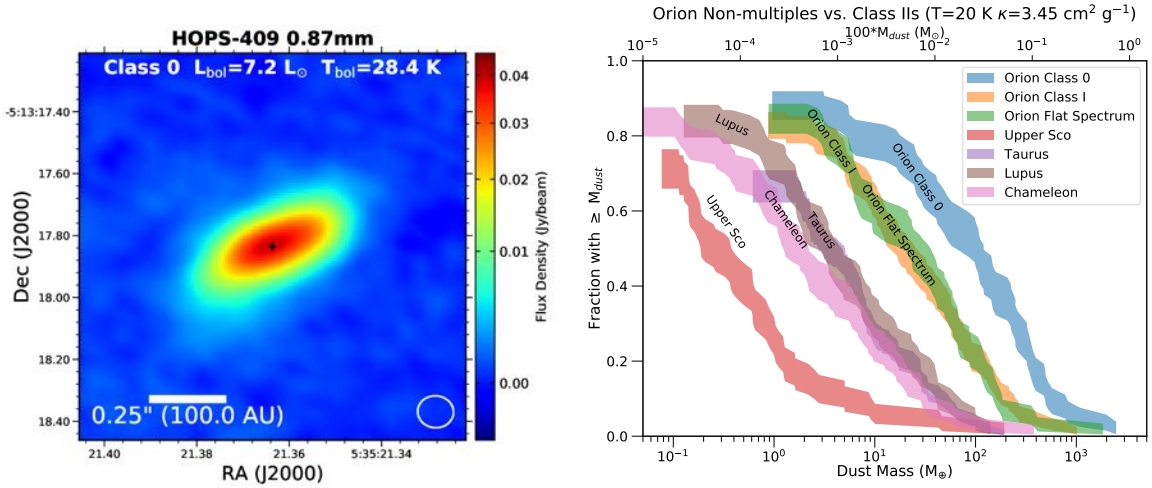

Figure 1: The left panel shows an example dust continuum image from the survey toward an edge-on Class 0 disk around the protostar HOPS-409 at 0.87 mm. The right panel shows the distributions of dust disk masses for Protostars in Orion, divided by class, and the dust disk mass distributions for Class II disks from other star forming regions. This shows the clear mass evolution from Class 0 to Class II where the disk populations of more-evolved populations have systematically lower dust masses.

Diagnostics of Stellar Mass Assembly Uncovered via Monitoring Protostellar Variability in the Sub-mm and Mid-IR.

D. JOHNSTONE[1]

[1] National Research Council Canada, Herzberg Astronomy & Astrophysics
doug.johnstone@nrc-cnrc.gc.ca

We have analyzed over half a decade of mid-IR and sub-mm observations monitoring protostar variability. Consideration of almost 5000 sources across the Gould Belt reveals that mid-IR variability is stronger and more likely to be dominated by long-term secular trends at earlier evolutionary stages (Park et al. 2021). A smaller sample observed in the sub-mm (Lee et al. 2021) supports this result (Figure 1). Comparing the strength of variability in the sub-mm directly with simultaneous mid-IR observations (Contreras-Pena et al. 2020), reveals excellent light-curve agreement, confirming our expectation that the sub-mm emission is directly related to the changing dust temperature in the protostellar envelope due to changes in the source (accretion) luminosity.

The measured timescales and amplitudes suggest that dynamic processes taking place within the inner, several au, protostellar disk play a role in modulating the mass assembly of deeply embedded protostars. For two protostars we have been able to analyse the variability more completely. The Class I source EC 53 (also known as V371 Ser) undergoes strong 18-month periodic variations (Figure 1: Top), observed from the near-IR through sub-mm, allowing for detailed analysis of the underlying physical processes (Lee et al. 2020). Similarly, the Class 0 (PBRS) source HOPS 373 underwent a burst event in 2019 (Figure 1: Second from top), providing a rich data set for analysis (Yoon et al. 2022).

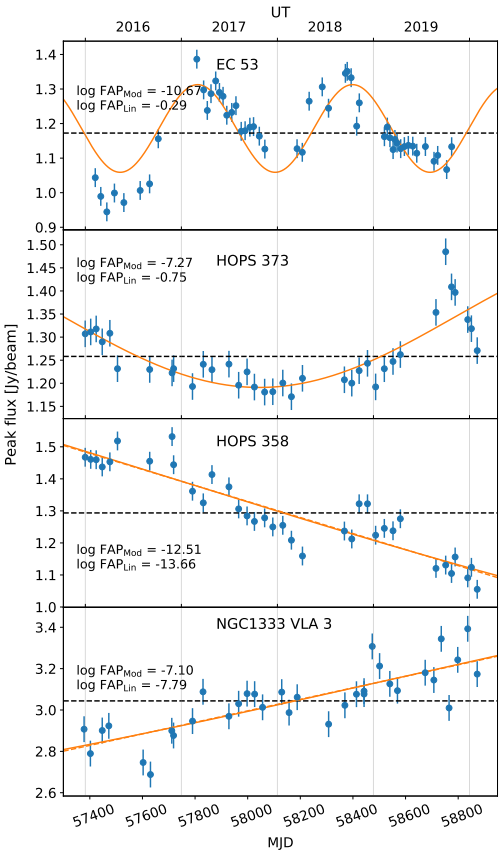

Figure 1: Representative light-curves of varying protostars observed in the sub-mm with the JCMT. The overlaid orange sinusoidal and linear fits qualitatively reveal long-term secular trends.

References:

Contreras Pena, Johnstone, Baek, Herczeg, Mairs, et al. 2020, MNRAS, 495, 3614
Lee, Johnstone, Lee, Herczeg, Mairs, et al. 2020, Apj, 903, 5
Lee, Johnstone, Lee, Herczeg, Mairs, et al. 2021, ApJ, 920, 119
Park, Lee, Contreras-Pena, Johnstone, Herczeg, et al. 2021, ApJ, 920, 132
Yoon, Herczeg, Lee, Lee, Johnstone, et al. 2022, ApJ, 929, 60

Dense clumps in the Milky Way: Physical properties and kinematics

F. WYROWSKI[1]

[1] Max Planck Institute for Radio Astronomy, wyrowski@mpifr-bonn.mpg.de

Parsec-scale massive dense clumps are the nurseries of star clusters. Current theoretical concepts triggered by new observational results highlight the importance of these coherent overdensities in giant molecular clouds as crucial structures channeling the inflow of material from parsec scales to scales of disks and stars. This talk will discuss unbiased, galaxy-wide dust continuum surveys of these clumps, such as the ATLASGAL 870 micron survey with the APEX telescope, and systematic spectroscopic follow-up programs to constrain further their physical and chemical conditions. Such molecular line observations of the clumps reveal also their large scale kinematics, including signatures for infall.

Probing accretion along filaments in creating shocks: First detection of extended SiO along filaments in the NGC6334 V

ATEFEH. AGHABABAEI[1], ÁLVARO. SÁNCHEZ-MONGE[1], PETER. SCHILKE[1], AND WONJU. KIM[1]

[1] Institute of Physics I, University of Cologne, babaei@ph1.uni-koeln.de

Star-forming clusters are found deeply embedded in filamentary molecular clouds. Filaments accrete material toward the central dense region, but how does accretion affect the medium in an early stage? To answer this question, we observed the massive protocluster NGC6334 V embedded in the filamentary cloud NGC6334. We detect a unique, widespread SiO emission with low-velocity components throughout the whole central hub of this cluster. SiO is a shock tracer, and shocks trace different phenomena (e.g., outflows, colliding flows, etc.) based on how fast or slow they travel. While high-speed shocks are commonly related to outflows, the physical process generating low-velocity shocks is not well understood. Some studies have reported the presence of a low-velocity SiO component in cloud-cloud collisions or colliding-flow events. In this work, we intend to study the effect of filamentary accretion in creating low-velocity shocks. We used spectral-line ALMA observations at 1.3 mm to identify filaments and compared these elongated features with large-scale APEX observational data. The comparison of ALMA and APEX data shows how the large-scale filaments seen with APEX are connected to the small-scale branches seen with ALMA. We also used different species, such as CH_3CCH, to map the temperature of the gas and the continuum emission to identify massive cores in the central region. The analysis of the SiO (2-1) line profile and spatial distribution reveals that 98% of SiO emission has a width of less than 10 km/s and 55% has a width of less than 2.5 km/s, suggesting the presence of slow-shocks in this region. The narrow velocity components emerge where filaments connect to the central hub and where no cores or outflows are detected. The SiO could be a sputtering product of shocks formed during the filament accretion process.

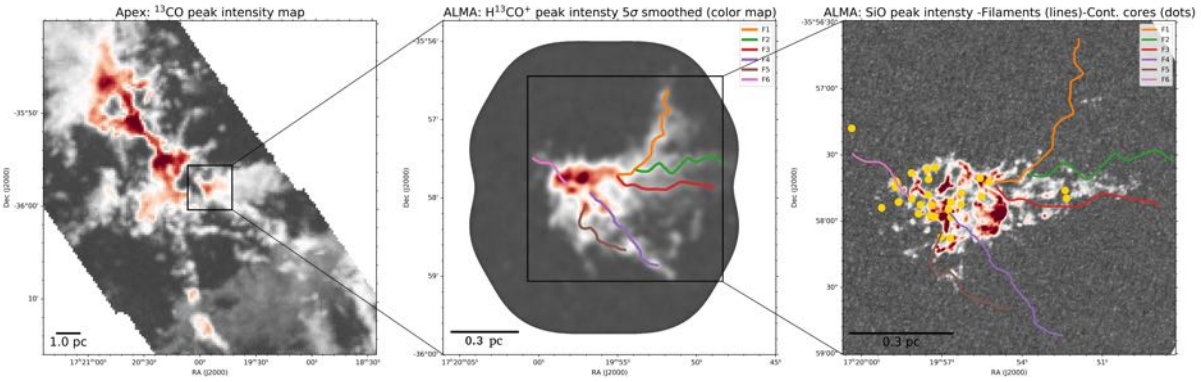

Figure 1: - Left: APEX ^{13}CO peak intensity map. - Middle: $H^{13}CO^+$ peak intensity map overlaid by filaments. The high-resolution ALMA observations reveal detailed filamentary structures compatible with previous low-resolution large-scale maps. - Right: SiO Peak intensity emission map overlaid by continuum cores and filaments. SiO emission brightens at the center and extends to the conversion point of filaments, where the dense core population is negligible.

From core to disk fragmentation in high-mass star formation

A. Ahmadi[1], H. Beuther[2], and C. Gieser[2], F. Bosco[2] Th. Henning[2], R. Kuiper[3], + CORE Team

[1] Leiden University, aahmadi@strw.leidenuniv.nl
[2] Max Planck Institute for Astronomy
[3] Institute for Theoretical Astrophysics, Center for Astronomy Heidelberg

There is growing consensus that the formation of high-mass stars proceeds through disk accretion, similar to that of lower mass stars. To this end, we have undertaken a large observational program (CORE) making use of interferometric observations from the NOrthern Extended Millimetre Array (NOEMA) for a sample of 20 high-mass protostellar objects in the 1.3 millimetre wavelength regime reaching 0.4" resolution (800 au at 2 kpc). We find rotational signatures in dense gas perpendicular to bipolar molecular outflows in most regions (see Fig. 1). Modelling the level populations of various rotational transitions of the dense gas tracer CH_3CN, we find the disk candidates to be on average warm ($\sim$200 K). Studying the Toomre stability of the disk-like structures reveals that most high-mass young stellar objects are gravitationally unstable and prone to disk fragmentation. Since most high-mass stars are found to have companions, disk fragmentation seems to be an important mechanism by which such systems may be formed. While observations at hundreds of au resolution have now shown that rotational signatures are common around such young and massive accreting protostars, it is difficult to differentiate between rotating and infalling envelope material and true disk structures which likely reside on much smaller scales. In this talk, I will take you on a tour across scales from our findings at hundreds of au resolution with NOEMA reaching down to sub 100 au observations with ALMA where we resolve disk scales. I will put into context how different modes of fragmentation can contribute to the final stellar mass distribution in high-mass star forming regions.

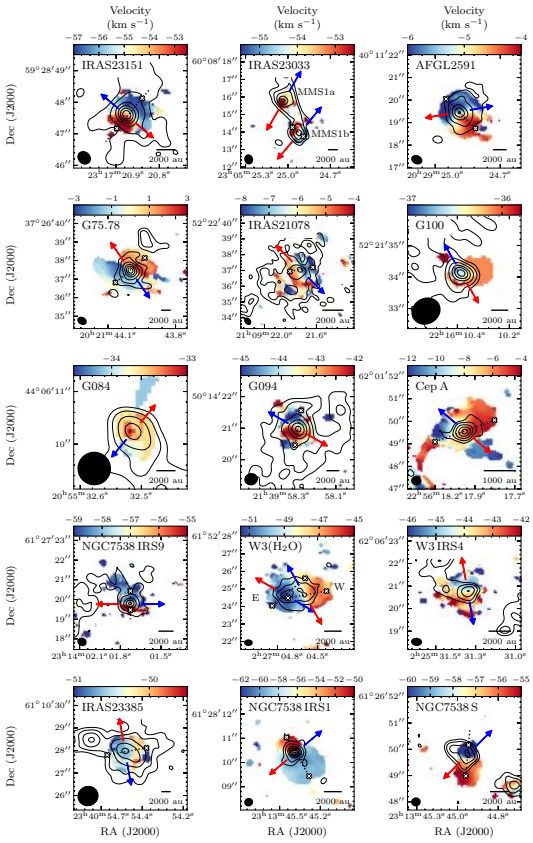

Figure 1: Intensity-weighted peak velocity (first moment) maps of CH_3CN (12_3-11_3) showing the dense gas kinematics for 15 sources in the CORE survey. The blue and red arrows correspond to the estimated directions of bipolar blueshifted and redshifted molecular outflows, respectively. The dotted lines indicate the position of the strongest velocity gradient tracing the disk.

Studying Dust Properties, Grain Alignment And Magnetic Field Structure With Multi-Wavelength Submillimeter Polarization

L. FANCIULLO[1,2] AND THE BISTRO COLLABORATION

[1] National Chung Hsing University, 145 Xingda Rd., South Dist., Taichung City 402, Taiwan (R.O.C.), lfanciullo.astro@gmail.com
[2] Academia Sinica Institute of Astronomy and Astrophysics, 11F of AS/NTU Astronomy-Mathematics Building, No.1, Sec. 4, Roosevelt Rd, Taipei 10617, Taiwan (R.O.C.)

Interstellar dust grains are generally non-spherical and their major axes tend to orient perpendicularly to magnetic field lines. The net result is that thermal emission from dust is polarized, and this polarization provides information on both dust itself, and on the orientation of interstellar magnetic fields. Thus, the study of polarized dust emission at submillimeter wavelengths is central to many astrophysical fields, including the study of dust properties, magnetic field mapping on both Galactic and molecular cloud scales, and CMB analysis (as a foreground).

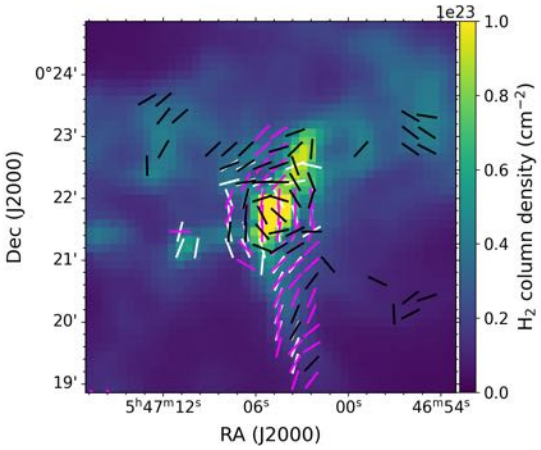

Figure 1: Polarization angles at 154 μm (white), 214 μm (magenta) and 850 μm (black) superimposed on a column density map of NGC 2071.

However, interpreting polarization is a non-trivial task. Polarization angles only provide a 2D picture of the 3D interstellar magnetic field structure. Also, the polarization fraction P/I, often used as a proxy for grain alignment efficiency, depends on additional factors such as the orientation and structure of the magnetic field and the optical properties of dust itself.

One way of breaking these degeneracies is to study polarized emission at multiple wavelengths. If dust temperature changes significantly along the line of sight, the emission of warm and cold dust will have different weight in different bands; the change of magnetic field orientation along the line of sight, then, can be inferred from the change of polarization angle with wavelength. If, conversely, dust temperature is uniform along the line of sight, the effects of magnetic field structure on P/I are expected to be independent of wavelength, so that the spectral *shape* of dust polarization is mainly determined by dust properties, and is a useful observable to constrain dust models.

I will show the results of a multi-wavelength polarimetric analysis of the star-forming region NGC 2071, using 850 μm data from the BISTRO large project at JCMT in combination with 154 μm and 214 μm data from the HAWC+ polarimeter on SOFIA. The data show a variation of polarization angle with wavelength (Fig. 1), which is likely a result of a change in magnetic field orientation with optical depth, although alternative explanations are discussed as well. I will further discuss which analysis techniques do not transfer well across wavelengths, and how including both short-wavelength ($< 250\,\mu$m) and long-wavelength data (~ 1 mm) was key to obtaining our results.

High-resolution dust mapping of Class 0 and I disks

M. MAUREIRA[1], J. PINEDA[1], D. SEGURA-COX AND P. CASELLI[1]

[1] Max Planck for Extraterrestrial Physics, maureira@mpe.mpg.de
[2] University of Texas, Austin

The formation of both stars and planets appears to be more closely knit together than previously thought. New observational evidence suggests that it is already during the protostellar stages, i.e., when accretion is at its peak, and the stellar mass is set, when the first generation of planets might begin forming. These embedded disks (Class 0 and I) are expected to be more massive and thus prompt to gravitational instabilities, resulting in the formation of planets and multiple stellar systems. In addition, these young disks also show various sizes and multiple system configurations, likely associated with anisotropic accretion from the surroundings and internal dynamics. Resolving the dust distribution in diverse young disks is crucial to directly constrain the initial conditions for planet formation and the star accretion process at disk scales. In this contribution, I will present new multi-wavelength ALMA observations that reveal the dust distribution down to 6 au for a diverse sample of Class 0/I disks. I will discuss the small-scale structures present in circumstellar and circumbinary disks. Likewise, I will also show the spatial variations of the spectral index in these systems, with implications for their physical structure (mass, temperature) and the process of dust accumulation and growth.

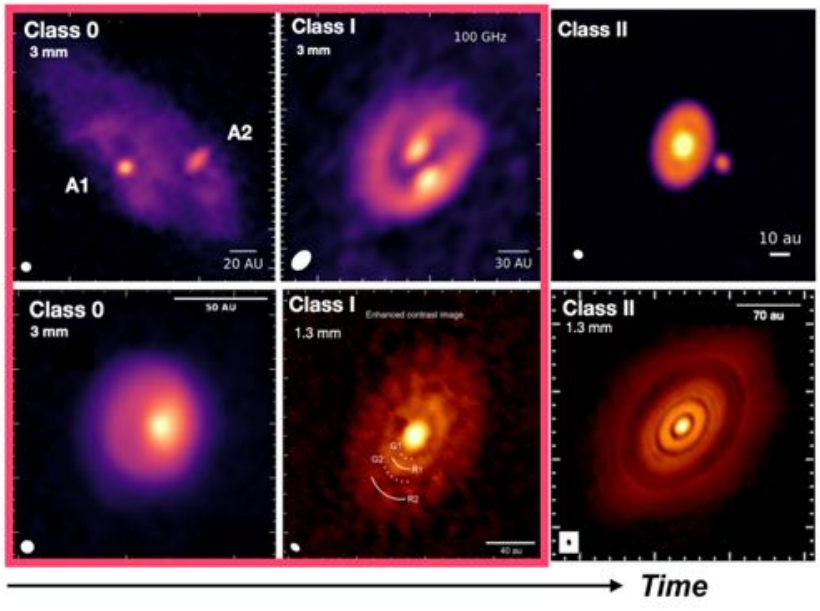

Figure 1: Gallery of protostellar (Class 0 and I) and protoplanetary disks (Class II) mapped with continuum ALMA high-resolution observations. Top: close multiple systems. Bottom: single or wide separation multiple systems. The red square highlights a few sources that are part of the sample I will present (see references).

References:

Andrews, Huang, Perez et al. ApJL, 869, L41 (2018)
Maureira, Pineda, Segura-Cox et al. ApJ, 897, 59 (2020)
Zamponi, Maureira, Zhao et al. MNRAS.tmp, (2021)
Alves, Girart, Padovani et al. A&A, 616, A56 (2018)
Segura-Cox, Schmiedeke, Pineda et al. Natur, 586, 228 (2020)
ALMA Partnership, Brogan, Pérez et al. ApJL, 808, L3 (2015)

Investigating Accretion onto Class 0 Protostars

S. T. MEGEATH[1] AND THE HOPS, ORIONTFE AND IPA TEAMS

[1] University of Toledo, s.megeath@utoledo.edu

At least half of a low mass star's mass is accreted in the Class 0 phase, yet due to their deeply embedded nature, accretion onto these protostars is poorly understood. We use mid to far-IR and sub-mm observations to investigate infall and accretion onto the rich population of Class 0 protostars within 500 pc studied by the HOPS and eHOPS programs. Using an ALMA ACA survey to trace combined 870 um envelope and disk fluxes and ALMA 12 meter data to measure the disk fluxes, we trace the evolution of Orion protostars from their envelope dominated Class 0 phase to disk dominated flat spectrum phase. We find that over this time, inferred mass infall rates decrease by a factor 100-1000 (Federman et al., in prep.). We then use the Spitzer Orion, YSOVAR and OrionTFE surveys to identify accretion driven outbursts from the Class 0 protostars. The erupting protostars are studied through a combination of Spitzer, WISE, Herschel and SOFIA observations (Zakri et al. 2021). We show that Class 0 protostars have outbursts with amplitudes of a factor of ~ 5 every 440 years; more frequent than the more evolved Class I and flat spectrum protostars. This high rate may result from disk instabilities driven by the rapid mass infall. A significant fraction of the stellar mass appears to be accreted during these bursts, although with substantial variations between the protostars. Finally, we overview a Cycle 1 JWST project, Investigating Protostellar Accretion. IPA will use the IFUs on NIRSpec and MIRI to search for accretion lines from five deeply embedded protostars spanning two orders of magnitude in current (proto)stellar mass.

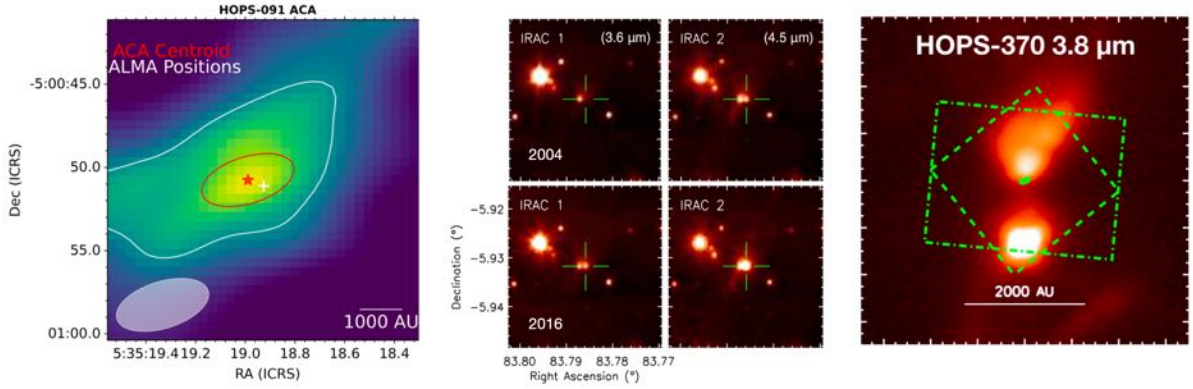

Figure 1: **Left:** ACA image of the envelope surrounding the Class 0 protostar HOPS-91 (Federman et al. in prep.). **Middle:** The outburst of the HOPS 12 Class 0 protostar observed by Spitzer in the 3.6 and 4.5 μm bands (Zakri et al. 2021), **Right:** 3.8 μm image of the intermediate mass HOPS 370 protostar. The green rectangles show the planned JWST IFU fields for this protostar.

References:

Zakri, Wafa, et al. 2022, The Astrophysical Journal, 924, L23
Megeath, S. T. et al. 2021, JWST Proposal. Cycle 1, ID. #1802

Formation and environment of multiple protostellar systems in Perseus

N. M. MURILLO[1]

[1] Star and Planet Formation Laboratory, RIKEN, nadia.murillomejias@riken.jp

The range of separations and configurations of multiple protostellar systems raise the question of what factors influence the formation of these systems. Models have probed the effect of several factors on the formation of multiple protostellar systems, but few observational constraints are available to test the modeled scenarios. In addition to the arrangement of protostellar components in multiple systems, the distribution of molecular gas reveals the dynamical processes within the system. Observations show physical and chemical variation among the components of multiple protostellar systems. However, the reason for this variation is not well understood, and few physico-chemical models of multiple protostellar systems have been done.

A survey of protostellar systems in Perseus including single and multiple protostars located in clustered and non-clustered regions, spanning evolutionary stages from Class 0 to Class II is used to study these questions. Using single dish observations 88.6–110.2 GHz, 215.2–220.4 GHz, and 360.1–362.7 GHz together with ALMA ACA observations in Band 6 and 7, the gas from molecular cloud scales ($>$10000 AU) down to the inner envelope scales ($\sim$1000 AU) is probed. Gas temperature, density, and mass are derived from the observations, and compared to multiplicity, evolutionary stage, region, bolometric luminosity from the SED, and envelope mass from 850 μm continuum. Molecular cloud gas temperature maps and gas kinematics are compared with the location of protostellar systems, and between clustered and non-clustered regions. The results of this survey indicate that gas temperature and density are not related to multiplicity, but rather the availability of gas mass is key in multiple star formation. Combining the results of this survey with existing observations of molecular inventories at $\lesssim$100 AU scales provides a way to explore physical and chemical variations between components.

Comparison of the results from the Perseus survey with other regions and mass ranges provides a broader vie of the factors that influence multiple star formation and their molecular gas environment.

Filament or sheet? The effects of the viewing angle on star formation

S. REZAEI KH.[1,2], AND J. KAINULAINEN[2]

[1] Max Planck Institute for Astronomy, Heidelberg, Germany sara@mpia.de
[2] Chalmers University of technology, Gothenburg, Sweden

Star formation properties of the molecular clouds are primarily derived from various observational quantities such as shape and column density. These observations, however, are limited to the 2D projected view of the clouds in the plane of the sky. Interstellar medium appears highly filamentary; specifically in regions of higher column densities which typically correspond to higher star formation rates. Nevertheless, there have been observations of molecular clouds such as California which show relatively low star formation efficiency despite its filamentary shape in the plane of the sky and its column densities in the same range as that of Orion A molecular cloud with an order of magnitude higher star formation rate. This raises the question of whether or not shape and column density are reliable tools to evaluate star formation efficiency of the molecular clouds.
We look into this subject via mapping the 3D structure of the clouds in dust using the latest Gaia data, combined with 2MASS and WISE photometry. We discover that, despite the apparent filamentary structure in the plane of the sky, California is a flat ∼120-pc-long sheet extending along the line of sight. We show that not only Orion A and California differ substantially in their 3D shapes, but also Orion A has considerably higher density substructures in 3D than California. This result presents a compelling reason why the two clouds have different star formation activities.
We expand our analysis to a larger sample of the local star-forming regions, and show how the clouds' surface area, mass, and surface density changes significantly with different viewing angles. Our results underline the importance of 3D information in interpreting star formation relations and challenge studies that rely solely on the column density thresholds to determine star formation properties in molecular clouds.

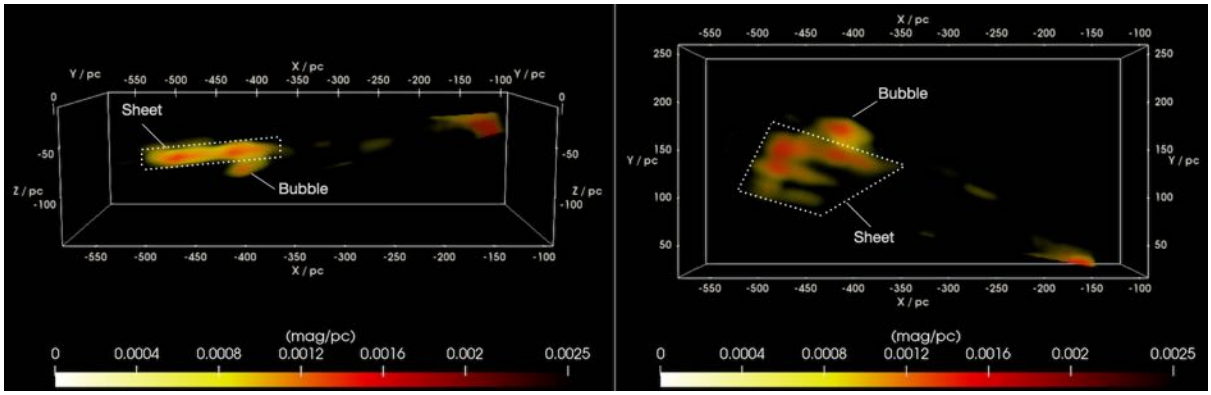

Figure 1: 3D substructures of the California molecular cloud projected from two viewing angles.

References:
Rezaei Kh., S., & Kainulainen, J., 2022, ApJ Letters, in press (Arxiv:2204.10892)
Kainulainen, J., Rezaei Kh., S., et al. 2022, A&A, 659, L6
Rezaei Kh., S. et al. 2020, A&A, 643, A151

LEGO: Observing the Milky Way to unravel Molecular Cloud Populations and Lifecycles in Galaxies

JENS KAUFFMANN[1] & THE LEGO COLLABORATION

[1] MIT Haystack Observatory, jens.kauffmann@mit.edu

Star formation is the key astrophysical process that converts baryonic matter into the stars and planets that form the backbone of galaxy structure. Consequently, the details of the star formation process have a substantial impact on the fundamental structure of galaxies, such as the spatial distribution of stellar populations and their metalicity. ALMA, and in future the ngVLA, therefore spend substantial fractions of their time on constraining the details of the star formation process in galaxies — but most of this important work must be done using *indirect* methods, as detail in extragalactic molecular clouds cannot be meaningfully resolved with physical beam sizes of $5\ \mathrm{pc} \cdot (d/\mathrm{Mpc}) \cdot (\vartheta_{\mathsf{beam}}/\mathrm{arcsec})$. The LEGO Large Program on the IRAM 30m-telescope, which images molecular clouds in the Milky Way, provides important data to *"calibrate"* these indirect methods, in many cases for the first time on the basis of observational data instead of theoretical models.

We provide an overview and status update on LEGO, which obtains the most comprehensive wide-field spectroscopic views of molecular clouds available to date. The survey has by now imaged two dozen clouds at frequencies 70–115 GHz. This work samples numerous astrophysically important molecules like CO, HCN, CS, and N_2H^+, and it generatesfor the first time a substantial sample of cloud-integrated line luminosities for these species. Emission from these molecules is, for example, widely used to probe the density and temperature structure of extragalactic molecular clouds. The LEGO data now can be used to test these methods used for such in well-studied galactic clouds, and to use this information to provide extragalactic work with improved and validated data analysis methods.

LEGO has for example already shown that emission from HCN is not a straightforward tracer of dense gas in galaxies (Kauffmann et al. 2017; Barnes et al. 2021), in contrast to what is frequently assumed in extragalactic research (e.g., Gao & Solomon 2004). Here we present new data on well-studied dense and cold molecular clouds that are representative of the onset of star formation (Broadmeadow et al., in prep.; Anderson et al., in prep.) — and that are esentially devoid of HCN emission, thus further questioning the use of HCN as a tracer of dense gas.

We also discuss how LEGO equips us with tools needed to unravel the molecular cloud populations in galaxies. Specifically, LEGO provides us with the cloud-averaged line luminosities needed to learn how different "types" of molecular clouds (e.g., very dense ones, or those disrupted by star formation feedback) can be identified from line ratios alone, and this knowledge can then be used to constrain the composition of cloud populations (e.g., relative ratio of clouds with and without star formation feedback) that would explain spectra observed in other galaxies. Initial results from LEGO (Broadmeadow et al., in prep.) reveal a rich diversity in cloud-averaged line ratios, highlighting the power of line ratios to constrain the properties of molecular clouds.

References:

Kauffmann, J., et al. 2017, A&A, 605L, 5
Barnes, A., et al. 2020, MNRAS, 497, 1972
Gao, Y., and Solomon, P.M. 2004, ApJ, 606, 271

Testing Star Formation Models in the Nearest Major Merger

A. BEMIS, A. R.[1], B. WILSON, C. D.[2]

[1] Leiden Observatory, Niels Bohrweg 2, 2333 CA Leiden, The Netherlands
bemis@strw.leidenuniv.nl
[2] McMaster University, 1280 Main Street West, Hamilton, Ontario, Canada

The Antennae (NGC 4038/9) is a prototypical major merger, and at 22 Mpc away ($1'' \sim 100$ pc) it is a useful target for studying star formation in turbulent environments. We present Cycle 6 ALMA observations of molecular gas at $\sim$cloud-scales, including CO and CN $J = 1 - 0$ emission and the radio continuum in bands 3 and 6. Recent work shows CN scales with HCN and is potentially a useful tracer of dense gas. We use the CN/CO ratio to estimate the dense gas fraction at $\sim$cloud-scales, and we compare CN emission with HCN Cycle 1 observations at > 200 pc scales to assess how well CN and HCN are tracing the dense, star-forming gas. The band 3 radio continuum is used to estimate the star formation rate. Results are compared against predictions of gravoturbulent models of star formation, and a radiative transfer analysis is performed by adopting the lognormal gas volume density Probability Density Function that is tied to these models of star formation.

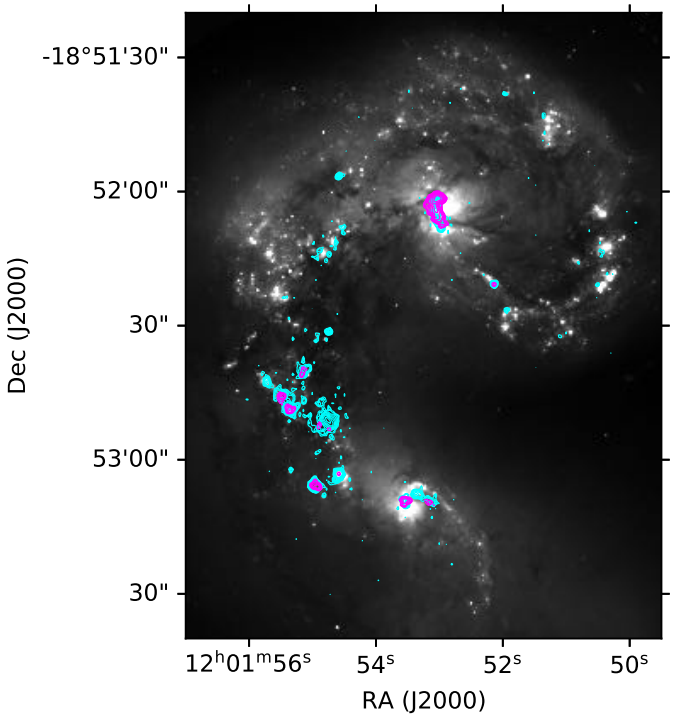

Figure 1: The Cycle 6 CN $J = 1 - 0$ (magenta) and 100 GHz radio continuum (cyan) emission at 90 pc resolution, overlaid on a *Hubble Space Telescope* composite optical image of the Antennae.

The SOFIA Massive (SOMA) Star Formation Survey and the open-source python package sedcreator

R. FEDRIANI[1] AND J. C. TAN[1,2]

[1] Chalmers University of Technology (Sweden), ruben.fedriani@chalmers.se
[2] University of Virginia (USA)

Massive stars have dramatic impacts throughout the universe at different scales and are one of the reasons you are reading this abstract today. But their birth, deep within dusty molecular clouds, is literally shrouded in uncertainty. The formation of massive protostars is still an open question and there is still a lot to be understood. Theories range from Core Accretion, i.e., a scaled-up version of low-mass star formation, to Competitive Accretion at the crowed centres of forming star clusters, to Stellar Collisions. The SOMA survey aims at understanding the basic formation mechanisms governing massive stellar birth through multi-wavelength observations but also through radiative transfer (RT) modelling of their spectral energy distributions (SEDs).
In this talk, I will present the current status of the SOFIA Massive (SOMA) Star Formation Survey for which more than 40 sources have been observed in the mid-infrared with SOFIA/FORCAST and that have been combined with Spitzer and Herschel observations. These data were used to construct SEDs and to fit a grid of RT models. To do this, we used the open-source python package sedcreator which will also be presented to the community. This package includes a number of convenient tools to measure fluxes on any astronomical image and to fit to a set of models. We find evidence that relatively massive protostars can form across a range of clump mass surface density environments, which contradicts some models for the required conditions of massive star formation. However, we see a trend that to form the most massive protostars, i.e., $m_* > 25\,M_\odot$, the mass surface density $(\Sigma_{\rm cl})$ needs to be $> 1\,{\rm g\,cm^{-2}}$. Our favoured explanation for this result is the Turbulent Core Accretion model prediction that the star formation efficiency of a core due to internal protostellar feedback is higher in higher $\Sigma_{\rm cl}$ environments.

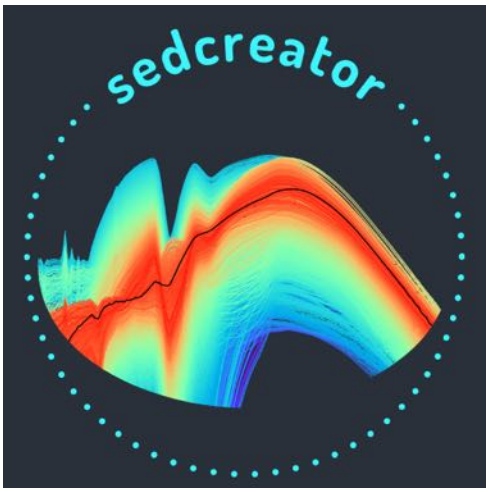

References:
https://github.com/fedriani/sedcreator

Isolated Massive Star Formation in G28.20-0.05

CHI YAN, LAW

[1]Chalmers University of Technology, chiyan.law@chalmers.se

Understanding the physical processes of massive star formation is essential in many aspect of astronomy. Infrared dark clouds have identified to be the progenitor of massive star and star cluster. However, it is remained an open question on the theory that describes the processes from cloud fragmentation, collapse, and formation of the protostars and star clusters. The high resolution and sensitivity of ALMA have opened up an unique window to probe deep into the distance embedded massive protostar forming region with great detail. Here we share report a ALMA high-resolution 1.3mm continuum and molecular line observations of the massive protostar G28.20-0.05 (Law et al. 2022, under review). Structure-finding analysis on the larger-scale continuum image indicates G28.20-0.05 is forming in a relatively isolated environment, with no other concentrated sources , i.e., protostellar cores, above $\sim 1\,M_{\odot}$ found from ∼0.1 to 0.4 pc around the source. The finding implies that a massive star can form in relative isolation and the dearth of other protostellar companions within the ~ 1 pc. The position of massive protostar is evidenced with a strong velocity gradient in the H30α emission toward the main continuum peak. It is evidence for a rotating, ionized disk wind, which drives a larger-scale molecular outflow. An infrared SED analysis indicates a current protostellar mass of $m_{*} \sim 24\,M_{\odot}$ forming from a core with initial mass $M_{c} \sim 400\,M_{\odot}$ in a clump with mass surface density of $\Sigma_{\rm cl} \sim 3\,{\rm g\,cm^{-2}}$.

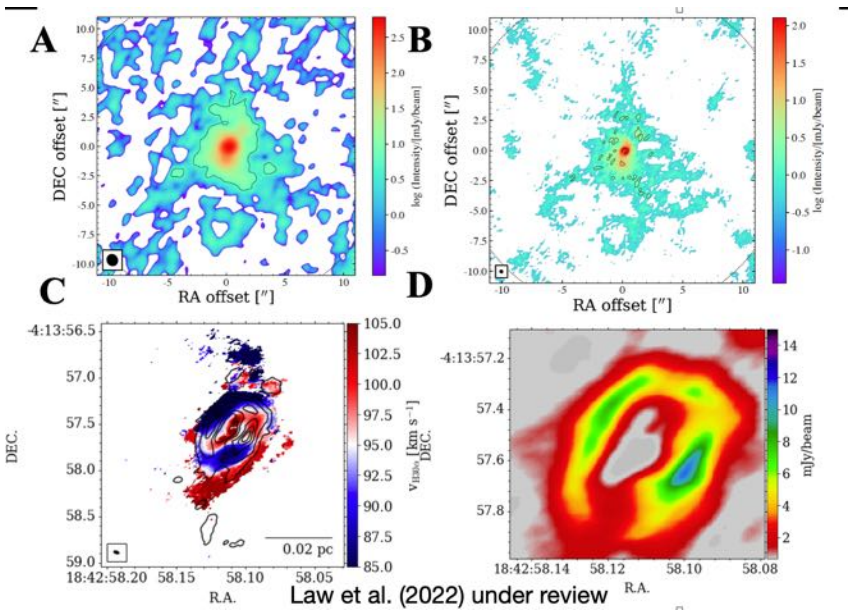

How do filaments form?

V. OSSENKOPF-OKADA[1]

[1] Universität zu Köln, I. Physikalisches Institut, ossk@ph1.uni-koeln.de

The wavelet decomposition of anisotropic structures introduced by Ossenkopf-Okada & Stepanov (2019) provides a versatile tool to quantify any filamentary structure without methological biases. It identifies filaments, measures the distribution of their widths and degrees of anisotropy in any two-dimensional data set.
As it can be applied in the same way to intensity maps and velocity maps it allows us to compare filamentary structures in density space with shock signatures in velocity space with respect to their spatial correlation. This provides a clue to the relative importance of self-gravity and external ram pressure for the formation of filaments. We can directly measure the shock-driven filament formation in hydrodynamic simulations.

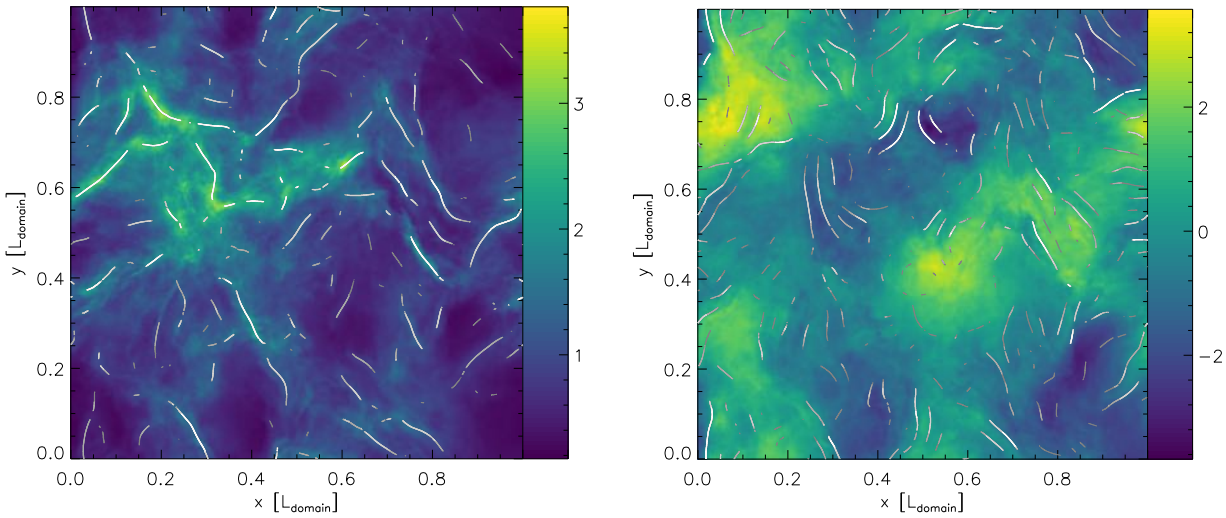

Figure 1: Column density and centroid velocity maps for a snapshot from the hydrodynamic simulations of Federrath et al. (2021), superimposed by the filament spines and the velocity shocks identified through the anisotropic wavelets sensitive to filaments with a width of $0.02\,L_{\rm domain}$. The brightness of the lines indicates the amplitude of the wavelet coefficients. One can see a frequent match in the locations of both types of anisotropic structures.

A comparison with observational data, however, shows that neither gravity nor large-scale flows are able to explain the observed structures in the Orion Molecular Cloud. Local feedback or magnetic fields must be responsible for the spatial offsets found between the intensity peaks and gradients in the velocity profiles of the existing molecular line data.

References:

Federrath, C., Klessen, R. S., Iapichino, L., & Beattie, J. R. 2021, Nature Astronomy, 5, 365
Ossenkopf-Okada, V. & Stepanov, R. 2019, A&A, 621, A5

The core population and kinematics of a massive clump: an ALMA view

E. REDAELLI[1], S. BOVINO[2], P. SANHUEZA[3], ET AL.

[1] Max-Planck-Institut für extraterrestrische Physik, eredaelli@mpe.mpg.de
[2] Departamento de Astronomía, Facultad Ciencias Físicas y Matemáticas, U. de Concepción
[3] National Astronomical Observatory of Japan, National Institutes of Natural Sciences

High-mass star formation theories make distinct predictions on the properties of the prestellar seeds of high-mass stars. Observations of the early stages of high-mass star formation can provide crucial constraints, but they are challenging and scarce. We investigated the properties of the prestellar core population embedded in the high-mass clump AG14.49 ($M_{\rm clump} = 5200\,{\rm M}_\odot$), and we studied the kinematics at the clump and the clump-to-core transition level. Our ALMA data consist of: Band 7 observations of the continuum emission and of o-$\rm H_2D^+(1_{1,0} - 1_{1,1})$, used to identify and study the core population and its properties; Band 6 data of dust thermal emission and $\rm N_2D^+$ (3-2) line; Band 3 observations of $\rm N_2H^+$ (1-0) transition, which traces the large scale gas kinematics. We performed dendrogram analysis of the o-$\rm H_2D^+$ data with the code SCIMES (1), identifying 22 cores. We have fitted their average spectra in LTE conditions, and we analysed their continuum emission at $0.8\,{\rm mm}$. We found that the cores are mostly low-mass, with $M_{\rm core} < 30\,{\rm M}_\odot$.

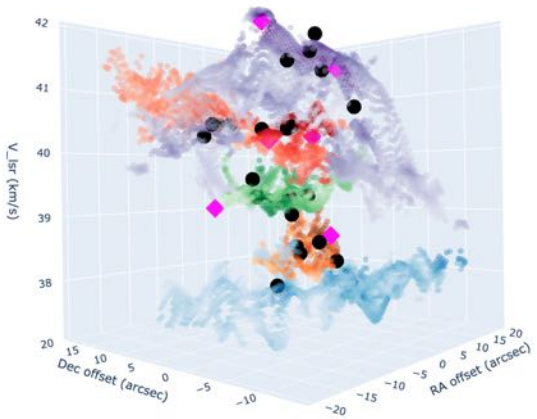

Figure 1: PPV plot of the results of the multi-component Gaussian fit performed on the $\rm N_2H^+$ data. The colors correspond to distinct hierarchical structures identified by ACORNS. The black circles and magenta diamonds show the positions of the prestellar and protostellar cores, respectively.

The analysis of the $\rm N_2H^+$ unveil a fairly complex kinematics within the clump. We fitted the data using a multi-component Gaussian analysis. The results of the fit were fed as an input to the hierarchical clustering algorithm ACORNS (2), which identifies five main coherent structures in ppv space (see Fig. 1). All of them are associated with $\rm H_2D^+$ cores and/or protostars, and they are active in star-formation. One of them, in particular, presents a filament-like structure that appears to be accreting mass towards one of the protostellar cores identified in outflow emission. We estimate a mass accretion rate towards the protostar of $\dot{M}_{\rm acc} \approx 2 \times 10^{-4}\,{\rm M}_\odot\,{\rm yr}^{-1}$, in agreement with other observational and numerical results. We conclude that the combination of o-$\rm H_2D^+(1_{1,0} - 1_{1,1})$ and $\rm N_2H^+$ (1-0) data represents a valuable diagnostic tool to investigate the dynamical properties of high-mass star-forming regions.

References:

(1) Colombo, D., Rosolowsky, E., Ginsburg, et al., 2015, MNRAS, 454, 2067
(2) Henshaw, J. D., Ginsburg, A., Haworth, T. J., et al. 2019, MNRAS, 485, 2457

Benchmarking the G351.77 protocluster: Gaia distance, gas mass, and star formation.

S. REYES[1], A. STUTZ[1], T. MEGEATH[2]

[1] Universidad de Concepcion, Concepcion, Chile reyes.r.simon.d@gmail.com
[2] University of Toledo, Toledo, OH, USA

I present ongoing work on the filamentary protocluster G351. The goal is to provide the necessary observational measurements for comparison to other better-studied and more nearby actively cluster-forming and gas-dominated regions, such as Orion A (Megeath et al. 2016) and the Integral Shaped Filament (ISF) where the Orion Nebula Cluster (ONC) star cluster is forming (e.g., Stutz & Gould 2016, Stutz 2018). We begin by noting that preexisting literature distances, arguably the most fundamental "nuisance parameter", are poorly constrained (with variations of factors > 2). Hence, we begin by analyzing the Gaia eDR3 parallaxes, proper motions and extinctions to obtain a distance constraint of $\sim$ 1.5 kpc. This analysis integrates 2MASS and GLIMPSE measurements, and potentially will include VVV as well. In this framework, we can then measure the gas mass and related metrics, such as the mass-to-length (M/L) profile of the filament. The starting point of this analysis is the Hershel column density map, N(H), and the above distance. Finally, we characterize the properties of the point-sources within G351, isolating the young stellar objects (YSOs) (Gutermuth et al. 2009) and complementing with YSOs from public catalogs. This allows us to estimate star formation rates (SFRs) and, in combination with the mass, efficiencies (SFEs). We then compare G351 with the Orion A cloud. In particular, the enclosed M/L profile of G351 is at least as high as for the ONC/M42, and much higher than for the ISF. Despite this high M/L, G351 is forming significantly fewer YSOs (by factors of $\sim$ 5). In order to explain as much as possible its particular SF activity in the framework of its large M/L, this begs the question of what could be the physical conditions that govern this cloud, such as a very young evolutionary state, or other possible sources of support against collapse (such as magnetic fields).

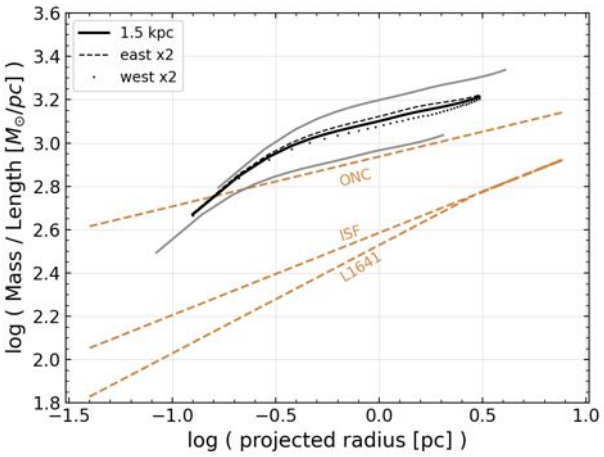

Figure 1: G351 enclosed line mass (M/L) profile (black curves) from Herschel data, averaged over the filament structure and assuming 1.5 kpc distance. Gray curves correspond to the M/L for the typical 1 and 2 kpc distances reported in literature and represent the uncertainty for this G351 measurement. The profiles of the Orion A structures (orange curves) are taken from Stutz & Gould (2016) and Stutz (2018).

References:

Gutermuth, R. A., Megeath, S. T. et al. 2009, ApJS, 184, 18
Megeath S. T. et al. 2016 AJ 151 5
Stutz & Gould 2016, A&A 590, A2
Stutz 2018, MNRAS 473, 4890–4899

On the traceable signatures of episodic accretion in embedded binary YSOs

R. RIAZ[1], D.R.G. SCHLEICHER[2], S. VANAVERBEKE[3], AND RALF S. KLESSEN[4]

[1] Centro de Investigación en Astronomía, Universidad Bernardo O'Higgins, Av. Viel 1497, Santiago, Región Metropolitana, Chile, rafeel.riaz@ubo.cl
[2] Departamento de Astronomía, Facultad Ciencias Físicas y Matemáticas, Universidad de Concepción, Av. Esteban Iturra s/n Barrio Universitario, Casilla 160-C, Concepción, Chile
[3] Centre for mathematical Plasma-Astrophysics, Department of Mathematics, KU Leuven, Celestijnenlaan 200B, 3001 Heverlee, Belgium
[4] Universität Heidelberg, Zentrum für Astronomie, Institut für Theoretische Astrophysik, Albert-Ueberle-Str. 2, 69120 Heidelberg, Germany

We explore the state of turbulence in the Jeans unstable molecular gas cores and its possible connection to episodic accretion in the resulting young stellar objects (YSOs). We focus on the formation and evolution of the embedded binary systems and report strong accretion bursts between the two companions with a recurrence time-scale of about 1 kyr. In the collapsing gas cores with subsonic velocity dispersion, we find that the secondary companion is more active than the primary companion such that the peak value of the mass accretion rates in the former is as high as 2 $\times 10^{-2}$ $M_\odot$ yr^{-1}. This makes the secondary companion of such binary systems a potential candidate to leave observable traces of episodic accretion in the surrounding gas. In general, our simulations suggest an order of magnitude more intense accretion bursts in prestellar cores with subsonic velocity dispersions than in gas cores with supersonic velocity dispersions. However, the simulations with supersonic turbulence in the prestellar gas cores show the formation of a number of binary YSOs in which the primary companion appears more active in accreting material from the nearby gas reservoir. This finding indicates a potential formation-channel of binary systems with extreme mass ratios.

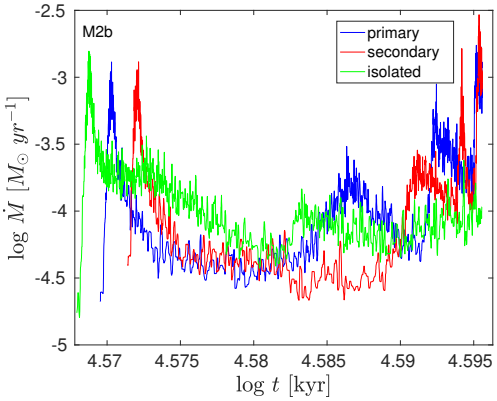

Figure 1: Accretion rates for the primary (blue), secondary (red), and isolated protostars (green) in models M2b (i.e. gas core with subsonic velocity dispersion). The accretion rate is given in units of $M_\odot$ yr^{-1} and the time is in kyr (Riaz et al. 2021).

References:

Riaz R., Schleicher D., Vanaverbeke S., Klessen R. 2021, MNRAS, 4, 6061

A detailed kinematic analysis of the DR21 Main outflow

SKRETAS I. M. [1], WYROWSKI F.[1], MENTEN K.[1], BEUTHER H.[2] AND THE CASCADE TEAM

[1] Max Planck Institute for Radioastronomy, iskretas@mpifr-bonn.mpg.de
[2] Max Planck Institute for Astronomy

Context: Molecular outflows are commonly detected originating from forming stars. One of the most famous such outflows is that associated with the DR21 Main located in the Cygnus-X molecular cloud. The outflow is believed to arise from a forming massive star and extends close to the plane of the sky. Recent work has suggested the existence of a new type of explosive outflows, formed by the collapse of protostellar clusters. Since then it has been suggested that DR21 Main actually represents an example of this new type of outflows (Zapata et al. 2013).
Aims: Exploring in detail the kinematics and structure of the DR21 Main outflow, using several different molecular tracers, we aim to determine the true nature of the DR21 outflow.
Methods: As part of the MPG-IRAM Observatory Programs (MIOP) CASCADE, we have imaged emission from various molecular lines toward the Cygnus-X molecular cloud system, including DR21, with both the IRAM 30m telescope and the NOEMA interferometer. The nature of these observations (low and high angular resolution respectively) allows for the examination of the outflows kinematics and its structure at large and small scales simultaneously.
Results: Integrated intensity maps of HCO+ emission observed with the IRAM 30m telescope reveals the well known structure of DR21, with a clear bipolar outflow. The clear separation of the two outflow lobes and the simultaneous red- and blue-shifted emission detected in both of them confirm the assumed orientation of the outflow as being close to the plane of the sky. Higher spatial resolution integrated intensity maps constructed using NOEMA observations show no sign of fillamentary outflow structures, a primary characteristic of explosive outflows as described in Zapata et al. (2017). In addition position-velocity maps of HCO+, HNC, HCN and H2CO IRAM 30m show a symmetrical velocity distribution for the two outflow lobes, a behaviour more like that of a clear bipolar outflow than the more chaotic nature expected from an explosive outflow. Additionally, signs of interaction between the outflow and a cold, dense structure located west of DR21 Main are found in zeroeth, first and second moment maps.
Conclusions: Overall, the revealed structure of the DR21 Main outflow suggests that it is most likely a typical bipolar outflow, and is therefore not a proper candidate for the newly proposed type of explosive protostellar outflows. At the same time, further investigation is required in order to properly identify the nature of the apparent interaction between the outflow and the dense structure near the west lobe.

References:
[1]Zapata, L. A., “A 10,000 Year Old Explosion in DR21”, The Astrophysical Journal, vol. 765, no. 2, 2013.
[2]Zapata, L. A., “Molecular Outflows: Explosive versus Protostellar”, The Astrophysical Journal, vol. 836, no. 1, 2017.

Submillimeter water masers in Young Stellar Objects

I. DE GREGORIO-MONSALVO[1], S. GIL[2], A. SANTAMARÍA-MIRANDA[1], A. PÉREZ-SÁNCHEZ[3], J.F. GÓMEZ[4], A. PLUNKETT[5], AND M. SCHREIBER[6]

[1] European Southern Observatory, Chile, idegrego@eso.org
[2] Pontificia Universidad Católica, Chile
[3] Allegro ALMA ARC Node, The Netherlands
[4] Instituto de Astrofísica de Andalucía, IAA-CSIC, Spain
[5] National Radio Astronomy Observatory, USA
[6] Universidad de Valparaíso, Chile

Water is one of the few molecules capable of producing maser emission in star-forming regions and it has been detected in a wide range of masses from low to massive young stellar objects. Previous studies in the past decades have focused on the water maser transition at 22 GHz, making use of facilities operating at centimeter wavelengths. Water masers at 22 GHz constitute a good tracer of mass-loss activity in young stars of all masses. In low-mass protostars these are mostly present during the very first stages of evolution and they tend to be located close to the central protostar when the most powerful mass-loss phenomena are present. Recent studies suggest these masers trace also mass loss phenomena in intermediate and high mass sources.
The water molecule shows several maser transitions at submillimeter wavelengths, which makes last generation of submillimeter telescopes like APEX and ALMA excellent facilities to follow up in the submillimeter range the studies done in the past decades at 22 GHz.
In this poster we present a survey of submillimeter water maser transitions at 321 and 325 GHz in a sample of young stellar objects with a wide range of masses, from high to low-mass. We show a preliminary analysis of the results of these surveys, including a study of the detection rates and fux density ratios at different transitions, which is related to density and temperature conditions of the masing regions. We also present an analysis of the velocity structure of different maser lines, which in combination with future higher angular resolution studies could reveal if the presence of jet-like structures is something expected across all range of masses. This is particularly interesting in the case of high-mass young stars since it impacts directly in their possible formation mechanisms.

Session IIIc: The ISM and Molecular Clouds: abundances, chemistry and microphysical processes

The Molecular Composition of Interstellar Clouds and what we learn from it

DAVID A. NEUFELD[1], ARSHIA JACOB[1]

[1] William H. Miller III Department of Physics and Astronomy
Johns Hopkins University, Baltimore, Maryland, USA neufeld@pha.jhu.edu

Observations at ultraviolet, visible, and particularly infrared and radio wavelengths provide a wealth of information about the molecular inventory of the interstellar medium (ISM). Because of the different chemical pathways responsible for their formation and destruction, different molecules probe specific aspects of the interstellar environment. Carefully interpreted with the use of astrochemical models, they provide unique information of general astrophysical importance, yielding estimates of the cosmic ray density, the molecular fraction, the ultraviolet radiation field, the dissipation of energy within the turbulent ISM and the age of interstellar gas clouds

Chemistry and molecular cloud properties in nearby galaxies

N. HARADA[1], S. MARTÍN[2], J. MANGUM[3], AND ALCHEMI COLLABORATION

[1] National Astronomical Observatory of Japan, nanase.harada@nao.ac.jp
[2] European Southern Observatory / Joint ALMA Observatory
[3] National Radio Astronomy Observatory

Starburst and active galactic nuclei influence the chemical and physical properties of the interstellar medium surrounding them. Recent development of high angular resolution, high sensitivity instruments enabled multi-species, multi-transition survey to study such molecular cloud properties in nearby galaxies. In this talk, I will present chemical and physical properties in starburst galaxies, an AGN-host galaxy, a merger. In particular, I will focus on results from the ALCHEMI survey, an ALMA large program of wide-frequency spectral scan (Figure 1, Martín et al. 2021). Our results show that even the lower-sensitivity data from 7-m array detected 78 species with $\sim$750 transitions. From our chemical compositions, the cosmic-ray ionization rates are found to be elevated by at least a few orders of magnitude compared with that in the Galactic disk clouds (Holdship et al., 2021, 2022, Harada et al. 2021). Both excitation and chemical compositions exhibit signs of shocks at the orbital intersections where the gas flows into the central region of NGC 253 (Humire et al. 2022). In addition, our survey made a first extragalactic detection of phosphorus-bearing species.

References:

• D. Haasler, V. Rivilla, S., Martín et al. (2021) A&A, 659, 158
• N. Harada, S. Martín, J. Mangum et al. (2021) ApJ, 923, 24
• J. Holdship, S. Viti, S. Martín et al. (2021) A&A, 654, 55
• J. Holdship, J. Mangum, S. Viti et al. (2022), A&A, in press
• P. Humire, C. Henkel, A. Hernández-Gómez et al. (2022) A&A, in press
• S. Martín, J. Mangum, N. Harada, et al. (2021) A&A, 656, 46

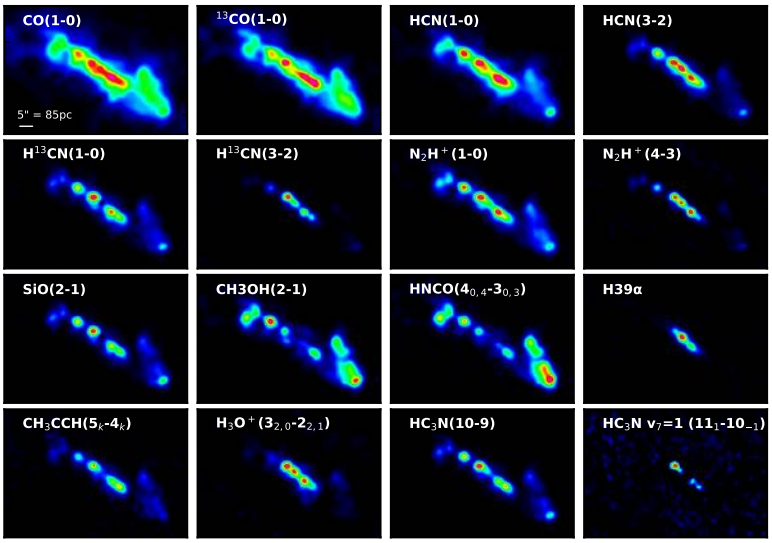

Figure 1: Integrated intensity images of selected transitions in the central region of the starburst galaxy from the ALCHEMI survey.

Multi dimension analysis of molecular clouds: the example of the Orion-B cloud

M. GERIN[1], J. PETY[2], E. BRON[1], A. ROUEFF[3], AND THE ORION-B CONSORTIUM

[1] LERMA, Observatoire de Paris, PSL Research University, Sorbonne Université and CNRS, France, Maryvonne.gerin@obspm.fr
[2] IRAM, Saint Martin d'Hères, France. [3] Aix Marseille University, CNRS, Centrale de Marseille and Institut Fresnel, Marseille, France.

Instead of mapping the emission of a single line towards molecular clouds, current receivers enable simultaneous spatial and spectral surveys of the ISM. The ORION-B project aims at obtaining a five square degree map of a subset of the Orion-B molecular cloud over the 3mm spectral window at 30" (0.05 pc) and 0.5 kms^{-1} resolution. This unprecedented spatial and spectral coverage allows to probe how the cloud structure and chemical abundances are related over a wide range of column density, incident UV radiation and volume density. The quality and volume of the data also require new analysis methods that provide trustable estimates of the physical conditions, molecular column densities and abundances and their associated uncertainties. This presentation will discuss the observations and data analysis strategy and introduce the new methods that are currently deployed in the ORION-B team. A particular emphasis will be put on the determination of the molecular column densities, physical conditions and abundances from the acquired information, and on possible steps in the future.

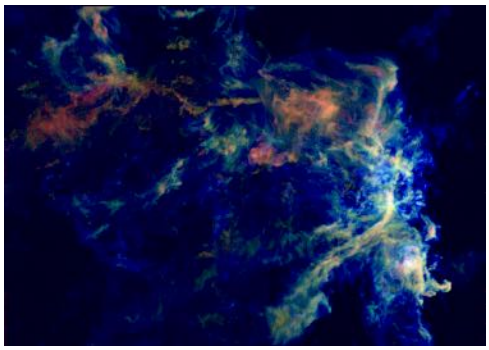

Figure 1: *CO emission towards the Orion B molecular cloud. The CO(1-0) peak temperature is coded in Blue, ^{13}CO(1-0) in Green and C^{18}O(1-0) in red.*

References:

Bron et al., A&A, 610, 12 (2018)
Bron et al., A&A, 645, 28 (2021)
Gratier et al., A&A, 599,100 (2017)
Gratier et al., A&A, 645, 27 (2021)
Orkisz et al., A&A, 599, 99 (2017)
Orkisz et al., A&A, 624, 113 (2019)
Pety et al., A&A, 599, 98 (2017)
Roueff et al., A&A, 645, 26 (2021)

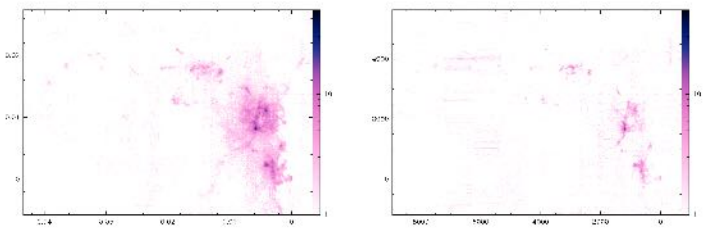

Figure 2: *Left HCO$^+$ (1-0) integrated intensity, Right HNC(1-0) integrated intensity. Both lines are displayed using the same logarithmic intensity scale.*

Cosmic rays: shaping dynamics and chemistry in star-forming regions

MARCO PADOVANI[1]

[1] INAF-Osservatorio Astrofisico di Arcetri, Firenze, Italy
marco.padovani@inaf.it

In recent years, exciting developments have taken place in the identification of the role of cosmic rays in star-forming environments. Observations from radio to infrared wavelengths and theoretical modelling have shown that low-energy cosmic rays (< 1 TeV) play a fundamental role in shaping the chemical richness of the interstellar medium, determining the dynamical evolution of molecular clouds. I will summarise in a coherent picture the main results obtained by observations and by theoretical models of propagation and generation of cosmic rays, from the smallest scales of protostars and circumstellar discs, to young stellar clusters, up to Galactic scales. I will also discuss new fields that will be explored in the near future thanks to new generation instruments, such as: SKA and its precurors, for the synchrotron emission; JWST for the estimate of the cosmic-ray ionisation rate; CTA, for the γ-ray emission from high-mass protostars.

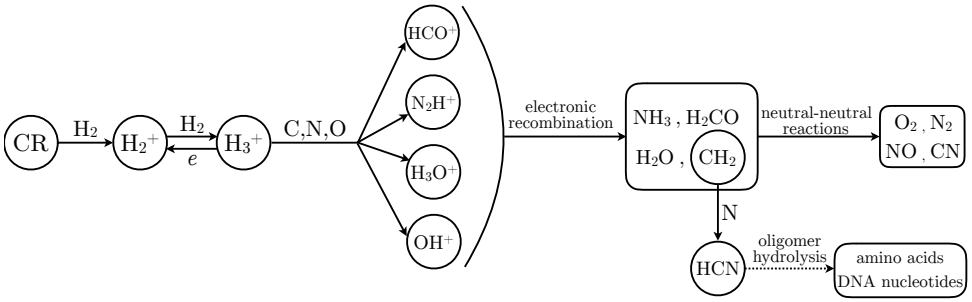

Figure 1: Simplified chemistry network induced by cosmic rays in molecular clouds.

References:
Padovani, M. et al. 2009, A&A, 501, 619
Padovani, M. et al. 2011, A&A, 530, A109
Padovani, M. et al. 2013, A&A, 560, A114
Padovani, M. et al. 2014, A&A, 571, A33
Padovani, M. et al. 2015, A&A, 582, L13
Padovani, M. et al. 2016, A&A, 590, A8
Padovani, M. et al. 2018, A&A, 614, A111
Padovani, M. et al. 2018, A&A, 619, A144
Padovani, M. et al. 2018, A&A, 620, L4
Padovani, M. et al. 2020, SSRv, 216, 29
Padovani, M. et al. 2021, A&A, 649, A149
Padovani, M. et al. 2021, A&A, 651, A116
Padovani, M. et al. 2022, A&A, 658, A189

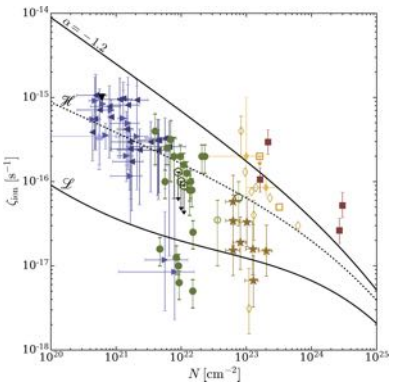

Figure 2: Cosmic-ray ionisation rate as a function of the H_2 column density. Comparison between models and observations.

Molecular cloud formation in metal-poor gas

S. GLOVER[1]

[1] Zentrum für Astronomie, Universität Heidelberg

In the Milky Way and in other metal-rich spiral galaxies, there is a clear correlation between molecular gas, as traced by CO emission, and star formation. Observations of local metal-poor dwarf galaxies show that this correlation begins to break down at low metallicity, but it remains unclear whether this is just because CO becomes a poor tracer of molecular gas in these conditions, or whether star formation starts to become associated with clouds dominated by atomic hydrogen. In this talk, I review recent theoretical work on this topic and discuss the opportunity that JWST offers to distinguish between these scenarios.

TEMPO: Tracing The Evolution of Massive Protostellar Objects: Fragmentation and Chemical Properties

G. A. FULLER[1,2], A. AVISON[1,3], N. ASABRE FRIMPONG[1], YONGXIONG WANG[1]

[1] Jodrell Bank Centre for Astrophysics, The University of Manchester,
g.fuller@manchester.ac.uk
[2] I. Physikalisches Institut, University of Cologne, [3] SKA Observatory

The Tracing Evolution in Massive Protostellar Objects (TEMPO) project is a study of a colour-luminosity selected sample of 38 massive star forming regions observed with ALMA at 1.3mm. Using the spectral line free continuum emission we explore the fragmentation, clustering and flux density properties of this sample of massive star forming protoclusters to investigate how and if these properties change as a function of luminosity and colour. In this presentation we will discuss the fragmentation properties of the sources and how the flux budget is distributed among the fragments. Methods of line-free continuum channel selection within ALMA data and a generalised approach for distinguishing sources which are potentially star-forming from those which are not, utilising interferometric visibility data will be discussed. The sources show a range of molecular species including complex organic molecules. We will also discuss the properties of the spectra and the chemical composition of the circumstellar regions of the objects. Focussing on CH_3CN, CH_3OH and other nitrogen and oxygen containing complex species, we will discuss how the properties of the molecular emission change as a function of luminosity and colour of the sources. This will be used to investigate how the physical and chemical properties of the circumstellar regions can be used to probe the evolution of the sources.

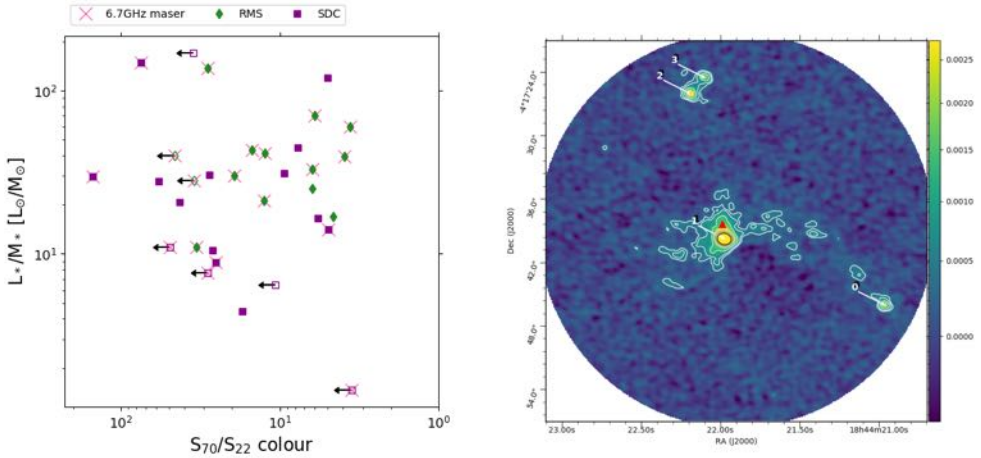

Figure 1: *Left:* The distribution of the TEMPO sources in the L/M – S(70μm)/S(22μm) plane. The markers indicate the original survey from which the sources are drawn and whether they are associated with a 6.7 GHz Class II methanol maser. Open markers with arrows indicate sources with upper limits at 22μm. *Right:* Example of the combined aggregate bandwidth continuum image for SDC28.277-0.352_1. The red triangle indicates the position of a 6.7GHz methanol maser.

HyGAL: Characterizing the Galactic ISM with observations of hydrides and other small molecules – First Results

A. M. JACOB[1,2], D. A. NEUFELD[1], P. SCHILKE[3], W-J. KIM[3] AND THE HYGAL TEAM

[1] William H. Miller III Department of Physics & Astronomy, Johns Hopkins University, Baltimore, MD 21218, USA, ajacob51@jhu.edu
[2] Max-Planck-Institut für Radioastronomie, Auf dem Hügel 69, 53121 Bonn, Germany,
[3] I. Physikalisches Institut, Universität zu Köln, Zülpicher Str. 77, 50937 Köln, Germany

One of the fundamental questions in modern astronomy concerns the life cycle of molecular material in the universe and addressing how molecular clouds are formed. Given, that atomic and molecular hydrogen gases form the major components of the neutral interstellar medium (ISM), cloud formation must involve the transition from regions dominated by HI gas to those dominated by H_2 gas. While this phase transition is determined by the environmental conditions in the ambient gas it is primarily driven by changes in the pressure or density (or column density). In addition, the chemical transition from gas which is mainly atomic to gas which is mainly molecular is a critical step in initiating the growth of chemical complexity in the ISM both locally and across Galactic scales. Therefore, understanding the processes responsible for this phase transition are crucial.

While this topic is highly complex, absorption spectroscopy of hydrides (molecules/molecular ions with a heavy atom covalently bonded to one or more hydrogen atoms) performed over the past decade have provided a wealth of new information about their use as sensitive tracers of different phases of the ISM. Moreover, being light molecules, their fundamental rotational transitions lie at terahertz frequencies, a frequency window for which SOFIA provides a unique access to. In this talk I will introduce HyGAL, a SOFIA Legacy program aimed to address several questions related to the HI-to-H_2 phase transition and star-formation in general using observations of hydrides (see, Jacob et al. 2022), such as (1) What is the distribution of the H_2 fraction in the ISM? (2) How does the density of low-energy cosmic-rays vary within in the Galaxy and (3) What is the nature of interstellar turbulence and what mechanisms lead to dissipation?

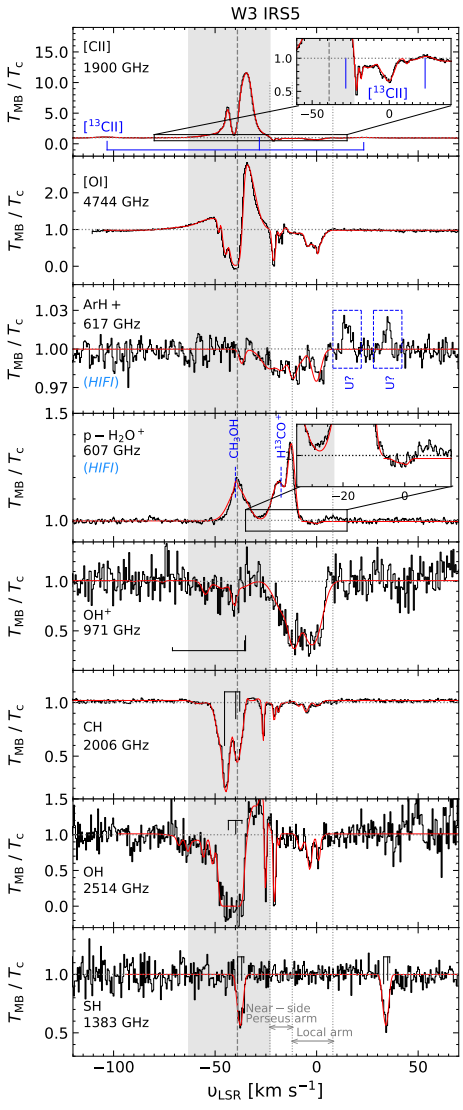

Figure 1: From top to bottom: The normalized spectra of the HyGAL species (C^+, O, ArH^+, p-H_2O^+, OH^+, CH, OH and SH) toward W3 IRS5 in black alongside their fits in red.

References:

Jacob, A. M., Neufeld, D. A.,(2022), ApJ, in press

HyGAL, II. The absorption line survey with the IRAM 30m telescope

W.-J. KIM[1], P. SCHILKE[1], D. A. NEUFELD[2], A. M. JACOB[2], D. SEIFRIED[1], A. SANCHEZ-MONGE[1], S. WALCH[1], E. FALGARONE[3], B. GODARD[4], F. WYROWSKI[5], V.S. VEENA[5], K. M. MENTEN[5], T. MÖLLER[1]

[1] I. Physikalisches Institut, Universität zu Köln, Zülpicher Str. 77, 50937 Köln, Germany, wonjukim@ph1.uni-koeln.de
[2] William H. Miller III Department of Physics & Astronomy, Johns Hopkins University, Baltimore, MD 21218, USA
[3] Laboratoire de Physique de l'ENS, ENS, Université PSL, CNRS, Sorbonne Université, Université de Paris, 24 rue Lhomond, 75005 Paris, France
[4] LERMA, Observatoire de Paris, PSL Research University, CNRS, Sorbonne Universités, F-75014 Paris, France
[5] Max-Planck-Institut für Radioastronomie, Auf dem Hügel 69, 53121 Bonn, Germany

As a part of the SOFIA Legacy Program HyGAL, we report the absorption line survey for simple molecules in Galactic diffuse and translucent clouds. We surveyed absorption lines at 2 and 3 millimeter wavelengths using the IRAM 30m telescope toward 15 millimeter continuum sources, which are massive star-forming regions located in the first and second quadrants. We detected HCO^+ absorption lines toward 14 sightlines, which contains 79 foreground cloud components, as well as HCN, HNC, C_2H, and $c-C_3H_2$ toward most lines of sight. In addition, CS and H_2S absorption lines are found in at least half of the continuum sources. The spectral data obtained were analyzed to characterize the chemical and physical properties of the interstellar medium statistically. The column density ratios of the seven molecular species observed are very similar to the previous observation of absorption lines from diffuse clouds at high latitudes. Combining the data sets of the SOFIA hydrides and the 30m simple molecules, we find that there are three groups of species, the ion, neutral and molecular species (see Figure 1). We also find higher H_2S abundances in diffuse clouds ($X(H_2S) \sim 10^{-8}$ to 10^{-7}) than in translucent clouds ($X(H_2S) \sim 10^{-9}$ to 10^{-8}). Such a sudden decrease in H_2S abundances from diffuse to translucent clouds possibly indicate the evidence of the first depletion of sulfur (S+) during the translucent phase in absorption clouds.

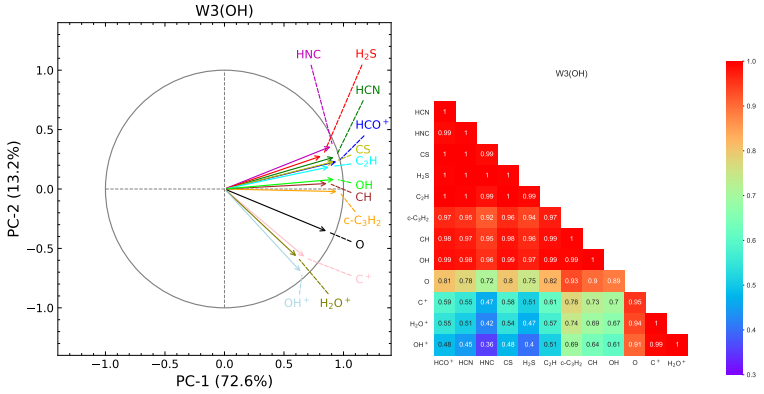

Figure 1: *Left*: Variable correlation circle plot for the first and second PCA dimensions toward W3(OH). *Right*: Correlation coefficients between different pairs of species shown as the heat map.

Hot molecular cores associated to the brightest far-infrared clumps in the Southern Milky Way

M. MERELLO[1], L. BRONFMAN[1], E. MENDOZA, [2], ET AL.

[1] Departamento de Astronomía, Universidad de Chile, Chile. mmerello@das.uchile.cl
[2] Departamento de Ciencias Integradas, Universidad de Huelva, Spain.

High-mass stars (M$>$ 8 M$\odot$) and star clusters are born deeply embedded in dusty condensations called molecular clumps. Once new protostars heat their surrounding dense dust and gas, they provoke the evaporation of ice mantles around dust grains. This Hot Molecular Core (HMC) phase is characterized by high values of gas temperature and density ($T_{gas} \sim 100$ K, n=$10^5 - 10^8$ cm^{-3}), high luminosities ($> 10^4$ L$_\odot$), and the presence of a rich spectrum of organic species.
Here we present our study of HMC candidates, using the APEX telescope. Our sample gathers ∼80 luminous sources selected from the Hi-GAL survey, associated with dense gas emission and in an advanced stage of evolution as traced by their luminosity-to-mass ratio, distributed between the III & IV Galactic Quadrants within a distance of 7 kpc. For this sample, we have conducted molecular line observations on a large range of frequencies (170 - 400 GHz) of different tracers of dense gas (HCN, HCO^+, CO, CS, HC_3N) and their isotopologues, shocked material (SiO), and temperature tracers (CH_3CCH, CH_3CN, CH_3OH). This is a valuable sample for astrochemical studies, e.g. allowing the detection of formamide (NH2CHO) and the isocyanic acid (HNCO), which are important pre-biotic species that can produce molecules containing peptide bonds, such as simple amino acids.

In particular, we present first detections in some of these sources of water emission, either by 183.31 GHz masers or thermally excited lines of $H_2^{18}O$ $3_{1,3} - 2_{2,0}$ and $4_{1,4} - 3_{2,1}$. Results of this work allowed us to determine physical properties of environmental gas of clumps, detect and characterize their very energetic molecular outflows, construct rotational diagrams of CH3CCH k-ladders over energies E_{up}/k= 50-350 K, and model their emission through LTE approximations, and associate the $H_2^{18}O$ emission to heated gas with $T_{ex} > 100$K. Finally, we will show preliminary results of conducted follow up studies on selected sources, leading to detections of deuterated water (HDO), first detections of high transitions of SiO (J=16-15/15-14/14-13) with APEX at $\sim 600-700$ GHz, and ALMA/ACA observations of 9 outer Galaxy sources.

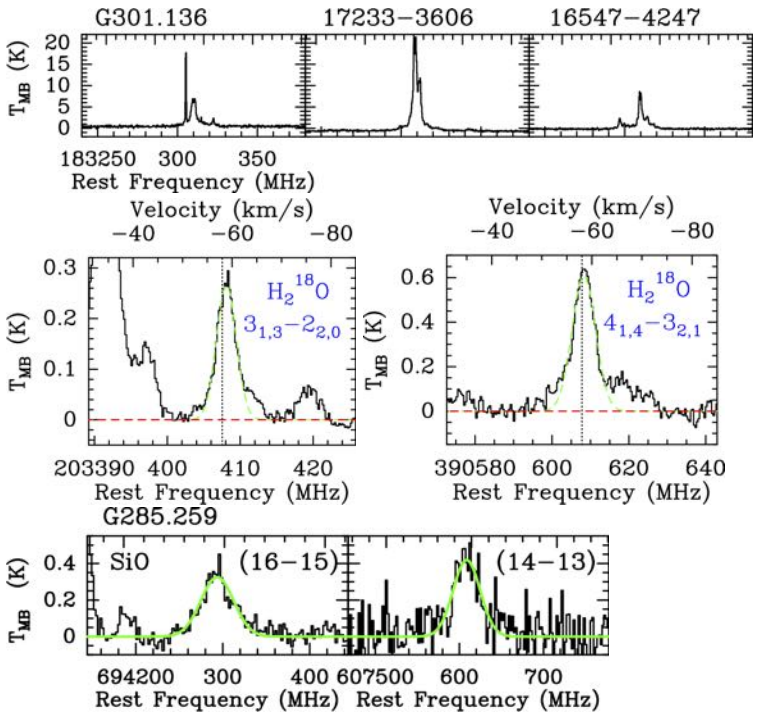

Figure 1: Top: Examples of discovered 183.31 water masers. Middle: Detection of the two $H_2^{18}O$ lines for 16164-5046. Fit line shows LTE model with $T_{rot} = 218$ K and N=6.0×10^{14} cm^{-2}. Bottom: Detection of SiO J=16-15/14-13 on G285.259.

Resolving Taurus Protoplanetary Disks down to a few au scale with ALMA Super-resolution Imaging

M.YAMAGUCHI[1,*], T.TSUKAGOSHI[2], T.MUTO[3], H.NOMURA[4,5], T.NAKAZATO[4], S.IKEDA[6,5], N.HIRANO[1], AND R.KAWABE[4,5],

[1] Academia Sinica Institute of Astronomy and Astrophysics, [2] Ashikaga University, [3] Kogakuin University, [4] National Astronomical Observatory of Japan, [5] Graduate University for Advanced Studies, [6] The Institute of Statistical Mathematic, * masayuki.yamaguchi.astro@gmail.com

ALMA high-resolution observations have spatially resolved disk substructures such as gaps and rings, likely generated by forming planets in the regions. The observed disks are, however, biased toward large disks ($r > 50$ au), and disk substructures of compact disks ($r < 50$ au) dominant in low-mass star-forming regions have not been well investigated. Increasing gap detections in not only large disks but also compact ones are crucial for confirming the overall tendency in the architecture of the disk substructure.

Here we present extremely high resolution ($< 0''.1$) images of the 1.3 mm continuum emission from 42 Taurus disks (their dust disk radii ranging from $8-200$ au). We used the ALMA archival data of Band 6. For the image reconstruction, we applied the sparse modeling (SpM) imaging technique that possibly improves the fidelity and spatial resolution of the ALMA images [1, 2]. We obtained images with spatial resolutions of $0''.02 - 0''.1$ ($3 - 14$ au), which is $2 - 3$ times better than those of the conventional CLEAN images.

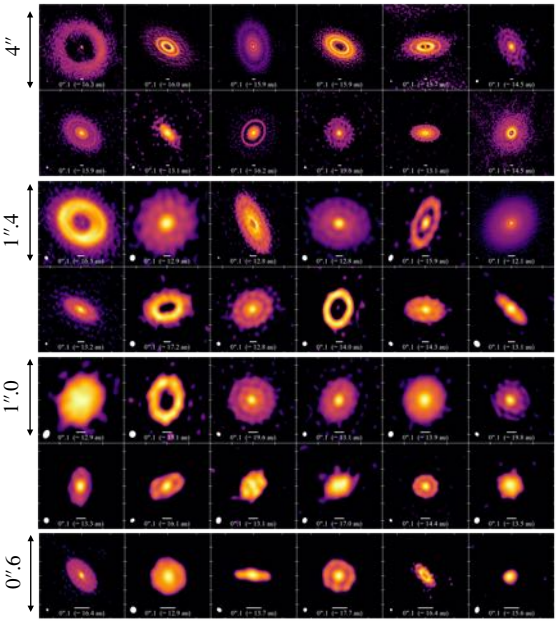

Figure 1: Gallery of 1.3-mm (Band 6) dust continuum images for 42 Taurus protoplanetary disks.

Figure 1 shows the SpM images of the 42 disks. We found that 18 disks have substructures with gaps & rings, 15 disks have ones with abrupt changes in the slopes of the radial intensity profile but not identified as gaps (i.e., unresolved gaps), and four disks have a ring alone. It is shown that the substructures are common even for the compact disks. In a total of the disks, we found 25 gaps & rings and 30 unresolved gaps. The relation between the gap size (calculated from a product of the gap width and depth) and the spectral type of the central star has been analyzed in the sample including eight DSHARP disks. We found that the sizes of the gaps at larger radii ($r > 20$ au) show the dependence on the stellar spectral type: the gap sizes in the A-F-G- type stars are larger by an order of magnitude than those in the M-K-type stars. Assuming that the gaps are caved by the planets and their sizes are proportional to the planetary masses, the observed gap size v.s. spectral type correlation implies the positive correlation between the planetary mass and the stellar mass.

References:

1.M.Yamaguchi, K.Akiyama, T.Tsukagoshi, T.Muto, et al, 2020, ApJ, Vol. 895, p84
2.M.Yamaguchi,T.Tsukagoshi, T.Muto, H.Nomura, et al. 2021, ApJ, Vol.923, p121

Large scale deuteration of molecules in the Cygnus-X molecular cloud complex

I. B. CHRISTENSEN[1], F. WYROWSKI[1], AND THE CASCADE TEAM

[1] Max-Planck-Institut für Radioastronomie, Auf dem Hügel 69, D-53121, Bonn, Germany,
ibarlach@mpifr-bonn.mpg.de

Probing the initial conditions and early stages of high-mass clumps is key for our understanding of the formation of high-mass star clusters. In the cold, dense natal molecular cloud that gives birth to new stars, deuterated molecules are efficiently formed. Deuteration is mainly driven by the reaction H_3^+ + HD $\rightarrow$ H_2D + H_2 + 230 K, which is exothermic and proceeds at low temperature (below 25 K) leading to a high degree of deuteration in clumps hosting young stellar objects. At low temperatures, DCO^+ is primarily formed through H_2D^+. DCN and DNC are formed through deuteration, also at low temperatures, from HCN and HNC. As the temperature increases DNC is destroyed or DCN is formed more efficiently, leading to a higher DCN/DNC-ratio in warmer environments. NH_2D is formed through NH_3 reacting with deuterated ions as well on the grain surfaces through hydrogenation/deuteration of N. Observing the ground state transitions of deuterated molecules provides a unique view on the conditions of the cold phases, hence gives an insight of the early-stages of high-mass star formation.

In the frame of the Cygnus All-scale Survey of Chemistry and Dynamical Environments (CASCADE), we aim to explore the large-scale structure of deuterated molecules in the cloud complex Cygnus X at 3-mm wavelength, an ideal hunting ground for massive clumps. The large-scale structure of deuterated molecules towards high density regions in Cygnus-X is mapped. A total of 12 sub-regions within Cygnus-X are mapped in lines from NH_2D, DCO^+, DCN and DNC, the deuterated molecules that show the most extended emission. There are clear differences in the morphology of these molecules' distributions that allow us to constrain the chemical and physical conditions in the star-forming clumps and their cloud environments.

Motte et al. (2007) detected 129 dense cores using the IRAM-30m telescope at 1.2-mm wavelength, and Cao et al. (2019) used Spitzer, Herschel, the JCMT, and the IRAM 30-m telescope and detected 151 massive dense clumps. Of these, 66 clumps of the Motte-catalogue and 60 clumps of the Cao-catalogue are covered in the MIOP Cygnus-X, and 82 individual clumps of between the catalogues are identified with CASCADE. With a 4σ confidence, DCO^+ is observed in 66% of the clumps, DCN in 37%, DNC in 76%, NH_2D in 70% and N_2D^+ is observed in 11%, where at least one of these deuterated molecules is observed in 72 clumps. We found strongly increased deuterium fractionation at 0.2 pc-scales in the Cygnus-X cloud complex where the median of observed DCO^+/HCO^+ is 0.018, DCN/HCN is 0.01, DNC/HNC is 0.013, N_2D^+/N_2H^+ is 0.055 and the highest deuteration is observed in NH_2D/NH_3 of 0.207.

References:

Cao, Y., Qiu, K., Zhang, Q., et al. 2019, ApJS, 241, 1
Motte, F., Bontemps, S., Schilke, P., et al. 2007, A&A, 476, 1243

Modeling excitation conditions on luminous high-mass star forming regions using CH3CCH

PAULA DÍAZ[1], LEONARDO BRONFMAN[1], MANUEL MERELLO[1], AND EDGAR MENDOZA[2]

[1] Departamento de Astronomía, Universidad de Chile, Chile. paulabdiazs@gmail.com
[2] Departamento de Ciencias Integradas, Universidad de Huelva, España.

Methyl acetylene (CH3CCH) it's typically used to explore physical conditions in star-forming regions, since it works as an excellent temperature tracer. Its rotational transitions obey the following features. First, due to the spatial symmetry of this molecule, they are characterized by the quantum numbers J (the total angular momentum) and K (its projection on the principal symmetry axis). Secondly, they appear closely spaced in frequency and exhibiting the so-called K-ladder emission lines. Lastly, they are purely thermal, therefore they follow an LTE behavior and, as a consequence, they are suitable for LTE rotational diagrams. These diagrams allow to compute the excitation temperature and column density for the detected transitions of the molecule.

In this work, we present detections of CH3CCH K-ladders in the transitions J=10-9, J=12-11, J=13-12 and J=23-22, collected with the APEX telescope, toward a sample of 7 luminous clumps, from our survey of hot molecular core (HMC) candidates. The rotational diagrams of CH3CCH produced for each source show a clear change in excitation temperature and column density for transitions with energy above $E_{up}/k = 200\ K$. The latter statement is sustained by the fact that LTE models that use a single excitation temperature and column density fail in emulating the CH3CCH emission, and better simulations can be obtained when two excitation components are considered (See Fig 1). These results may illustrate the spatial distribution of the CH3CCH transitions within the HMC candidates.

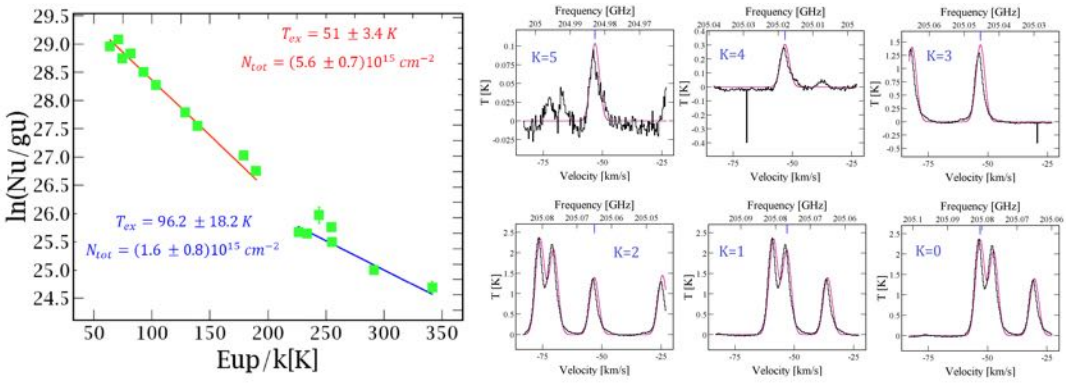

Figure 1: **LEFT:** Rotational diagram of CH3CCH in HMC G333.125-0.424 (G333). **RIGHT:** K-ladder of the transition J=12-11 of G333. In black is the observed spectrum, and in purple is the two components LTE model.

Modeling snowline locations in protostars

N. M. Murillo[1], T.-H. Hsieh[2], and C. Walsh[3]

[1] Star and Planet Formation Laboratory, RIKEN, nadia.murillomejias@riken.jp
[2] Max-Planck-Institut für extraterrestrische Physik
[3] School of Physics and Astronomy, University of Leeds

Snowline locations are responsible for a range of effects during the formation and evolution of stars, such as setting the chemical composition of the envelope and disk. This in turn influences the formation of planets through changing the elemental compositions of solids and affecting the collisional properties and outcomes of dust grains. Snowlines can also reveal echoes of past accretion bursts, lending insight into the formation process of stars. A numerical chemical network coupled with a grid of cylindrical-symmetric physical models is used to identify what parameters alter snowline locations, and their observational tracers. Snowline locations move to larger radii (i.e., away from the heating source) with increasing luminosity and decreasing envelope densities (Fig. 1). The snowline radius of molecules with low sublimation temperatures ($\lesssim$30 K), such as CO, shift inwards along the disk mid-plane when a disk(-like) structure is present. For molecules that sublimate at higher temperatures ($\sim$100 K), such as H_2O, the presence of a disk concentrates these molecules to compact regions ($<$100 AU) around the protostar by limiting the outward shift of snowline positions. Successful observational measurements of snowline locations are strongly dependent on spatial resolution, and inclination of the protostellar cloud core.

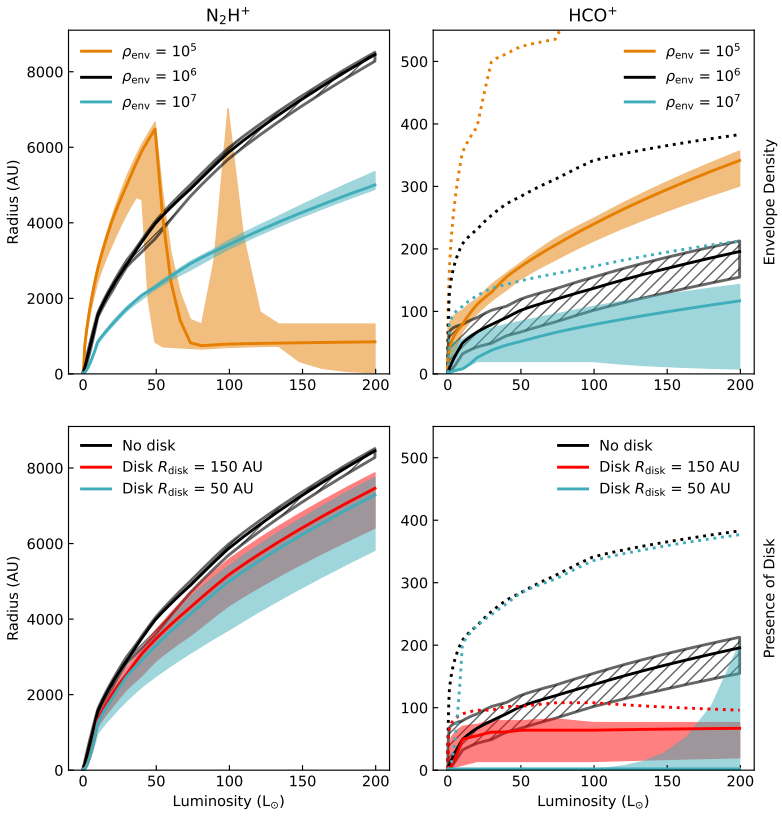

Figure 1: *Peak radius of N_2H^+ (left) and HCO^+ (right) simulated emission versus luminosity for changes in envelope density (top row), and presence of disk (bottom row). The solid line shows the peak radii for inclination i = 45°. The shaded area indicates the range of peak radii with i = 0° (face-on) and 90° (edge-on) for N_2H^+, and i = 15° (face-on) and 90° (edge-on) for HCO^+. The dotted line on the right panels shows i = 0° for HCO^+.*

Chemical differentiation of massive Young Stellar Objects and Ultra-Compact HII regions

M. A. TRINIDAD[1], J. L. VERBENA[2]

[1] Departamento de Astronomía, Universidad de Guanajuato, Apartado Postal 144, 36000, Guanajuato, Guanajuato México,
[2] I. Physikalisches Institut, Universität zu Köln, Zülplicher Str. 77, 50937 Köln, Germany,
verbena@ph1.uni-koeln.de

It is known that, in general, all stars are formed in molecular clouds under gravitational collapse of molecular dense gas. Two of the earliest phases of high-mass star-forming process are the young stellar object (YSO) and the ultra-compact (UC) HII region. In order to study these phases, we carried out a systematic survey toward a sample of 98 massive YSOs and UC HII regions. We aim to characterize their chemical environment and evolutionary state, for which we carried out observations with the 30 m IRAM radiotelescope. We observed the molecular lines at the 3 mm band (e.g. N_2H^+, NH_2D (1-0), CS (2-1), HCN (1-0) and HCO^+, SO (32-21), $C^{34}J$(2-1), C_2H, $H^{13}CN$, CH_3CN, etc.). These observations allow us to study the chemical content of different star formation environments at their earliest evolutionary phases. This survey will help us to 1) study the chemical and dynamical evolution of the observed sources 2) study how star formation varies as function of environment, 3) estimate the density of the molecular clumps and investigate the existence of a density threshold for the formation of a dense core, and 4) study the variation of abundance of molecular lines in different galactic environments. Additionally, we investigate the kinematics of the molecular gas close to YSOs and UC HII regions (e.g. outflow, infall, rotation), as well as the evolutionary state of the sources.

INFUSE: Observing the Non-radiative to Radiative Shock Transition in the Cygnus Loop SNR with a Rocket-Borne FUV Integral Field Spectrograph

E. M. WITT[1] AND B. T. FLEMING[2]

[1] Laboratory for Atmospheric and Space Physics, emily.witt@lasp.colorado.edu
[2] Laboratory for Atmospheric and Space Physics

Supernova remnants (SNRs) have long been studied in the X-ray, ultraviolet (UV), optical, and infrared (IR) bandpasses with important tracers of the interaction between SNR shocks and the ISM material they collide with are found in the far-ultraviolet (FUV). While X-ray data traces non-interactive, non-radiative shocks and optical/IR data traces interactive, radiative shocks, spectral lines in the FUV such as O VI ($v_{sh} > 160$ km/s, $T = 300$ kK) and C IV ($T = 100$ kK) trace the transition region between the two, where the ISM and SNR material first begin to interact (Danforth et al., 2001).

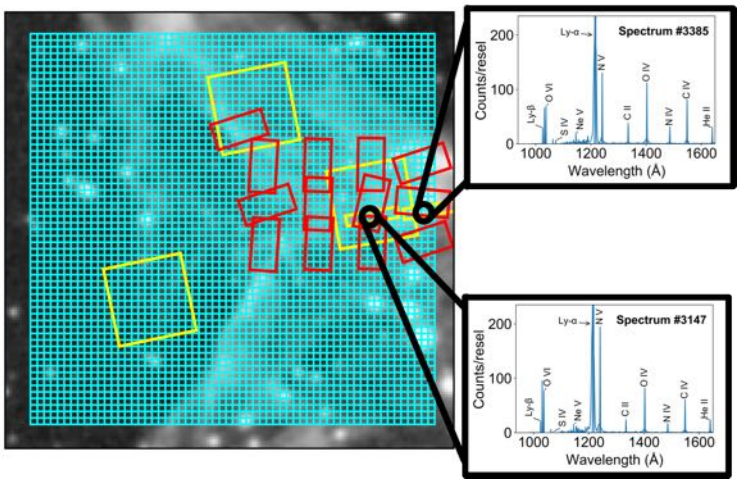

Figure 1: XA region of the Cygnus Loop with the INFUSE FOV overlaid. Each cyan square corresponds to one 1D INFUSE spectra. Sample 1D spectra are shown for illustration purposes. Apertures corresponding to one 1D *FUSE* and *IUE* spectra are shown in yellow and red, respectively. Underlying picture from the blue filter archive of the Digitized Sky Survey 2 (DSS2).

Previous FUV studies, attempting to link X-ray and IR observations of shock fronts in the Vela SNR and the Cygnus Loop have suffered either from one of three problems: large apertures and sparse sampling, wide FOV but limited angular resolution, or small angular coverage and sparse spatial sampling due to limited observation time (Witt et al., 2018). The spectral features that trace shock fronts occur in the Cygnus Loop on arcsecond scales, with structure that requires 3D spectroscopic mapping to adquately trace (Figure 1). The INtegral Field Ultraviolet Spectroscopic Experiment (INFUSE), a sounding rocket payload under development by the Colorado Ultraviolet Spectroscopy Program (CUSP), will be the first far ultraviolet (1000 - 2000 Å) integral field spectrograph (IFS) in space. With the INFUSE sounding rocket, spectroscopy mapping of emission features over a broad field-of-view at moderate angular resolution will be possible for the first time.

References:

Danforth, C. W., Blair, W. P., and Raymond, J. C. 2001, AJ, 122, 938-953
Witt, E. M., Fleming, B. T., France, K., et al. 2018, SPIE Proc., 10699, 9-19

Modelling the main galactic cooling lines with a clumpy PDR model

C. YANITSKI[1], V. OSSENKOPF-OKADA[1], AND M. RÖLLIG[1]

[1] I. Physikalisches Institut der Universität zu Köln, yanitski@ph1.uni-koeln.de

By now there have been large-scale Milky Way surveys of the dust continuum and many spectroscopic lines. These must be utilised so we may better understand and constrain the physics of the interstellar medium (ISM). Of course a precise match of all features is never possible, but the large-scale structure and the typical line ratios and intensities should be reproduced in a statistically significant way. In that context, Cubick et al. (2008) has already demonstrated that the KOSMA-τ photon-dissociation region (PDR) code can model the line emission from the Milky Way with very few assumptions and constraints. This approach has been extended to arbitrary geometries in the novel PDR code `kosmatau3d` (based on the work by Andree-Labsch et al. 2017), now also accounting for the dust pumping, continuum emission, and the full velocity structure. The code uniquely accounts for the clumpy structure of the inhomogeneous ISM. We then solve the radiative transfer equation relative to the observer to create synthetic observations of intensity and optical depth (providing position-position-velocity datacubes).

We find that much of the observed structure in the spectroscopic maps can be replicated by simple axisymmetric distributions of the dense and diffuse gas mass (traced with atomic and molecular hydrogen), average density, cosmic ray ionisation rate, and far-UV radiation. We also find these `kosmatau3d` synthetic observations are able to replicate the molecular ring and certain galactic arm features (see Figure 1) even without an explicit implementation of the spiral structure of the Milky Way. This suggests the structure seen in the galactic position-velocity diagram arises to a large extent from the rotation of the galaxy and the molecular ring, and thus offers insight into the interpretation of galactic longitude-velocity diagrams.

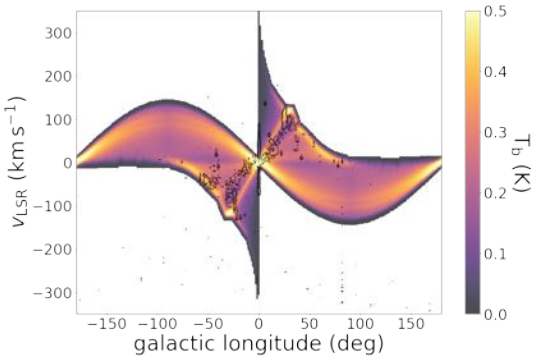

Figure 1: This figure shows the [CII] position-velocity diagram along the galactic plane ($\beta_{\mathrm{gal}} = 0$). Overlaid are contours of the Galactic Observations of Terahertz C+ (GOT C+) project (Pineda et al. 2013) with levels 0.5 K (dashed) and 1 K (solid). This plot shows which features simply arise from the velocity structure of the Milky Way.

References:

Andree-Labsch, S., Ossenkopf-Okada, V., Röllig, M. 2017, A&A, 598, A2
Cubick, M., Stutzki, J., Ossenkopf, V., et al. 2008, A&A, 488, 623
Pineda, J. L., Langer, W. D., Velusamy, T., et al. 2013, A&A, 554, A103

Probing physical conditions and UV radiation fields in the Gy 3-7 cluster in the outer Galaxy with SOFIA/FIFI-LS

NGÂN LÊ[1], AGATA KARSKA[2,1], MIGUEL FIGUEIRA[3,1], AGNIESZKA MIROCHA[4], CHRISTIAN FISCHER[5], MAJA KAŹMIERCZAK-BARTHEL[5], RANDOLF KLEIN[6], MARTA SEWIŁO[7,8,9], CARSTEN KÖNIG [2], FRIEDRICH WYROWSKI[2], KARL M. MENTEN[2] , WILLIAM J. FISCHER[10], LARS E. KRISTENSEN[11], JOHN J. TOBIN[12], AND MACIEJ KOPROWSKI[1]

[1] Institute of Astronomy, Faculty of Physics, Astronomy and Informatics, Nicolaus Copernicus University, Grudziądzka 5, 87-100 Toruń, Poland, agata.karska@umk.pl
[2] Max-Planck-Institut für Radioastronmie, Auf dem Hügel 69, 53121 Bonn, Germany
[3] National Centre for Nuclear Research, ul. Pasteura 7, 02-093 Warsaw, Poland
[4] Astronomical Observatory of the Jagiellonian University, ul. Orla 171, 30-244 Kraków, Poland
[5] Deutsches SOFIA Institut, University of Stuttgart, Pfaffenwaldring 29, D-70569 Stuttgart, Germany
[6] SOFIA/USRA NASA Ames Research Center P.O. Box 1, MS 232-12 Moffett Field, CA 94035, USA
[7] Exoplanets and Stellar Astrophysics Laboratory, NASA Goddard Space Flight Center, Greenbelt, MD 20771, USA
[8] Department of Astronomy, University of Maryland, College Park, MD 20742, USA
[9] Center for Research and Exploration in Space Science and Technology, NASA Goddard Space Flight Center, Greenbelt, MD 20771, USA
[10] Space Telescope Science Institute, 3700 San Martin Dr., Baltimore, MD 21218, USA
[11] Niels Bohr Institute, Centre for Star & Planet Formation, University of Copenhagen, Øster Voldgade 5-7, DK-1350 Copenhagen K, Denmark
[12] National Radio Astronomy Observatory, 520 Edgemont Rd., Charlottesville, VA 22903, USA

Far-infrared (far-IR) line emission traces the bulk of gas cooling in deeply-embedded parts of star forming regions and informs about the on-going heating processes (e.g., shocks, UV radiation). However, gas cooling and heating might differ with the environment e.g., the metallicity of the region. Gy 3-7 is an embedded cluster in the CMa-l224 star-forming region in the outer Galaxy, at a distance of $\sim$1 kpc, with the estimated metallicity Z of $\sim 0.55 - 0.73\ Z_{\odot}$, providing an ideal laboratory to investigate the impact of metallicity on the far-IR gas cooling.

Here, we present the result of SOFIA/FIFI-LS spectral maps of CO lines from J=14-13 up to 30-29, OH line at 79 μm, [C II] at 158 μm, and [O I] at 63 and 145 μm over the $2' \times 1'$ region on the Gy 3-7 cluster. We use CO transitions $J_{\rm up} \leq 22$ to calculate the spatial distribution of CO rotational temperatures across the cluster. We use ionic and atomic lines and models of photodissociation regions to derive the strengths of UV radiation field and H_2 number densities. The ratio of molecular to atomic far-IR line luminosities from protostars in Gy 3-7 is compared to values found in similar sources in the Milky Way and in the Magellanic Clouds. This comparison shows a decreasing trend of far-IR molecular line cooling with metallicity, hinting at the possible impact of metallicity on the physical and chemical conditions of star forming regions in the outer Galaxy.

UV radiation and large-scale outflow from DR 21 with SOFIA FIFI-LS

A. Mirocha[1,2], A. Karska[2], M. Figueira[2,3], Y.-L. Yang[4], N. Le[2], Ch. Fisher[5], M. Kaźmierczak-Barthel[5], R. Klein[6], L. Looney[7], A. Beck[5], S. Latzko[5], Ch. Iserlohe[5], S. Colditz[5], W. Vacca[6] and A. Krabbe[5]

[1] Astronomical Observatory, Jagiellonian University, Kraków, Poland, agnieszka.mirocha@doctoral.uj.edu.pl
[2] Institute of Astronomy, Nicolaus Copernicus University, Toruń, Poland [3] National Centre for Nuclear Research, Warszawa, Poland [4] Department of Astronomy, University of Virginia, Charlottesville, VA 22904, USA [5] Deutsches SOFIA Institut, Stuttgart, Germany [6] SOFIA-USRA, USA [7] Department of Astronomy, University of Illinois, USA

Energetic processes are an integral part of the massive stars' evolution. They impact the physics and chemistry of molecular clouds, as well as the galaxy as a whole. The DR21 star-forming region is known to host one of the largest and most luminous outflows in the Milky Way. Additionally, energetic UV photons create a photodissociation region (PDR) in the neighbourhood of central protostar(s).

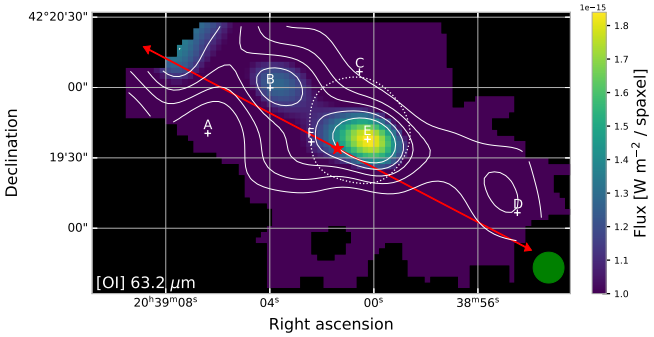

Figure 1: Integrated intensity map of [O I] 63.2 μm toward DR21. Red star shows the position of the driving source of the outflow (Dobashi et al. 2019) , and red arrows show the outflow direction based on the H_2 $v = 1 - 0$ S(1) observations (Garden et al 1986).

By studying the SOFIA FIFI-LS spectroscopic data of high-J CO lines, [OI], [CII], and [OIII] lines, we aim at quantifying the gas energetics of the outflow and determine the UV field strengths and gas densities in the PDR region. The spatial extent of line emission differs between various far-IR lines. The [OI] 63.2 μm line is detected symmetrically in both outflow lobes, and resembles the high$-J$ CO emission. On the contrary, [C II] and the [O I] line at 145.5 μm show a more compact pattern. In the poster, we will show how the total far-IR line cooling changes across the DR21 outflow tracing its energetics and physical processes. We will also show the estimate of the UV radiation field strengths toward PDR region of DR21.

References:

Dobashi, K., Shimoikura, T., Katakura, S., Nakamura, F., & Shimajiri, Y. 2019, PASJ, 71, S12
Garden, R., Geballe, T. R., Gatley, I., & Nadeau, D. 1986, MNRAS, 220, 203

Session IV: Laboratory Astrophysics

Greetings from the Laboratory: Recent developments in Laboratory Astrophysics

T.F. GIESEN, G.W. FUCHS, A.A. BREIER AND M. KAUFMANN

University of Kassel, Institute of Physics, 34132 Kassel, Germany
t.giesen@uni-kassel.de

Interstellar molecules accompany the life cycle of stars, which begins with the contraction of cold gas in giant molecular clouds and ends with the ejection of processed matter from dying stars and supernova remnants. The physical and chemical processes and conditions of interstellar matter are reflected in the spectra of gas-phase molecules. Spectroscopic detections of interstellar molecules with world-class telescopes such as ALMA, SOFIA, and, in the future, the James Webb telescope, provide an enormous amount of spectral data of breathtaking accuracy and sensitivity. A complete interpretation of the astronomical spectra is only possible by comparison with high-precision laboratory data that provide information about the chemical composition, isotopic abundances, ionization fraction, temperatures, and velocities of the gas.

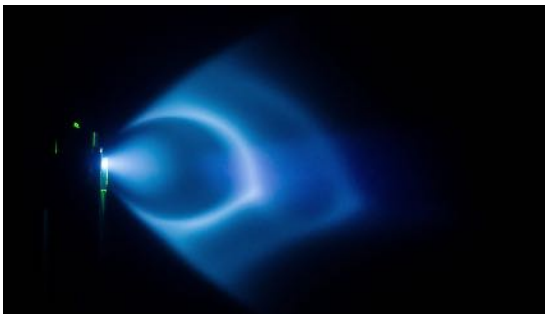

Figure 1: Supersonic expansion of a molecular plasma forming cold reactive molecules.

Despite the enormous amount of laboratory data already available in molecular databases, the evolution of telescope instrumentation to ever-higher sensitivity and spatial resolution will require new, high-precision laboratory data, which will also require new laboratory techniques. Chirped-pulse microwave techniques, high-quality cavity-enhanced spectroscopy, frequency comb-assisted precision spectrometers, and resonance-enhanced multiphoton ionization spectrometers are just a few examples of instruments that have contributed to recent progress in laboratory astrophysics. In addition, sophisticated methods for the generation of short-lived molecules in discharge and laser ablation sources, as well as the storage of molecular ions in cold multipole ion traps and cryogenic storage rings, have opened new horizons for the study of interstellar molecules under laboratory conditions.

The wealth of new, high-precision laboratory measurements comprises spectral data for complex organic molecules, including their stable isomers. With the discovery of methyloxirane in space, chiral molecules have become the focus of new laboratory investigations. From ortho/para ratios of small stable species and from isotopic abundances, time-dependent interstellar processes can be studied in which molecules act as astronomical clocks. Radioactive molecules will also be important in this context. New data on small metal oxides will reveal possible pathways to the origin of cosmic dust formation. Spectroscopic data on molecular ions will help to better understand chemically important ion-neutral reaction pathways. Last but not least, with the successful launch of the James Webb telescope, the infrared region will become spectrally more important, which has already triggered many new laboratory investigations in this particular frequency range. This overview talk will provide insights into the development of new laboratory techniques for the investigation of astrophysically relevant molecules using examples from the Kassel laboratory astrophysics group.

Broad band millimeter astronomical and laboratory observations: The QUIJOTE line survey of TMC-1 and the GACELA experimental setup

J. CERNICHARO[1]

[1] Department of Molecular Astrophysics. Institute of Fundamental Physics (CSIC). C/Serrano 121. Madrid (Spain) jose.cernicharo@csic.es

I present the instrumental developments that have been performed in the framework of the ERC Synergy project Nanocosmos in the field of radio astronomy and molecular spectroscopy. Extremely sensitive radio receivers using HEMT amplifiers have been built to develop the GACELA gas cell for rotational spectroscopy in the frequency ranges 31-50 and 72-116 GHz. Similar receivers have been also installed at the Yebes 40m radiotelescope for radioastronomical observations and molecular astrophysics studies. Several molecules have been observed with GACELA (Cernicharo et al. 2019) and searched for in space towards Orion, SgrB2, IRC+10216, and TMC-1.
An ultradeep line survey of the cold prestellar cloud TMC-1 (QUIJOTE; Cernicharo et al. 2021) is under way with the Yebes 40m telescope (see Fig. 1) and its extremely sensitive receivers. QUIJOTE has allowed the discovery of more than 30 new molecular species, including eight cations, one anion, seven neutral S-bearing species, radicals, and a large number of hydrocarbons including the first identification of a non functionalized polycyclic aromatic hydrocarbon in space, indene (C_9H_8).

Figure 1: The 40 m radiotelecope of the Yebes Observatory observing TMC-1 on January 2021. It is located on the Alcarria Plateau (Castilla La Mancha) at 60 km from Madrid and 950 m of altitude. It was built in 2007.

References:
Cernicharo, J., Gallego, J.D., López-Pérez, et al.: 2019, A.&A., 626, A34
Cernicharo, J., Agúndez, M., Kaiser, R., et al.: 2021, A.&A., 652, L9

Quantum calculations of formation and destruction rates of molecules for ISM models

OCTAVIO RONCERO[1]

[1] Instituto de Física Fundamental, CSIC, c/ Serrano 121, 28006 Madrid (Spain),
octavio.roncero@csic.es

The accuracy of reactive rate constants need to be increased to bound the possible chemical routes that drives the abundances observed in different environments in the interstellar medium, specially in gas phase. In many cases, the experimental determination of such rate constants presents difficulties or some uncertainties, and accurate quantum simulations can go a long way to provide them, specially in some limiting cases. In this work we shall present theoretical rate constants for different current problems of interest in the astrochemical field. First, the role of chemical pumping in Photodissociation Regions for $H_2(v>>0)$ with M (Zanchet et al. 2019, Goicoechea et al. 2021) (M=C, N, O and S, in neutral and cationic forms), paying special attention to spin-orbit transitions in the cases of S^+ and N^+. Second, some key reactions for the formation and destruction of CS molecule in cold molecular clouds, as a key molecule to follow the sulfur abundance (Bulut et al. 2021). Third, the gas phase reactions of organic molecules (OM), like H_2CO and CH_3OH, with OH at low temperatures (del Mazo Sevillano et al. 2019). An overview of the methods used will be given, which varies with the size of the molecular systems and the process studied and conditions. Also the effect on Astrophysical model will be discussed.

References:

Bulut, N., Roncero, O., Aguado, A. et al, 2021, A&A, 646, A5
del Mazo-Sevillano, P., Aguado, A., et al. 2019, J. Phys. Chem. lett., 10, 1900
Goicoechea, J. R., Aguado, A., Roncero O., et al. 2021, A&A, 647, A10
Zanchet, A., Lique, F., Roncero, O. et al., 2019, A&A, 626, A103

Origin of Cosmic Dust - An Experimental Approach

TH. HENNING[1]

[1] Max Planck Institute for Astronomy, Koenigstuhl 17, D-69117 Heidelberg, Germany
henning@mpia.de

Refractory cosmic dust particles are originally formed in high-temperature condensation processes occuring in the outflows of evolved stars or supernova ejecta. After the grains are injected into the interstellar medium they are heavily modified by radiation fields and finally destroyed by shocks. An efficient reformation of dust particles under the low-temperature conditions of interstellar space is necessary in order to explain the dust content of our and other galaxies (see, e.g., Zhukovska et al. 2018).

The talk will discuss experimental results which support the observationally-based hypothesis that dust grains and PAHs can form under the low-temperature conditions of interstellar space. In liquid helium experiments at temperatures of 1.7 K, carbon atoms and molecules were indeed found to condense into a partially graphitized carbonaceous solid (Krasnokutski et al. 2017). In a comprehensive experimental approach, the formation and growth of refractory dust components was investigated (Rouillé et al. 2020). The experiments were based on the annealing of neon-ice matrices which contained initially isolated precursors of silicate and carbonaceous grains. During the annealing process the formation of silicate particles and carbonaceous grains was observed. A remarkable result is the fact that the silicates and the carbonaceous grains are chemically separated, supporting grain models with individual silicate and carbon components. We will also discuss the formation of PAHs in low-temperature processes (see, e.g., Zhao et al. 2018).

References:

Krasnokutski, S.A. et al. 2017, ApJ 847, 89, 2017.
Rouillé, G., Jäger, C., Henning, Th. 2020, ApJ 892, 96, 2020
Zhao, L. et al. 2018, Nature Astronomy 2, 973.
Zhukovska, S., Henning, Th., Dobbs, C. 2018, ApJ 857, 94.

High-resolution spectroscopy of astrophysically relevant molecular ions

O. ASVANY[1], S. THORWIRTH[1], P. C. SCHMID[1], T. SALOMON[1] AND S. SCHLEMMER[1]

[1] I. Physikalisches Institut, Universität zu Köln, Zülpicher Str. 77, 50937 Köln, Germany,
asvany@ph1.uni-koeln.de

High-resolution rovibrational and pure rotational spectra for molecular ions of astrophysical interest have been recorded in the Cologne laboratories. Recent examples include CN^+, $CH_2NH_2^+$, $CH_3NH_3^+$, c-$C_3H_2^+$, l-$CCCH^+$, and $HCCCO^+$. These species have been investigated using ion trap instruments which feature mass selection via quadrupole mass analyzers, long storage times in cryogenic 22-pole ion traps, and cooling of the ions via He buffer gas to temperatures as low as 4 K. Due to the low number of stored ions (typically less than 10^5), so-called action spectroscopic techniques have to be applied, in which the ion count is used as the spectroscopic signal. As the ion counting efficiency is close to unity, action spectroscopy can be very sensitive. Several such action spectroscopic schemes have been developed in-house during the last couple of years. Recent technical advances along these lines are demonstrated for the ions l-$CCCH^+$ and $HCCCO^+$ in this contribution. The advantage of using mass-selected, cryogenically cooled ions is that very clear spectroscopic information is obtained, with only a handful of lines, but which can be intense and have very narrow linewidths. This allows to obtain accurate frequency information and to resolve overlapping lines. An example of such an approach is the first rotational spectrum of protonated methylamine, $CH_3NH_3^+$, shown in the adjacent Figure. A comparison with spectroscopic simulations reveals that this symmetric top molecule is not rigid, but exhibits torsional motion between the CH_3 and NH_3 subunits. This result and the other laboratory rotational data presented here will further support and guide radio-astronomical searches of these species in space. A first search of $CH_3NH_3^+$ in the Sgr B2(N) and (M) regions was performed but unfortunately without a clear detection.

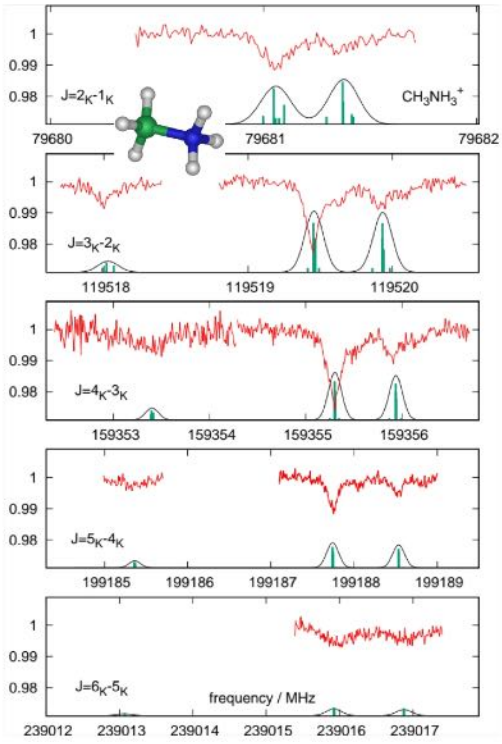

Figure 1: Measured rotational transitions $J'_K \leftarrow J''_K$ $(K = 0, 1, 2)$ of $CH_3NH_3^+$ (red trace). The simulations (green sticks and black line) are based on a rigid symmetric rotor model.

References:
Thorwirth, S., Schreier, P., Salomon, T., et al., 2019, Astrophys. J. Lett., 882, L6
Markus, C.R., Asvany, O., Salomon, S., et al. 2020, Phys. Rev. Lett., 124, 233401
Schmid, P. C., Thorwirth, S., Endres, C. P., et al. 2022, Front Astron Space Sci, 8, 805162

High-resolution ro-vibrational spectroscopy of cyclopropenyl cation: The ν_4 C–H anti-symmetric stretching band

D. GUPTA[1], P. C. SCHMID[1], M. MIES[1], AND S. SCHLEMMER[1]

[1] I. Physikalisches Institut, Universität zu Köln, Zülpicher Straße 77, 50937 Köln, Germany, gupta@ph1.uni-koeln.de

The cyclopropenyl cation, *c*-$C_3H_3^+$, is the smallest aromatic hydrocarbon ion and is considered to be an important player in the ion–molecule reaction network in space. While it has evaded an astronomical detection till now, the spectroscopic study reported in this work provides information for *c*-$C_3H_3^+$ to be a potential search target by the James Webb Space Telescope. We have obtained its gas-phase ro-vibrational spectrum for the ν_4 C–H anti-symmetric stretching fundamental band in high resolution with the band centre around 3.1 μm. The experiment was performed in the cryogenic 22-pole ion trap instrument, LIRtrap (Paul et al.). Our work is in good agreement with previous available data in this region from Zhao et al. where the *c*-$C_3H_3^+$ cations were generated in a supersonically expanding planar plasma discharge. Those authors used continuous-wave cavity ring-down spectroscopy for their studies. Courtesy mass selection prior to storing the ions in the trap, our spectrum is comprised only of lines of the desired cyclopropenyl cation. The spectrum shown in Fig. 1 below exhibits the typical structure of an oblate top molecule with C_{3v} symmetry. It is dominated by a "2 B" rotational spacing with some substructure due to distortions present for a close to rigid symmetrical rotor. Details of fitting this regular spectrum will be discussed and compared to the previous results.

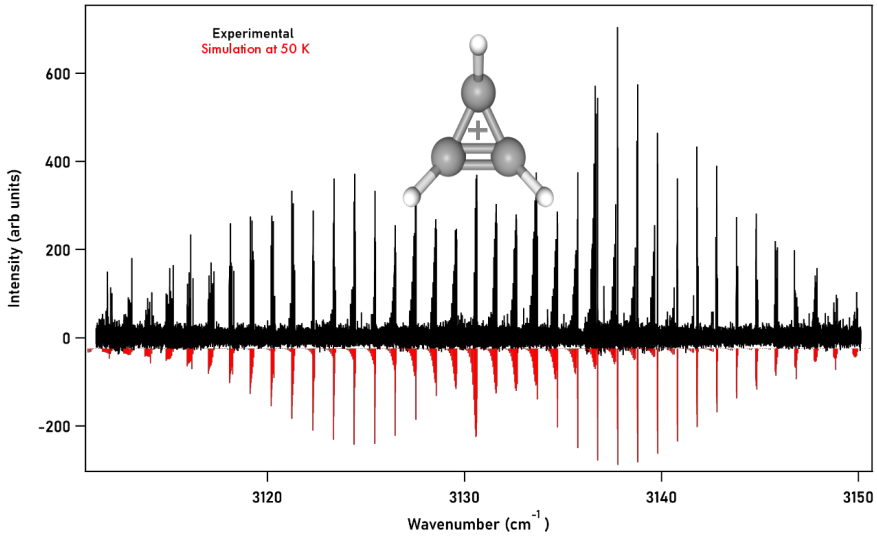

Figure 1: Experimental and simulated spectrum of *c*-$C_3H_3^+$.

References:
Paul, W., Lückel, B., Schlemmer, S., Gerlich, D. 1995 Int. J. Mass Spectrom. and Ion Proc., 149, 373.
Zhao, D., Doney, K. D., Linnartz, H. 2014 ApJL 791 L28.

On the spectroscopy of acylium ions: infrared action spectroscopic detection of NCCO $^+$

O. ASVANY[1], M. BAST[1], S. SCHLEMMER[1] AND S. THORWIRTH[1]

[1] I. Physikalisches Institut, Universität zu Köln, Köln, Germany bast@ph1.uni-koeln.de

The linear $\mathrm{N}\equiv\mathrm{C}-\mathrm{C}\equiv\mathrm{O}^+$ ion has been studied spectroscopically for the first time using the Free Electron Laser for Infrared eXperiments, FELIX, at Radboud University (Nijmegen, The Netherlands) in combination with the 4K 22-pole ion trap facility FELion.[a] The vibrational spectrum of $NCCO^+$, shown in Figure 1, was observed in the range from 500 to 1400 and 2000 to 2500 cm^{-1} using resonant photodissociation of the correponding Ne-complex while monitoring the depletion of the ion-Ne cluster signal as a function of wavenumber. Spectroscopic assignment of vibrational bands relies on comparison against results from high-level quantum-chemical calculations performed at the CCSD(T) level of theory and very good agreement is found.

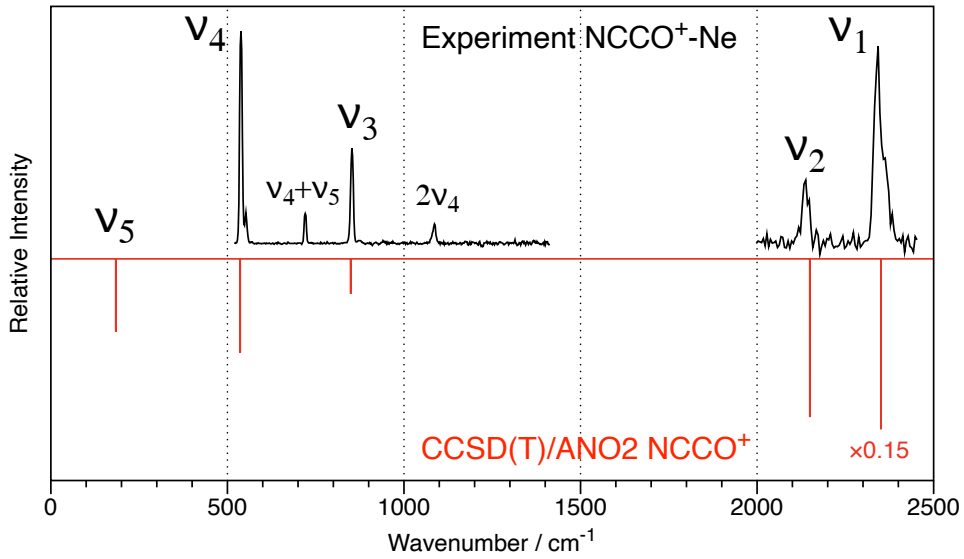

Figure 1: IRPD vibrational spectrum of $NCCO^+$-Ne. Studied with FELIX between 500 - 1400 cm^{-1} and 2000 - 2500 cm^{-1} in comparison to the quantum-chemical calculations.

References:

[a] Jusko et al. 2019, Faraday Discuss. 217, 172

LLWP - Updates on a new Loomis-Wood Software at the Example of Acetone-$^{13}C_1$

L. BONAH[1], O. ZINGSHEIM[1], H. S. P. MÜLLER[1], J.-C. GUILLEMIN[2], F. LEWEN[1], AND S. SCHLEMMER[1]

[1] I. Physikalisches Institut, Universität zu Köln, Köln, Germany, bonah@ph1.uni-koeln.de
[2] ENSC, Univ. Rennes, Rennes, France

Acetone-$^{13}C_1$ is a complex organic molecule with two internal methyl ($-CH_3$) rotors having relatively low barriers to internal rotation of 251 cm^{-1} [1]. This leads to two low-lying torsional modes and five internal rotation components resulting in a dense and complex spectrum. Similar conditions can be found in many complex molecules, with isotopologues, hyperfine structure, and interactions being additional factors for the presence of even more crowded spectra than that of acetone.

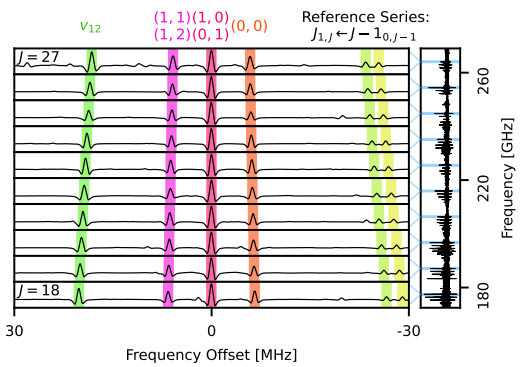

Figure 1: Loomis-Wood plot of Acetone-$^{13}C_1$ displaying the typical triplet pattern of the internal rotation.

Measurements of acetone-$^{13}C_1$ were performed with an isotopically enriched sample in the frequency range from 37-1102 GHz. Loomis-Wood plots (LWPs) are one approach to improve and fasten the analysis of such crowded spectra. Here, an updated version of the LLWP software was used which relies on LWPs for fast and confident assignments. Additionally, LLWP focuses on being user-friendly, intuitive, and applicable to a broad range of assignment tasks. The software will be presented here and is available together with its full documentation at llwp.astro.uni-koeln.de. Predictions of acetone-$^{13}C_1$ created with ERHAM [2-3] allow for future radio astronomical searches.

References:

[1] P. Groner, *J. Mol. Struct.* **550-551** (2000) 473-479.
[2] P. Groner, *J. Chem. Phys.* **107** (1997) 4483-4498.
[3] P. Groner, *J. Mol. Spectrosc.* **278** (2012) 52-67.

Spectroscopic studies of acylium- and thioacylium ions

S. THORWIRTH[1], O. ASVANY[1], T. SALOMON[1], M. BAST[1], M. E. HARDING[2], J. L. DOMÉNECH[3], AND S. SCHLEMMER[1]

[1]I. Physikalisches Institut, Universität zu Köln, Köln, Germany sthorwirth@ph1.uni-koeln.de
[2] Institut für Nanotechnologie, Karlsruher Institut für Technologie (KIT), Karlsruhe, Germany
[3] Instituto de Estructura de la Materia (IEM-CSIC), Madrid, Spain

Acylium- and thioacylium ions, R-CO^+ and R-CS^+, are a class of molecular ions of relevance for astrochemistry that have received relatively little attention from molecular spectroscopy so far. Triggered by our first spectroscopic study of the polyatomic HC_3O^+ and HC_3S^+ species (Thorwirth et al. 2020), it was not long until these two ions as well as the methyl variant CH_3CO^+ were detected in space (Cernicharo et al. 2021, and references therein). With this contribution, we would like to present a status report on the spectroscopic studies of acylium- and thioacylium ions at Cologne that make use of various action spectroscopy schemes in combination with state-of-the-art ion trap machinery.

References:

Thorwirth, S., Harding, M. E., Asvany, O., et al. 2020, Mol. Phys. 118, e1776409
Cernicharo, J., Cabezas, C., Bailleux, S. et al. 2021, Astron. Astrophys. 646, L7

First high resolution spectroscopy of the ν_2 antisymmetric C-C-stretching mode of I-C_3H^+

M. BAST[1], J. BÖING[1], T. SALOMON[1], S. THORWIRTH[1] AND S. SCHLEMMER[1]

[1] I. Physikalisches Institut, Universität zu Köln, Köln 50937, Germany boeing@ph1.uni-koeln.de

The I-C_3H^+ ion plays an important role as an intermediate in the carbon chemistry of the interstellar medium, as it enables the formation of more complex hydrocarbon molecules. After its first detection in the horsehead PDR region via its rotational lines[1], laboratory measurements of the rotational[2] and the vibrational spectra[3] were performed. These provided accurate information about the vibrational states and their band positions, which we used in combination with quantum chemical calculations to start our investigation. Here, we report first high resolution infrared measurements of the ν_2 antisymmetric C-C-stretching mode of I-C_3H^+ around 2089.8 cm^{-1} at a temperature of about 40 K. For the experiment the mass selected ions are stored in a cryogenic 22-pole ion trap instrument where they are overlapped with the infrared light of a mode-hop-free quantum cascade laser (QCL). Excitation of the ions is recorded by appropriate action spectroscopic techniques.

References:

[1] J. Pety et al., A&A 548(2012) A68.,
[2] B. McGuire et al., Ap. J. 774(2013)56
[3] S. Brünken et al., Astrophys. J. Lett. 783(2014)L4
[4] S. Brünken et al., J. Phys. Chem. A 123(2019)8053

Session V: Observatories and Instrumentation: Future Opportunities

Scientific capabilities enabled by future millimeter through FIR instrumentation and observatories

JOHANNES STAGUHN

Johns Hopkins University & NASA/GSFC jstaguhn@jhu.edu

The Far-infrared (FIR) allows an unobscured and unbiased census of baryons in galaxies throughout the universe from the very early times. Technical progress in observational capabilities has ramped up in recent years, reaching a point where we can expect to design background limited space-based FIR observatories. Unprecedented sensitivities and mapping speeds for those missions will be enabled by advanced detectors, powerful readout systems, and cryogenic optics and cooling technologies. The payback for these developments will come in form of up to four orders of magnitude of improvement in sensitivities over past FIR missions, with spectroscopic mapping speeds that are a million plus times faster than what has been obtained so far. With that, future observatories will allow the astronomical community to address a wide range of scientific questions with unprecedented precision, ranging from measurements of masses of protoplanetary disks, detailed observations revealing the role of water, ice, and volatiles in planet formation, and open new windows on the interplay between AGN, the interstellar medium and its associated star formation which drives the evolution of metallicity in the universe.
I will describe the progress in technologies that will lead to these significant observational capabilities, ranging from enhanced ground-based sub-millimeter interferometers to space-based FIR observatories that could be launched as early as in the mid 2030s.

The ALMA Wideband Sensitivity Upgrade

JOHN CARPENTER[1]

[1] Joint ALMA Observatory (john.carpenter@alma.cl)

The Atacama Large Millimeter/submillimeter Array (ALMA) is the most sensitive telescope ever built for high-resolution observations at millimeter and submillimeter wavelengths. To enhance ALMA as a world leading facility for millimeter/submillimeter astronomy, the ALMA partnership established the ALMA Development Program to promote hardware, software, and infrastructure improvements for ALMA. The top priority of the ALMA Development Program over the next decade is the Wideband Sensitivity Upgrade, which will at least double ALMA's system bandwidth with improved sensitivity and scientific capabilities. This goal requires upgrading the receivers and most of the digital electronics, including the correlator, as well as the ALMA software that drives the system. The Wideband Sensitivity Upgrade will afford significant improvements for every future ALMA observation. The impact will span the vast array of astronomical topics for continuum or spectral line science. The impact will be particularly profound for high spectral resolution surveys (< 0.2 km/s) of molecular clouds and protoplanetary disks, where the instantaneous correlated bandwidth will increase by 1-2 orders of magnitude over current capabilities (see Figure 1). This talk will summarize the Wideband Sensitivity Upgrade and the expected scientific impact.

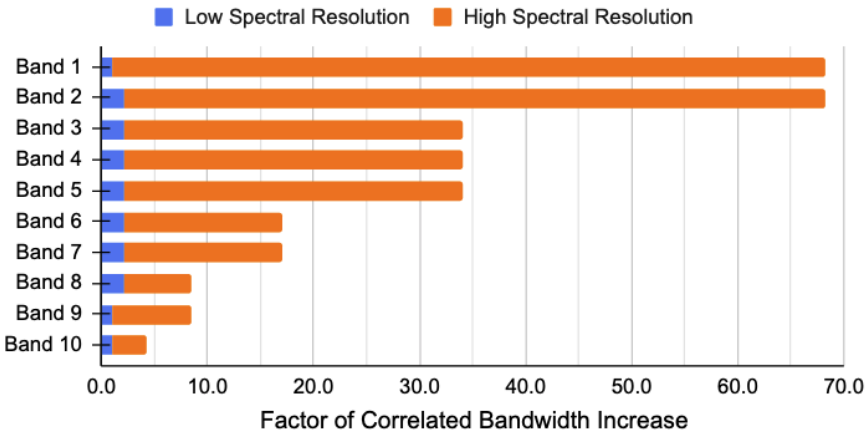

Figure 1: Factor increase in the correlated bandwidth over the current ALMA system that will be enabled by the ALMA Wideband Sensitivity Upgrade for the $2\times$ bandwidth upgrade. Results for shown for two spectral resolution regimes: "Low Spectral Resolution" (blue) which is defined by the best spectral resolution that the current ALMA correlator can achieve at full correlated bandwidth (7.5 GHz per pol), and "High Spectral Resolution" (orange), which is defined by the goal of reaching 0.1-0.2 km/s resolution in every ALMA band at maximum correlated bandwidth (16 GHz per pol). The increase in bandwidth will further double when the $4\times$ bandwidth upgrade is completed. The Wideband Sensitivity Upgrade will enable up to a factor of 70 increase in the correlated bandwidth at high spectral resolution, enabling efficient molecular line surveys of molecular clouds, circumstellar disks, and evolved stars.

IRAM Observatories today and tomorrow

R. NERI[1]

[1] Institut de Radioastronomie Millimétrique, F-38406 Saint-Martin d'Hères neri@iram.fr

NOEMA and the IRAM 30-meter telescope were designed and built to provide world-class observing capabilities for thousands of researchers across the world. The two observatories together, provide a unique combination of cutting-edge technologies to help researchers address key astronomical questions. Both facilities offer a range of outstanding capabilities today that will continue to be expanded as part of IRAM's long-term development strategy. Current capabilities and those expected in the near future are presented here.

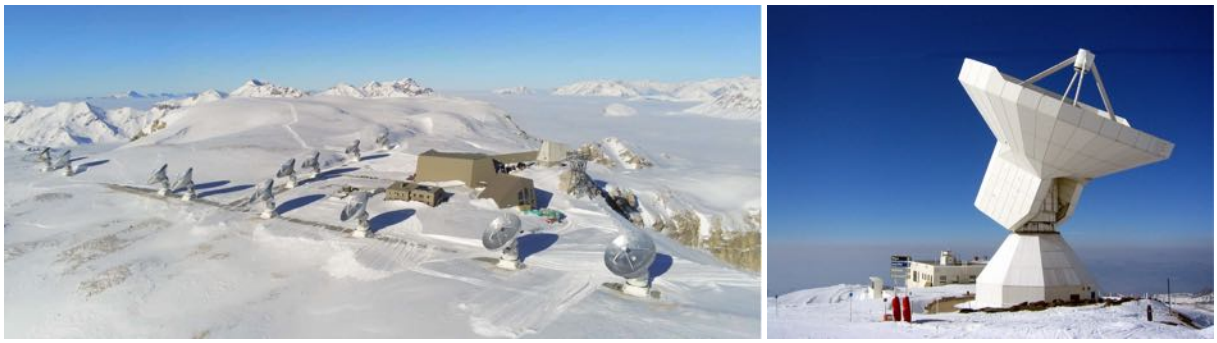

Figure 1: Left: view of the NOEMA observatory (France) as seen from the southeast. The twelve antennas are arranged in the most compact configuration. Right: the 30-meter telescope (Spain). NOEMA and the 30-meter telescope are operated by IRAM, an international research institute supported by the CNRS (France), MPG (Germany) and IGN (Spain).

Star and planet formation: Upcoming opportunities in the space-based infrared

FLORIS VAN DER TAK[1,2]

[1] SRON Netherlands Institute for Space Research, vdtak@sron.nl
[2] Kapteyn Astronomical Institute, University of Groningen

While ALMA, VLA and JWST are revolutionizing our view of star and planet formation with their unprecedented sensitivity and resolution at submm, radio, and near-IR wavelengths, many outstanding questions can only be answered with observations in the thermal (mid- and far-) infrared domain. In particular, how do interstellar clouds develop filamentary structures and dense cores? What are the masses and luminosities of objects at the earliest stages of star formation? What are the gas masses of planet-forming disks, and how do these disks disperse during planet formation? How is refractory and volatile material distributed within the disks, and how does this evolve with time? This talk reviews how upcoming and planned balloon-borne and space-based telescopes for the mid- and far-infrared will address these questions, and outlines which further missions will be needed beyond 2030, when the ELTs will be in full operation.

Chilean involvement in astronomy instrumentation projects

R. REEVES[1,2,3,4]

[1] CePIA, Universidad de Concepción , rreeves@udec.cl
[2] ANID-Basal CATA2 ACE210002
[3] Millennium Nucleus TITANS
[4] ANID-Fondecyt 1181620

In this talk, we review historical aspects regarding the development of the astronomical instrumentation field in Chile, the relationship with governmental funding, the current situation across the country, and views for the establishment of a community towards the future. We will cover from the early participation in specific projects, contributing with basic manpower, to the establishment of development labs that provide engineering support to solve the needs of existing large facilities, not only for Chile. While the scientific aspect of astronomy has grown in Chile significantly over the past two decades, instrumentation is developing at a lower pace. This is because besides the required support in human resources, the area needs institutional and governmental decided actions to invest in infrastructure and equipment. We explore how the interplay between developing scientific instrumentation and technology transfer to industry may open a new avenue for a faster development of astronomical instrumentation in Chile, where base funding to support manpower and equipment in astronomy instrumentation laboratories is basically non-existent.

CCAT-prime: status and science prospects

G.J. STACEY[1] ON BEHALF OF THE CCAT-PRIME CONSORTIUM

[1] Cornell University gjs12@cornell.com

We will report on the CCAT-prime Project, including the science, the Fred Young Submillimeter Telescope (FYST) and instrumentation, and the schedule. The FYST is a 6-m telescope sited at 5600 m elevation near the summit of Cerro Chajnantor in northern Chile. Its site, together with its very large field-of-view (FoV) optics and high surface accuracy, low-emissivity surface enables pursuit of low surface brightness science over large fields. Our science goals include: tracing the formation and evolution of star forming galaxies from the epoch of reionization to the cosmic peak of star formation activity through wide-field, broad-band [CII] line imaging and dust continuum surveys; constraining thermodynamics and feedback in galaxy clusters through the Sunyaev-Zeldovich effects on the CMB; improving constraints on primordial gravitational waves through precision removal of polarization foregrounds; and tracing local star formation processes through velocity-resolved spectroscopy at 30" to 100° sized scales in the Galaxy. These goals are realized though sensitive wide-field surveys. In addition to the Mod-Cam first light camera, we are constructing Prime-Cam, a large FoV direct detection imager, and CHAI, a multi-beam submillimeter heterodyne spectrometer. Prime-Cam has seven instrument modules, four are currently under construction: three polarmetric cameras (at 280, 350, and 850 GHz) and a 210-420 GHz Fabry-Perot imaging spectrometer, EoR-Spec. CHAI will have 128 pixels covering important lines in the short submillimeter windows. The CCAT-prime team is an international group of universities, led by Cornell University. The CCAT-prime telescope is being designed and built by Vertex Antennentechnik GmbH with first science expected in 2024.

Current and Future Space/Airborne Observatories for ISM Studies

M. MEIXNER[1], B. SCHULZ[2]

[1] Stratospheric Observatory for Infrared Astronomy (SOFIA)/USRA Science Mission Operations, mmeixner@usra.edu
[2] Deutsches SOFIA Institut, Universität Stuttgart

The interstellar medium emits a tremendous amount of radiation in the infrared (3 to 500 μm) that represents the majority of the light emitted by a galaxy. The Stratospheric Observatory For Infrared Astronomy (SOFIA, Special issue articles, 2018) covers this entire wavelength range with 5 instruments including spectrometers, imagers and polarimeters. James Webb Space Telescope (JWST, Gardner et al. 2006) covers the short wavelength infrared (0.6 to 28 μm) with 4 instruments including spectrometers and imagers. I will briefly introduce each current facility through its science and capabilities and discuss how they work in concert to achieve a wholistic view of the ISM. The Astro2020 Decadal survey recognizes the importance of the far-infrared (far-IR). For the future, they recommend a potential probe and a large IR/far-IR observatory that may cover the wavelength range of 3 to 500 μm. I will introduce current concepts under consideration for far-IR probes and the large mission study concept for the far-IR, Origins Space Telescope (Meixner et al. 2019; 2021).

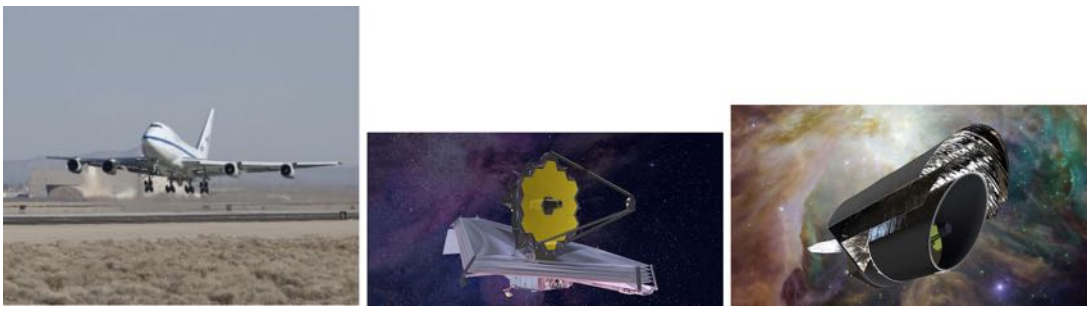

Figure 1: The Stratospheric Observatory For Infrared Astronomy (SOFIA, left), the James Webb Space Telescope (JWST, center), the Origins Space Telescope concept (Origins, right)

References:

Ali, Z. A., et al., 2018, J. Astron. Instrum., Vol 7, 1840002
Ennico, Kimberly, et al., 2018, J. Astron. Instrum., Vol 7, 1840012
Fischer, Christian, et al., 2018, J. Astron. Instrum., Vol 7, 1840003
Gardner, J., Mather, J.C,m Clampin, M. et al., 2006, Space Science Reviews, Volume 123, Issue 4, pp.485-606
Harper, Doyal A., et al., 2018, J. Astron. Instrum., Vol 7, 1840008
Herter, T. L., et al., 2018, J. Astron. Instrum., Vol 7, 1840005
Leppik, K., et al., 2018, J. Astron. Instrum., Vol 7, 1840010
Meixner, M., Cooray, A., Leisawitz, D., et al. 2019, arXiv:1912.06213
Meixner, M., Cooray, A., Leisawitz, D., et al. 2021, Journal of Astronomical Telescopes, Instruments, and Systems, Volume 7, id. 011012
Pfüller, Enrico, et al., 2018, J. Astron. Instrum., Vol 7, 1840006
Risacher, C., et al., 2018, J. Astron. Instrum., Vol 7, 1840014
Richter, M. J., et al., 2018, J. Astron. Instrum., Vol 7, 1840013
Reinacher, Andreas, et al., 2018, J. Astron. Instrum., Vol 7, 1840007
Temi, Pasquale, et al., 2018, J. Astron. Instrum., Vol 7, 1840011

The APEX Telescope: current status and future developments

NICOLAS REYES[1], CHRISTOPHER HEITER, CARLOS DURAN[2], RODRIGO PARRA, AND BERND KLEIN[2]

[1] Max Planck Institute fur Radioastronomy, nreyes@mpifr-bonn.mpg.de
[2] European Southern Observatory

The Atacama Pathfinder Experiment (APEX) is a 12 meters submillimeter telescope located at Llano de Chajnantor, Chile. The site, at 5.100 m above sea level, is well known as one of the best sites for submillimeter observations on earth. It allows for regular observations in the 350 um atmospheric window and occasional observations up in the 200 um band. The telescope has been in continuous operation since 2005 as a cooperation between the Max Planck Institut, the European Southern Observatory and the Onsala Space Observatory. Reference [1] presents an overall description of the telescope and its capabilities. After the first 10 years of operation the telescope was refurbished. Several telescope systems were updated with the aim of extending the lifetime of the telescope and facilitating full remote observations. The telescope was equipped with a new sub-reflector and new panels to reach a 10 um RMS surface accuracy, improving the telescope aperture efficiency in the higher bands of observation. On following we will review the results of the last surface adjustments, and present the accurate modelling of the telescope we had used to improve the results of our alignment strategy. APEX is equipped with a full set of state-of-the-art, single-pixel heterodyne receivers covering the frequency range from 180 GHz to 720 GHz. Here we describe the development of the N-FLASH suite of receiver, partially commissioned in 2020, designed for simultaneous multi-band observations using dichroic filters. The telescope is also equipped with heterodyne cameras: LASMA, a 7-pixel 345GHz instrument, is currently in scientific operation with improved performance in terms of sideband rejection and IF frequency coverage. A third suite of instruments at APEX are large field-of- view bolometric cameras. We will focus on the final testing results of AMKID, a dual color (350 um and 870 um) instrument based on KIDs detectors. This instrument will be installed during the first half of 2023, opening a completely new range of science with APEX.

Binary file (standard input) matches

SPRITE: A Small Satellite for Mapping Shocked Interfaces in the ISM

B.FLEMING[1] AND THE SPRITE TEAM

[1] Laboratory for Atmospheric and Space Physics, University of Colorado,
Brian.Fleming@lasp.colorado.edu

The ultraviolet bandpass is a window into a host of important astrophysical processes in the ISM of galaxies, tracing shock heated interfaces between supernovae and the ambient ISM as well as the hot stars that drive galaxy evolution. Unfortunately, our access to the far-UV (100 - 200 nm) has largely been limited to point-source spectrographs that fail to capture to extended structure of diffuse clouds in both the Milky Way and nearby galaxies.

The Supernova Remnants and Proxies for ReIonization Testbed Experiment (SPRITE) is a small satellite that will change this paradigm. Set to launch in 2023, SPRITE is a 12U form factor (22.6 x 22.6 x 36.6 cm) no larger than a toaster oven that will explore the ISM of the Milky Way, Magellanic Clouds, and nearly galaxies to new depths. SPRITE is designed in part map both the scattered and absorbed star-light as well as cooling features from shocked gas at the ISM interface to 10 arcsecond scales. This survey will cover more than 50 remnants and star-formation regions in the Magellanic Clouds, the Cygnus Loop and Vela supernova remnants, and potentially several Milky Way superbubbles. SPRITE will also carry out a program of push-broom spectral mapping of low-redshift galaxies, such as M33, producing data cubes of star-formation and nebular features both within our galaxy and of our nearest companions. These data products will be archived on the Mikulski Archive for Space Telescopes (MAST) alongside data from many other space observatories, including Hubble.

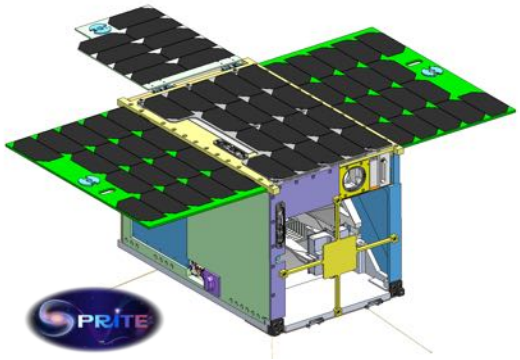

Figure 1: The SPRITE CAD Model.

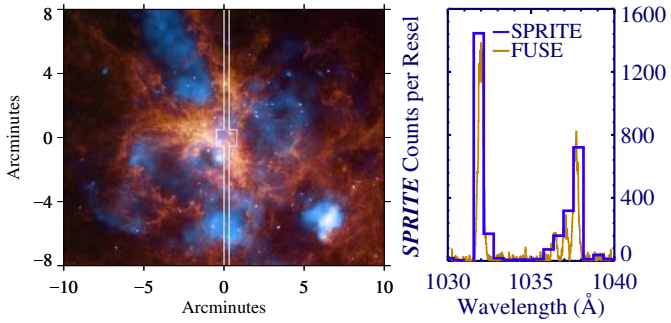

Figure 2: (Left) A portion of the 0.5° long SPRITE slit overlaid on 30 Doradus. (Right) O VI emission as detected by SPRITE from LMC SNR Henize 70.

As the first scientific astrophysics cubesat in a 12U format, SPRITE's 18 x 16 cm primary mirror and low-noise detector push the boundaries of sensitivity for a small, low-cost space mission. SPRITE also serves as an orbital testbed for new technologies to help enable a future UVOIR great observatory. We present a brief overview of the design, performance and timeline of SPRITE, as well as several points of discussion regarding the application of small satellites to the study of the ISM and galaxy feedback processes.

The CCAT-prime Heterodyne Array Instrument (CHAI)

U.U. GRAF[1], I. BARRUETO[1], G. GRUTZECK[2], C.E. HONINGH[1], K. JACOBS[1] M. JUSTEN[1], B. KLEIN[2], I. KRÄMER[2], H. KRÜGER[1], A. MAHMOOD[1], B. SCHMIDT[1], M. SCHULTZ[1] J. STUTZKI[1], S. VARGHESE[1], K. VYNOKUROVA[1], L. WEIKERT[1], S. WULFF[1]

[1] KOSMA, University of Cologne, Cologne/Germany; graf@ph1.uni-koeln.de
[2] Max Planck Institute for Radioastronomy, Bonn/Germany

We are building the CCAT-prime Heterodyne Array Instrument, a powerful mapping spectrometer for FYST. In its final configuration, CHAI will have 64 spatial pixels in each of two frequency bands. As a heterodyne spectrometer, it will be able to spectrally resolve even the most narrow astronomical lines.

CHAI is primarily targeted at mapping extended sources in the two neutral atomic carbon fine structure lines and the nearby rotational lines of carbon monoxide. The low frequency array (LFA) of CHAI will cover part of the 650 μm window, giving access to the [CI] $^3P_1 \rightarrow ^3P_0$ and CO $J = 4 \rightarrow 3$ lines. The HFA will operate in the 350 μm window, covering [CI] $^3P_2 \rightarrow ^3P_1$ and CO $J = 7 \rightarrow 6$ simultaneously. The field of view of the two square 8×8 pixel arrays will be $7.5' \times 7.5'$ for the LFA and $4.5' \times 4.5'$ for the HFA. The array footprints are illustrated in Fig. 1 overlaid on the [CII] map of the horsehead nebula (Risacher et al. 2016).

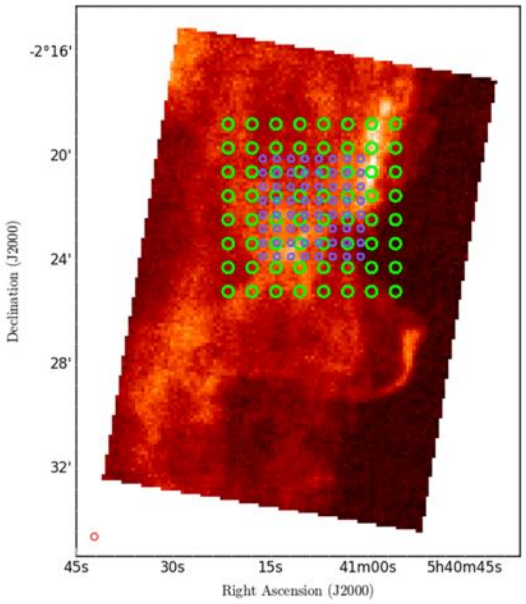

Figure 1: Overlay of the CHAI array footprint on a [CII] map of the horsehead nebula.

CHAI uses on-chip balanced mixers in a very compact focal plane unit. The local oscillator is coupled to the mixers using a waveguide system that guides the LO signal into the cryostat and distributes it to the individual mixers. The intermediate frequency output of each mixer is amplified, processed and analyzed in a highly integrated digital Fourier transform spectrometer, The IF bandwidth of 4 GHz corresponds to a velocity range of approximately 2500 km/s for the LFA and approximately 1500 km/s for the HFA, The geometry of FYST requires a relatively complex optics path from the telescope focal plane to the receiver cryostat. Part of the optics setup can be flipped out of the way to allow the telescope signal to pass to other instruments.

In our contribution we will describe the specifications, design and the development progress of the instrument.

The future of FIR astronomy, after SOFIA

H. ZINNECKER[1], A. KRABBE[2]

[1] Universidad Autonoma de Chile, Santiago hzinnecker50@gmail.com
[2] Deutsches SOFIA Institut, Univ. Stuttgart, Germany

We offer some critical comments on the premature shut-down of SOFIA announced by NASA/DLR, following the unusual recommendation by the US Decadal Report earlier this year. After reviewing some unique SOFIA observational results and its recent boost in productivity, we point out that productivity is not the ultimate metric to judge the success of an ongoing mission but that "unique discoveries" are an equally important metric (ignored by the Decadal Report and NASA/DLR's decision). Clearly the SOFIA FIR instruments GREAT, HAWC+, FIFI-LS as well as the mid-IR instruments EXES and FORCAST have contributed unique new knowledge of the interstellar medium, which we will briefly summarize ("the local truth"). FIR is key!

Now, considering that the SPICA FIR space telescope failed to be selected by ESA as a successor to Herschel, the closeout of SOFIA means that the future of FIR astronomy and survival of the FIR community is at stake (at risk). How to prevent this? The common claim that the 6.5m James Webb Space Telescope can replace SOFIA is shcwn to be false; while the ALMA/NOEMA ground-based submm telescope arrays will miss their synergy FIR complement, for at least a decade to come. A big loss.

We call for a discussion of the future of FIR astronomy in the near future, be it the use of other stratospheric re-usable platforms or fighting for a limited continuation of SOFIA observations with specific instrumentation, based on a reduced budget. We must also evaluate which key FIR science SOFIA has left out (such as H2 and HD rotational transition tracers of the ISM) and focus on detector technology to improve FIR sensitivity.

Superconductive devices for the CCAT-prime Heterodyne Array Receiver Instrument (CHAI)

I.BARRUETO[1], U. U. GRAF[1], C.E HONINGH[1], K. JACOBS[1], M.JUSTEN[1], M.SCHULTZ[1], S. WULFF[1], AND J. STUTZKI[1]

[1] 1. Physikalisches Institut, Universität zu Köln, barrueto@ph1.uni-koeln.de

CHAI is a dual colour heterodyne receiver for the 460-500 GHz and 780-820 GHz bands, each consisting of a square array of 8x8 pixels in a balanced mixer configuration. For each band the cryogenic (4K) 64 mixer block consist of 2x8 vertically stacked 1x4 pixel waveguide blocks. These blocks are fabricated in CuTe split block technology with 460x230 μm (480 GHz) and 240x140 μm (800 GHz) rectangular waveguides connecting the 3 LO power dividers and 4 mixers. Both mixers and LO power dividers, are fabricated on 9μm (480 GHz) and 5 μm (800 GHz) thick Silicon membrane chips in Niobium and Niobium titanium nitride superconducting technology respectively. The 480 GHz band mixers are the in-house made balanced mixers based on the design by Westig et al [2]. The 800 GHz mixers are currently being developed. The LO power dividers are 90° CPW branch line couplers with a Titanium Nitride load.

The LO power dividers and mixer devices have been tested on a 2-pixel test block, representing the physical half of the 1x4-pixel block (dotted red line in Fig. 1); the 2-pixel block contains one power divider and two balanced mixers. This simpler scheme allows to pretest basic components in a representative way.

Regarding the 800 GHz band, current developments are focused on the design and pertinent fabrication preparations of the balanced mixer. At the conference we will present test results for all relevant components: the 2-pixel block for the 480 GHz band as well as the designs for a 800 GHz band mixer.

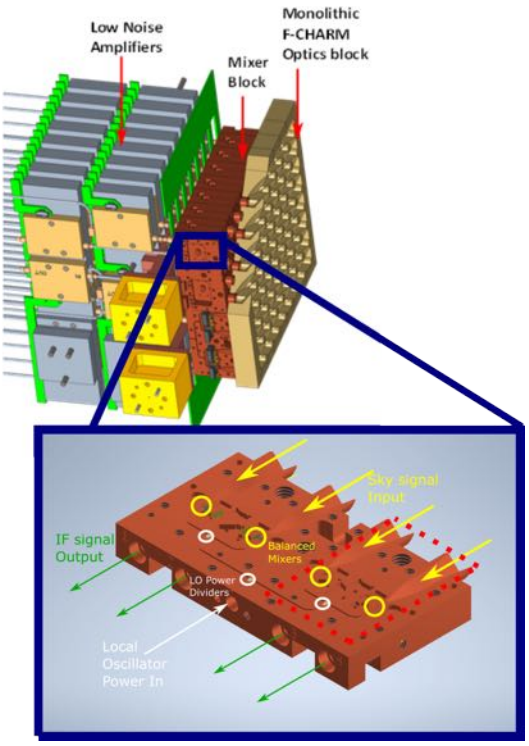

Figure 1: 3D of the Focal plane unit array with its main components labelled and a detailed image of a half 4-pixel block with its core components. The dotted red line marks the which part of the 4-pixel block which is being tested with the debugging 2-pixel block.

References:

M.P. Westig, K. Jacobs, J. Stutzki, M. Justen and C.E Honingh, Supercond. Sci. Technol. 24, 085012(2011).

The U-Board – A heterogeneous, closely coupled architecture for radio astronomy

G. GRUTZECK[1], B. KLEIN[1,2]

[1] Max-Planck-Institute for Radio Astronomy, ggrutzeck@mpifr-bonn.mpg.de
[2] University of Applied Sciences Bonn-Rhein-Sieg

Instrumentation for mm- and submm-astronomy as well as laboratory spectroscopy require phase-coherent signal generation and acquisition over wide bandwidths, combined with powerful signal processing. In mm- and submm-astronomy it is particularly important for both incoherent instrumentation, such as a readout for Microwave Kinetic Inductance Detectors (MKIDs), as well as coherent instrumentation, such as high-resolution spectrometers. In the field of laboratory spectroscopy the Chirped Pulse Spectroscopy (CPS) requires a wide-band, phase-coherent signal generation and acquisition.

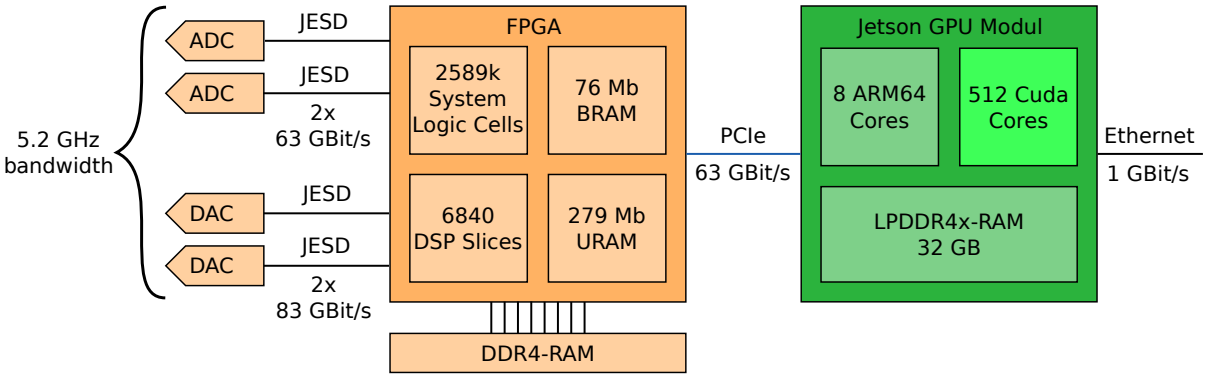

Figure 1: The analog frontend and heterogeneous architecture of the U-Board.

The U-Board has been developed to satisfy these requirements (s. figure 1). It combines a set of high speed Digital Analog Converters (DACs) and Analog Digital Converters (ADCs) with a closely coupled heterogeneous processing architecture, which combines the advantages of Field Programmable Gate Arrays (FPGAs) and Graphics Processing Units (GPUs). The ADCs and DACs form the analog frontend with an instantaneous bandwidth of 5.2 GHz. The two processing systems are closely coupled as they are connected via PCIe, which allows simple direct data transfer in both directions. This architecture allows to develop real-time streaming applications, which combine the hard realtime capabilities and integer processing power of an FPGA with the floating point processing power of a GPU. The architecture is completed by a processor, which controls the components. The signal processing is split between the FPGA and the GPU, according to the requirements of the applications, both for the signal synthesis as well as for the analysis. The MKID readout just as the signal generation and acquisition for the CPS are implemented and currently under commissioning. The detailed concept of the high-resolution spectrometer is currently under development.

References:

G. Grutzeck, B. Klein, I. Krämer, M. Heininger, A. Bell, The U-Board - a closely coupled, heterogeneous architecture, in prep.

Line Intensity Mapping with the EoR-Spec Instrument on FYST

T. NIKOLA[1], AND CCAT-PRIME COLLABORATION

[1] Cornell University, tn46@cornell.edu

The EoR-Spec (Epoch of Reionization Spectrometer) is one of the seven instrument modules of Prime-Cam, which is the main direct detection instrument on the 6 meter aperture FYST (Fred Young Submillimeter Telescope) located near the summit of Cerro Chajnantor in the Atacama desert in northern Chile above the ALMA plateau. With a spectral resolving power of $R \sim 100$ and a field of view of about 1.3 degrees it is optimized for its scientific goal, which is to map the redshifted [CII] 158 μm fine structure line from the epoch of reionization in many redshift intervals. The [CII] emission traces the signal of star formation from aggregation of galaxies and thus tracks the morphology of the ionization of the interstellar and intergalactic medium in this epoch. In this presentation I will outline the details of the Line Intensity Mapping observing plan and how the results will inform about the re-ionization of the early Universe.

CCAT-prime: New Holographic Metrology for the FYST Telescope and its Laboratory Test

X. REN[1], P. ASTUDILLO[2], U. U. GRAF[1], R. E. HILLS[3], S. JORQUERA[2], B. NIKOLIC[3], S. C. PARSHLEY[4], N. REYES[5], L. WEIKERT[1]

[1] I. Physikalisches Institut, Universität zu Köln, Köln, 50937, Germany, ren@ph1.uni-koeln.de
[2] Departamento de Astronomía, Universidad de Chile, Santiago, 7591245, Chile
[3] Cavendish Laboratory, University of Cambridge, Cambridge, UK
[4] Department of Astronomy, Cornell University, Ithaca, NY 14853, USA
[5] Max Planck Institute for Radio Astronomy, Bonn, Germany

We describe a novel holographic measurement system, including hardware design and new software approach, for measuring and setting the mirror surfaces of the FYST telescope. FYST is a 6-m diameter telescope sited at 5600m above sea level, which will observe at millimeter and sub-millimeter wavelengths, part of the CCAT-prime Observatory located in Chile. Under the best atmospheric condition, the site allows observations up to the 1500GHz (200-micron) atmospheric window. To preserve its best electromagnetic performance at all operating frequencies, the telescope must be aligned to achieve a surface accuracy of <10.7 microns. FYST is also one of the next-generation CMB telescopes. Its novel 'crossed-Dragone' optics which consists of two similar sized mirrors provides a very large field of view, but also presents new challenges for the holographic measurement and surface adjustment.

To improve the accuracy of the measurement a high-frequency (295.74GHz) artificial source is used. It is placed at 300m from the telescope providing a strong and stable signal and reducing the influence of atmospheric turbulence. In order to discriminate between the surface errors contributed by each of the two mirrors, 4 or 5 telescope beam maps are measured with the receiver mounted to well-separated positions in the focal plane. The details of this method are described by Ren et al. (2020, Proc. SPIE, 11445).

A small model of FYST (scale factor of $\sim$15) was constructed as a testbed to demonstrate the feasibility of our new holography method. A copper foil (thickness of 50 microns) is used to create some known 'piston' surface errors and construct phase error degeneracy between the two mirror surfaces. Applying the multi-map holography measurements on the testbed telescope, the errors can be successfully distinguished and measured with an accuracy of <5 microns. Large-scale error, such as twist of the whole mirrors, can also be measured. We conclude that the new holography metrology is particularly suitable to measure panel-to-panel errors (local surface errors) for crossed-Dragone telescopes. We expect that the accuracy of the holographic system will be further improved in the FYST telescope measurements, because the systematic errors in the laboratory like multi-reflections, inaccuracy of reference receiver beam and source vibrations, are negligible or can be accurately measured and corrected.

References:
Stephen C. Parshley, Michael Niemack, Richard Hills et al., 2018, Proc. SPIE 10700.
X. Ren, P. Astudillo, U.U. Graf, R.E. Richard et al., 2020, Proc. SPIE 11445.

Development of the automated tuning algorithm for the CCAT-prime Heterodyne Array Instrument (CHAI)

K. VYNOKUROVA[1], U.U. GRAF[1], C. BUCHBENDER[1], C.E. HONINGH[1], J. STUTZKI[1]

[1] KOSMA, University of Cologne, Cologne/Germany, vynokurova@ph1.uni-koeln.de

The CCAT-prime Heterodyne Array Instrument (CHAI) is one of the two instruments on the future Fred Young Submilimeter Telescope (FYST). The spectrometer is expected to map neutral atomic carbon fine structure [CI] $^3P_1 \rightarrow ^3P_0$ ($^3P_2 \rightarrow ^3P_1$) and carbon monoxide (CO) $J = 4 \rightarrow 3$ ($J = 7 \rightarrow 6$) lines in the 650 μm and 350 μm windows respectively. These observations will help to understand star formation processes in different environments from the Milky Way to nearby galaxies.

The spectrometer has 64 pixels in each of two frequency bands, arranged in square arrays, the LFA (low frequency array) and HFA (high frequency array). For optimum performance of the instrument, each pixel must be tuned individually. Due to the large pixel count, this can only be done efficiently in an automated approach.

Our on-chip balanced Superconductor-Insulator-Superconductor (SIS) mixers each have two junctions that need to be properly biased in order to minimize the noise temperature of the whole pixel. The mixer bias control algorithm has the following tasks:

- Calibrate the junction IV-curves
- Monitor each junction's operationg conditions
- Automatically optimize the mixer tuning

Both, the hardware and the software involved in these tasks, have to be very fast, to not limit the observing efficiency.

Our poster will describe the concept of the calibration and tuning algorithm, the functions that it will fulfill and show the progress made on the software as a whole.

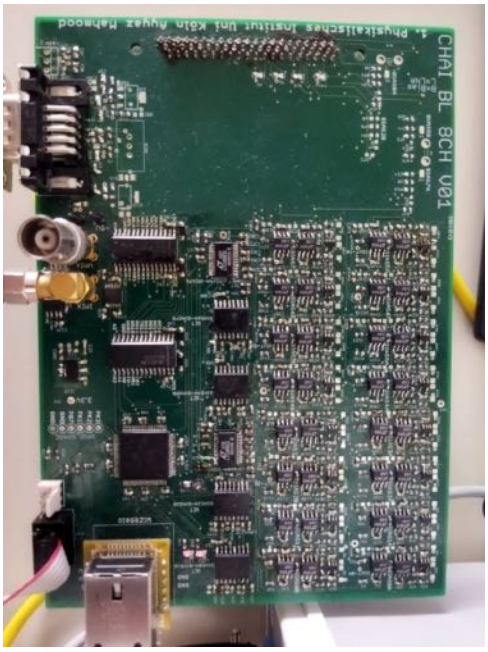

Figure 1: Prototype of a CHAI mixer bias board

Fostering (sub-)mm Astronomy in Chile through the new MPIfR-AIUC collaboration

JUAN-PABLO PÉREZ-BEAUPUITS[1,2], KARL MENTEN[2], VLADIMIR MARIANOV[1], CARLOS DURAN [3], ROLANDO DUNNER[1], AND FRIEDRICH WYROWSKI[2]

[1] Pontificia Universidad Católica (PUC), Santiago, Chile, jpereb@ing.puc.cl
[2] Max-Planck Institut für Radioastronomie, Bonn, Germany
[3] European Southern Observatory, Santiago, Chile

The Atacama Pathfinder EXperiment (APEX) observatory will enter a new era, starting from 2023. In this new era, substantial modifications of the administration and operations of the observatory will take place. The Max-Planck Institute for Radio Astronomy (MPIfR, Bonn) will play an exclusive leading role, with support from the Onsala Space Observatory (Chalmers University of Technology). In this new organization, Chilean institutions have the doors open to assume a more active participation (besides the guaranteed 10% of observing time) in the operations, as well as the scientific and technological exploitation of the observatory. In this context, the Center of Astro-Engineering of the Universidad Católica (AIUC) has signed a collaboration agreement with the MPIfR, to funnel Human Resources (as a first milestone) between the two institutions, and the APEX observatory. The formation of new qualified manpower, for both scientific and technology in (sub-)mm astronomy, can be built upon this foundation.

Session VI: Special Session on JWST first results

The James Webb Space Telescope: Advancing chemical and physical studies of star and planet formation

S.N. MILAM[1], B. SECONDAUTHOR[2], AND C. THIRDAUTHOR[2]

[1] NASA Goddard Space Flight Center, stefanie.n.milam@nasa.gov

In late 2021, the James Webb Space Telescope (JWST) was launched into space on an Ariane 5 rocket from French Guiana. JWST has unprecedented sensitivity and angular resolution, and will be the premier space-based facility for near- and mid-infrared astronomy (0.6-28.5 micron) for the next few decades. The 6.5-meter telescope is equipped with four state-of-the-art instruments which include imaging, spectroscopy, and coronagraphy. These instruments are already returning amazing spectra and images of star forming regions and revealing the dynamic processes not readily accessed with other observatories. One of first images, and arguably the most beautiful, revealed by JWST was the edge of a nearby, young, star-forming region called NGC 3324 in the Carina Nebula. This nebula is one of the largest and brightest in the sky, located approximately 7,500 light-years away in the southern constellation Carina. JWST reveals emerging stellar nurseries and individual stars that were obscured in visible images. Additionally, protostellar jets, are prominent throughout the image as well as the youngest sources, which appear as red dots in the dark, dusty region of the cloud. This image, and the others released over the last few months have demonstrated JWST's amazing capability in the Near to Mid-infrared for both imaging and spectroscopy. We are entering the next era of star and planet formation studies with JWST and will start to disentangle the complex processes involved on very detailed levels. This presentation will highlight the first images released from JWST and highlight upcoming programs in the first year of science. I will also discuss the capabilities and future proposal opportunities.

Figure 1: Four of the first images revealed by the James Webb Space Telescope, demonstrating the amazing imaging and spectroscopic capabilities for the next generation of star and planet formation studies, and beyond.

First results of the PHANGS/JWST Treasury program on star formation in nearby galaxies

M. BOQUIEN[1], J. LEE[2], K. LARSON[3], A. LEROY[4], K. SANDSTROM[5], E. SCHINNERER[6], D. THILKER[7], AND THE PHANGS TEAM

[1] Centro de Astronomía (CITEVA), Universidad de Antofagasta, Avenida Angamos 601, Antofagasta, Chile, mederic.boquien@uantof.cl
[2] Gemini Observatory / NSF's NOIRLab, 950 N. Cherry Avenue, Tucson, AZ 85719, USA
[3] Space Telescope Science Institute, 3700 San Martin Dr., Baltimore, MD 21218, USA
[4] Department of Astronomy, The Ohio State University, 140 West 18th Ave., Columbus, OH 43210, USA
[5] Center for Astrophysics and Space Sciences, Department of Physics, University of California, San Diego, CA 92093, USA
[6] Max-Planck-Institut für Astronomie, Königstuhl 17, D-69117, Heidelberg, Germany
[7] Department of Physics and Astronomy, The Johns Hopkins University, Baltimore, MD 21218, USA

Over the past few years, the PHANGS team has gathered an exceptional set of observations of main-sequence nearby galaxies with HST, ALMA, and MUSE to explore the physical processes at play at small scales in galaxies and ultimately help understand how galaxies form and evolve across cosmic times. These data will be complemented by the PHANGS-JWST Treasury Program, which provide NIRCam+MIRI imaging between 2 μm and 20 μm of 19 galaxies over more than 100 hours of observations. With its outstanding sensitivity and exquisite spatial resolution, JWST will revolutionize our understanding of galaxies. By resolving IR emission across these morphologically diverse galaxies into individual regions and clusters, the PHANGS-JWST observations will fuel diverse, high-impact science in the fields of star formation, feedback, interstellar medium physics and galaxy evolution. In this communication on behalf of the PHANGS-JWST team, I will show the spectacular NIRCam and MIRI data of the first three galaxies, NGC 628, NGC 1365, and NGC 7496. I will present a high-level overview of the first results of the investigations led by the team as well as showcase some of the major science questions that we will be able to address in the coming years. With the exceptional multi-wavelength PHANGS dataset we will be able to measure the timescales and efficiencies of the earliest phases of star formation and stellar feedback, build the first empirical models of how small dust grain properties depend on the local interstellar medium conditions, and quantitatively establish how dust-reprocessed starlight traces star formation activity, all across a representative range of conditions in the z=0 universe.

Early Science with PHANGS-JWST: New Insights into Small Dust Grains

J. SUTTER[1], K. SANDSTROM[1], J. CHASTENET[2], AND THE PHANGS TEAM

[1] Center for Astrophysics and Space Sciences, Department of Physics, University of California San Diego, jessica.sutter93@gmail.com
[2] Sterrenkundig Observatorium, Ghent University

We present early science results from JWST NIRCAM and MIRI observations of NGC 628, NGC 1365, NGC 7496, and IC 5332 from the Physics at High Resolution in Nearby Galaxies (PHANGS) sample. This initial set of galaxies includes a grand design spiral (NGC 628), two barred galaxies which host AGN (NGC 1365, 7496), and a lower metallicity environment (IC 5332). These data provide the first opportunity to determine the properties of polycyclic aromatic hydrocarbons (PAHs) at 5-10 pc scales in galaxies outside the Local Group. From these new data, we produce maps of the 3.3μm, 7.7μm, and 11.3μm PAH features. NIRCAM's unique ability to map the 3.3μm feature at high angular resolution reveals the structure of the mid-infrared emission in unprecedented detail. The combination of the three emission features provides estimates of the PAH grain sizes and charge across the disk of each galaxy. Preliminary analysis has shown that JWST is able to clearly distinguish and resolve PAH emission from different ISM phases. We find diffuse PAH emission smoothly distributed across each galaxy, with the exception of holes, often corresponding to the location of ionized gas traced by Hα emission. Through mapping the ratios of the PAH 7.7/11.3 features across each disk, we find the properties of the PAHs are relatively consistent across each individual galaxy with some variation in average charge with proximity to HII regions. Understanding the properties of the PAHs from these early JWST results will lay the groundwork for further studies of the complex interplay between the dust, gas, and stars that drives galaxy evolution. By comparing to the rich set of panchromatic observations already obtained as part of the PHANGS collaboration, we plan further studies of how the PAH emission is affected by the local conditions including metallicity, HI emission, and H_2 distribution and investigate what could be driving the evolution of the dust grains within the ISM.

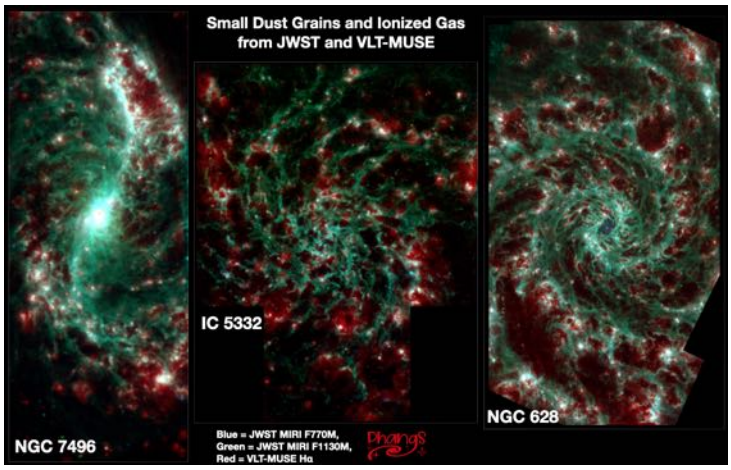

Figure 1: Maps of the first three galaxies observed by JWST: NGC 7496, IC 5322, and NGC 628. Blue and green are JWST MIRI F1130W and F770W, respectively. Red is Hα from VLT-MUSE.

JWST/MIRI Spectroscopy and Imaging of the Class 0 protostar IRAS 15398-3359

YAO-LUN YANG[1,2], JOEL D. GREEN[3], KLAUS M. PONTOPPIDAN[3], JENNIFER B. BERGNER[4], L. ILSEDORE CLEEVES[2], NEAL J. EVANS II[5], ROBIN T. GARROD[2], MIHWA JIN[6,7], CHUL HWAN KIM[8], JAEYEONG KIM[9], JEONG-EUN LEE[8], NAMI SAKAI[1], CHRISTOPHER N. SHINGLEDECKER[10], BRIELLE SHOPE[2], JOHN J. TOBIN[11], AND EWINE F. VAN DISHOECK[12,13]

[1] RIKEN, [2] University of Virginia, [3] STSci, [4] University of Chicago, [5] University of Texas, [6] GSFC, [7] Catholic University of America, [8] Seoul National University, [9] KASI, [10] Benedictine College, [11] NRAO, [12] Leiden Observatory, [13] MPE

The origin of complex organic molecules (COMs) in young Class 0 protostars has been one of the major questions in astrochemistry and star formation. While COMs are thought to form on icy dust grains via gas-grain chemistry, observational constraints on their formation pathways have been limited to gas-phase detection. Sensitive mid-infrared spectroscopy with JWST enables unprecedented investigation of COM formation by measuring their ice absorption features. We present an overview of JWST/MIRI MRS spectroscopy and imaging of a young Class 0 protostar, IRAS 15398-3359, and identify several major solid-state absorption features in the 4.9-28 μm wavelength range. These can be attributed to common ice species, such as H_2O, CH_3OH, NH_3, and CH_4, and may have contributions from more complex organic species, such as C_2H_5OH and CH_3CHO. The MRS spectra show many weaker emission lines at 6–8 μm, which are due to warm CO gas and water vapor, possibly from a young embedded disk previously unseen. Finally, we detect emission lines from [FeII], [NeII], [SI], and H_2, tracing a bipolar jet and outflow cavities. MIRI imaging serendipitously covers the south-western (blue-shifted) outflow lobe of IRAS 15398-3359, showing four shell-like structures similar to the outflows traced by molecular emission at sub-mm wavelengths. This overview analysis highlights the vast potential of JWST/MIRI observations.

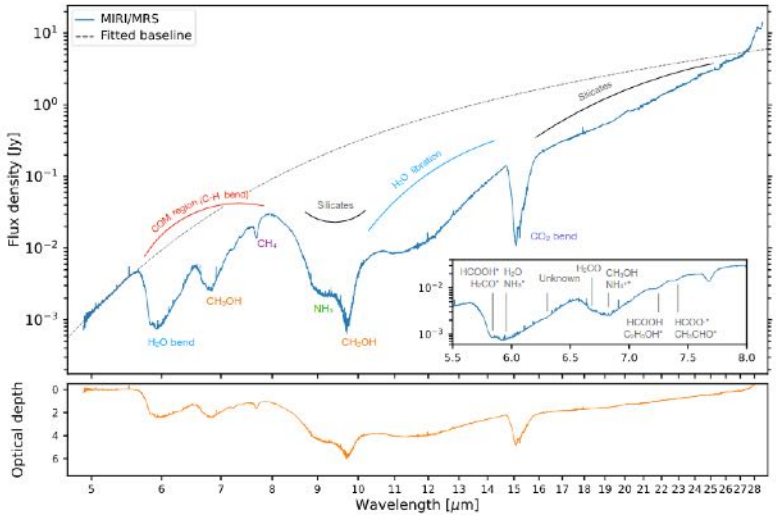

Figure 1: Top: Extracted MIRI MRS spectrum of the IRAS 15398-3359 point source, with major solid-state features indicated. The wavelength axis is in logarithmic scale. The dashed line illustrates the fitted continuum. Top (inset): Detail of the 5.5-8 μm region from same spectrum with secure and possible identifications labeled. Bottom: The optical depth spectrum derived using the continuum shown in the top panel.

List of participants

Last name	First name	Institution	Contribution	Page
Aghababaei	Atefeh	I. Physikalisches Institut, Universität zu Köln	Contributed talk	88
Ahmadi	Aida	Leiden University	Contributed talk	89
Álvarez-Gutiérrez	Rodrigo	Universidad de Concepción	Poster IIIa.P1	71
Aravena	Manuel	Universidad Diego Portales	Review	20
Asvany	Oskar	I. Physikalisches Institut, Universität zu Köln	Contributed talk	129
Baby	Aleena	I. Physikalisches Institut, Universität zu Köln	Poster IIIa.P2	72
Barrueto	Ignacio	I. Physikalisches Institut, Universität zu Köln	Poster V.P1	147
Bast	Marcel	I. Physikalisches Institut, Universität zu Köln	Poster IV.P1	131
Bemis	Ashley	Leiden University	Poster II.P1, IIIb.P1	44, 96
Böing	Julian	I. Physikalisches Institut, Universität zu Köln	Poster IV.P4	134
Bolatto	Alberto	University of Maryland	Invited talk	33
Bonah	Luis	I. Physikalisches Institut, Universität zu Köln	Poster IV.P2	132
Bonilla-Barroso	Andrea	Instituto de Radioastronomía y Astrofísica (IRyA-UNAM)	Contributed talk	64
Boquien	Médéric	Universidad de Antofagsta	Contributed talk	155
Bordier	Emma	EUROPEAN SOUTHERN OBSERVATORY	Contributed talk	65
Breloy	Isabelle	I. Physikalisches Institut, Universität zu Köln		
Briceño	Cesar	NOIRLab/CTIO/SOAR		
Bronfman	Leonardo	Universidad de Chile		
Bryant	Aaron	Deutsches SOFIA Institut, Universität Stuttgart	Contributed talk	37
Carpenter	John	Joint ALMA Observatory	Invited talk	137
Caux	Emmanuel	IRAP/CNRS-UPS-CNES		
Cernicharo	José	CSIC	Invited talk	126
Christensen	Ivalu Barlach	Max-Planck-Institut für Radioastronomie	Poster IIIc.P2	116
Congiu	Enrico	Departamento de Astronomia, Universidad de Chile	Poster II.P2	45
Cosentino	Giuliana	Chalmers University of Technology	Contributed talk	66
de Gregorio-Monsalvo	Itziar	ESO-Chile	Poster IIIb.P9	104
den Brok	Jakob	AIfA, University of Bonn	Poster II.P3	46
Díaz	Paula	Universidad de Chile	Poster IIIc.P3	117
Eibensteiner	Cosima	Argelander Institut für Astronomie (AIfA), Universtiy Bonn	Contributed talk	38

Last name	First name	Institution	Contribution	Page
Falgarone	Edith	Ecole Normale Supérieure	Invited talk	60
Fanciullo	Lapo	National Chung Hsing University	Contributed talk	90
Fedriani	Ruben	Chalmers University of Technology	Poster IIIb.P2	97
Fischer	Christian	Deutsches SOFIA Institut, Universität Stuttgart	Poster II.P13	56
Fissel	Laura	Queen's University	Invited talk	84
Fukui	Yasuo	Univ Nagoya	Invited talk	63
Fuller	Gary	The University of Manchester	Contributed talk	111, 62
Ganguly	Shashwata	University of Cologne	Poster IIIa.P3	73
Garay	Guido	Universidad de Chile	Invited talk	34
García	Pablo	NAOC	Poster IIIa.P4	74
Gerin	Maryvonne	Observatoire de Paris	Invited talk	108
Giesen	Thomas	Univertät Kassel, Institut für Physik	Review	125
Glover	Simon	University of Heidelberg	Invited talk	110
González	Jorge	Las Campanas Observatory	Poster II.P4	47
Graf	Urs	University of Cologne	Contributed talk	145
Grutzeck	Gerrit Fabian	Max-Planck-Institute for Radio Astronomy	Poster V.P2	148
Guerrero-Gamboa	Ruben	Instituto de Radioastronomía y Astrofísica (IRyA-UNAM)	Poster IIIa.P10	80
Guevara	Cristian	I. Physikalisches Institut, Universität zu Köln	Contributed talk	67
Gupta	Divita	I. Physikalisches Institut, Universität zu Köln	Contributed talk	130
Harada	Nanase	National Astronomical Observatory of Japan	Invited talk	107
Harrington	Kevin	ESO-Chile	Contributed talk	23
He	Hao	McMaster University	Poster II.P5	48
Henning	Thomas	MPIA Heidelberg	Invited talk	128
Herrera-Camus	Rodrigo	Universidad de Concepción	Contributed talk	24
Ibar	Edo	Universidad de Valparaiso	Contributed talk	25
Jacob	Arshia	Johns Hopkins University	Contributed talk	112, 106
Jakob	Holger	DSI Uni Stuttgart		
Johnstone	Doug	NRC Canada, Herzberg Astronomy and Astrophysics	Invited talk	86
Kabanovic	Slawa	I. Physikalisches Institut, Universität zu Köln	Poster IIIa.P5	75, 61
Kalari	Venu	Gemini Observatory/NSF's NOIRLab	Poster II.P6	49
Kaneko	Hiroyuki	Joetsu University of Education	Poster II.P7	50
Karoumpis	Christos	University of Bonn	Poster I.P3	30
Kauffmann	Jens	MIT Haystack Observatory	Contributed talk	95
Kausel	Gudrun	Unversidad Austral		

Last name	First name	Institution	Contribution	Page
Kavak	Umit	SOFIA Science Center/USRA/NASA ARC	Contributed talk	68
Kazmierczak Barthel	Maja	DSI Uni Stuttgart	Poster II.P14, IIIc.P8, IIIc.P9	57, 122, 123
Khan	Sarwar	Max-Planck-Institut für Radioastronomie	Poster IIIa.P6	76
Kim	Wonju	I. Physikalisches Institut, Universität zu Köln	Contributed talk	113
Klein	Bernd	Max-Planck Institute for Radioastronomy		
Klein	Randolf	USRA/SOFIA	Poster IIIa.P7	77
Kohno	Kotaro	University of Tokyo	Invited talk	21
Krabbe	Alfred	University of Stuttgart		
Law	Chi Yan	CHALMERS	Poster IIIb.P3	98
Madden	Suzanne	CEA, Saclay, France	Contributed talk	39
Maureira	Maria Jose	MPE	Contributed talk	91
Megeath	Tom	University of Toledo	Contributed talk	92
Mehta	Parit	I. Physikalisches Institut, Universität zu Köln	Poster IIIa.P11	81
Merello	Manuel	Universidad de Chile	Contributed talk	114
Milam	Stefanie	NASA Goddard	Invited talk	154
Morris	Mark	University of California, Los Angeles	Invited talk	36
Murillo	Nadia	RIKEN	Contributed talk	93
Neri	Roberto	IRAM	Invited talk	138
Neumann	Justus	Institute of Cosmology and Gravitation, University of Portsmouth	Poster II.P9	52
Nikola	Thomas	Cornell University	Poster V.P3	149
Ossenkopf-Okada	Volker	I. Physikalisches Institut, Universität zu Köln	Poster IIIb.P4	99
Padovani	Marco	INAF-Osservatorio Astrofisico di Arcetri	Invited talk	109
Patra	Sudeshna	Indian Institute of Science Education and Research Tirupati	Contributed talk	40
Perez-Beaupuits	Juan-Pablo	Pontificia Universidad Catolica de Chile	Poster V.P6	152
Peters	Christiana	DFG, Brasil		
Puschnig	Johannes	Argelander Institut für Astronomie Bonn	Poster II.P11	54
Rathjen	Tim	University of Cologne	Poster II.P12	55
Rebolledo	David	Joint ALMA Observatory - NRAO	Contributed talk	41

Last name	First name	Institution	Contribution	Page
Redaelli	Elena	Max Planck Institute for Extraterrestrial Physics	Poster IIIb.P5	100
Reeves	Rodrigo	Universidad de Concepción	Invited talk	140
Ren	Xiaodong	I. Physikalisches Institut, Universität zu Köln	Poster V.P4	150
Reyes	Nicolas	MPI für Radioastronomie	Invited talk	143
Reyes	Simon	Universidad de Concepción	Poster IIIb.P6	101
Rezaei	Sara	Max Planck Institute for Astronomy (MPIA)	Contributed talk	94
Riaz	Rafael	Centro de Investigaciones Astronómicas, Universidad Bernardo O'Higgins, Santiago	Poster IIIb.P7	102
Riechers	Dominik	I. Physikalisches Institut, Universität zu Köln	Contributed talk	26
Riquelme	Denise	MPIfR	Contributed talk	69
Roncero	Octavio	CSIC	Invited talk	127
Rubio	Monica	Universidad de Chile	Invited talk	35
Rybak	Matus	Sterrewacht Leiden	Invited talk	22
Salinas Cornejo	Javiera	Universidad de Concepción		
Sandoval	Nicolas	Universidad de Concepción	Poster IIIa.P8	78
Schlemmer	Stephan	I. Physikalisches Institut, Universität zu Köln		
Schulz	Bernhard	DSI Uni Stuttgart	Review	142
Simon	Robert	I. Physikalisches Institut, Universität zu Köln	Contributed talk	42
Skretas	Iason	Max-Planck Institute for Radioastronomy	Poster IIIb.P8	103
Solimano	Manuel	Universidad Diego Portales	Poster I.P1, I.P2	28, 29
Stacey	Gordon	Cornell University	Invited talk	141
Staguhn	Johannes	Johns Hopkins University & Nasa/GSFC	Review	136
Stutz	Amelia	Universidad de Concepcion	Review	83
Stutzki	Jürgen	I. Physikalisches Institut, Universität zu Köln	Contributed talk	70
Sutter	Jessica	University of California San Diego	Contributed talk	156
Syed	Jonas	Max-Planck-Institut für Astronomie	Poster IIIa.P9	79
Thorwirth	Sven	I. Physikalisches Institut, Universität zu Köln	Poster IV.P3	133
Tobin	John	NRAO	Invited talk, Contributed talk	85, 157
van der Tak	Floris	SRON	Invited talk	139
Verbena	Juan Luis	I. Physikalisches Institut, Universität zu Köln	Poster IIIc.P5	119

Last name	First name	Institution	Contribution	Page
Vieira	Daniel	I. Physikalisches Institut, Universität zu Köln	Contributed talk	27
Vynokurova	Kateryna	I. Physikalisches Institut, Universität zu Köln	Poster V.P5	151
Walch-Gassner	Stefanie	I. Physikalisches Institut, Universität zu Köln	Review	59
Wang	Tsan-Ming	Argelander-Institut für Astronomie		
Weiss	Axel	MPIfR	Contributed talk	43
Witt	Emily	University of Colorado, Boulder	Poster IIIc.P6	120
Wyrowski	Friedrich	MPI für Radioastronomie	Invited talk	87
Yamaguchi	Masayuki	ASIAA	Poster IIIc.P1	115
Yanitski	Craig	I. Physikalisches Institut, Universität zu Köln	Poster IIIc.P7	121
Yorke	Hal	NN	Review	32
Zinnecker	Hans	Universidad Autonoma de Chile	Contributed talk	146